

The Relationship Between Topography and Soil Moisture Distribution

by

Eddie James Humphries, Jr.

B.A. in Environmental Science and Engineering,
Harvard University

Submitted to the Department of
Civil and Environmental Engineering
in Partial Fulfillment of the Requirements for
the Degree of

Master of Science

CIVIL AND ENVIRONMENTAL ENGINEERING
at the

Massachusetts Institute of Technology
June 1996

© 1996 Massachusetts Institute of Technology
All rights Reserved

Signature of the Author _____

Environmental Engineering
May 23, 1996

Certified by _____

Elfatih A. B. Eltahir
Thesis Supervisor

Accepted by _____

Joseph M. Sussman
Chairman, Departmental Committee on Graduate Studies
Department of Civil and Environmental Engineering

Eng

MASSACHUSETTS INSTITUTE
OF TECHNOLOGY

JUN 05 1996

LIBRARIES

The Relationship Between Topography and Soil Moisture Distribution

by

Eddie James Humphries, Jr.

**Submitted to the Department of
Civil and Environmental Engineering
in Partial Fulfillment of the Requirements for
the Degree of Master of Science**

CIVIL AND ENVIRONMENTAL ENGINEERING

ABSTRACT

Soil moisture is an important component of the hydrologic cycle. The very nature of soil moisture makes it extremely difficult to measure at large spatial scales. In this thesis, a method is proposed to relate the distribution of soil moisture to topography. An equation with an explicit representation of elevation and soil moisture is derived from the basic principles of unsaturated flow. Treating elevation and soil moisture as random variables, this equation is used to relate the spectrum of soil moisture to the spectrum of elevation for the one- and the two-dimensional cases. This relationship depends on several soil and climate properties; the sensitivity of the relationship to these properties is analyzed and discussed. The variability of soil moisture resulting from variability in soil properties is also analyzed and compared with the variability resulting from topography.

To test the theoretical results, a field experiment is designed to measure soil moisture along a hillslope using neutron probe technology. Porosity and saturated hydraulic conductivity are also determined over the distance of the experimental site. The soil moisture measurements show the effects of two nearly equal but opposite forces: the forcing of the soil properties and the forcing of the elevation gradient. Because soil properties significantly affect soil moisture, it can be concluded that topography has an observable impact on soil moisture at the experimental site. The predictions made using the basic equation relating the effect of topography on soil moisture agreed well with the observed soil moisture conditions. Overall, this study shows that topography affects soil moisture in a quantitative manner and that this effect can potentially be used to better quantify the distribution of soil moisture

Thesis Supervisor : Elfatih A. B. Eltahir
Title : Assistant Professor

ACKNOWLEDGEMENTS

I would like to thank my advisor, Professor Elfatih Eltahir for his guidance and willingness to help me change research topics halfway through my graduate career.

The research for this thesis was supported by NASA.

I would like to thank Professor Howard Stone at Harvard University for his help in solving the partial differential equation in this thesis. Also thanks to Jeremy Pal and Sara Zion for help with my fieldwork, and to Janni Moselsky for typing my references at the last moment.

Also, endless thanks and appreciation for the love and support of my family.

Finally, immeasurable undying love and gratitude to my bride-to-be, Christine Zaleski, who kept me sane for two years at MIT and helped me out until the very end.

This work is dedicated to
Christine Ann Regina

TABLE OF CONTENTS

ABSTRACT	2
ACKNOWLEDGEMENTS	3
TABLE OF CONTENTS	5
LIST OF FIGURES	7
LIST OF TABLES	10
LIST OF NOTATIONS	12
CHAPTER 1: Introduction	13
1.0 Background	13
1.1 Importance of Soil Moisture as a Hydrologic Variable	13
1.2 Literature Review	14
1.3 Outline	18
CHAPTER 2: A Theory for the Relationship Between Soil Moisture and Topography	19
2.0 Introduction	19
2.1 Formulation of the Problem	19
2.2 Analytical Solutions to the Deterministic One-Dimensional Flow Equation	24
2.3 One-Dimensional Stochastic Analysis of the Steady-State Relationship Between Topography and Soil Moisture	30
2.4 One-Dimensional Example of the Distribution of Soil Moisture	39
2.5 Two-Dimensional Stochastic Analysis of the Steady-State Relationship Between Topography and Soil Moisture	51
2.6 Two-Dimensional Example of the Distribution of Soil Moisture	55
2.7 Comparison of One- and Two-Dimensional Results	65
2.8 Conclusions	68

CHAPTER 3: Effect of Soil Properties and Climate on Soil Moisture Variability	70
3.0 Introduction	70
3.1 Influence of Soil Properties on the Relationship of Soil Moisture to Topography	70
3.2 Sensitivity of the Soil Moisture-Topography Relationship to Soil and Climate Properties	74
3.3 Stochastic Analysis of the Relationship Between Soil Moisture and Soil and Climate	86
3.4 Example of Soil as a Forcing of Soil Moisture Variability	90
3.5 Conclusions	94
CHAPTER 4: Results of Field Experiments	96
4.0 Introduction	96
4.1 Background to the Site	96
4.2 Experimental Procedure	97
4.3 Relationship of Soil Water to Topography and Soil Properties	115
4.4 Predictions of the Theory Relating Soil Moisture to Topography	125
4.5 Conclusions	139
CHAPTER 5: Conclusions	141
5.0 Introduction	141
5.1 Soil Moisture Theory	141
5.2 Field Observations	142
5.3 Future Research	143
REFERENCES	144

LIST OF FIGURES

Figure 2.4.1: Elevation Contours of the Selected Region of New England	43
Figure 2.4.2: One-dimensional Observed Autocorrelation Function for New England Elevation	44
Figure 2.4.3: Autocorrelation of One-dimensional Simulated Soil Moisture	48
Figure 2.4.4: Distribution of Elevation in Central New England	49
Figure 2.4.5: Distribution of Soil Moisture from One-Dimensional Simulation	50
Figure 2.6.1: Observed Two-Dimensional Autocorrelation Function for Elevation in Selected Region in New England	59
Figure 2.6.2: Simulated Two-Dimensional Autocorrelation Function for Selected Region in New England	60
Figure 2.6.3: Latitudinal Autocorrelation of Two-Dimensional Simulation of Soil Moisture	61
Figure 2.6.4: Longitudinal Autocorrelation of Two-Dimensional Simulation of Soil Moisture	62
Figure 2.6.5: Autocorrelation Function of Two-Dimensional Simulated Soil Moisture Field in Two Dimensions	63
Figure 2.6.6: Distribution of Soil Moisture from Two-Dimensional Simulation	64
Figure 3.2.1a Sensitivity of Mean of Soil Moisture to α	76
Figure 3.2.1b Sensitivity of Variance of Soil Moisture to α	76
Figure 3.2.1c Sensitivity of Coefficient of Variation of Soil Moisture to α	76
Figure 3.2.2a Sensitivity of Mean of Soil Moisture to β	77
Figure 3.2.2b Sensitivity of Variance of Soil Moisture to β	77
Figure 3.2.2c Sensitivity of Coefficient of Variation of Soil Moisture to β	77
Figure 3.2.3a Sensitivity of Mean of Soil Moisture to c	79

Figure 3.2.3b Sensitivity of Coefficient of Variation of Soil Moisture to c	79
Figure 3.2.4a Sensitivity of Mean of Soil Moisture to D	81
Figure 3.2.4b Sensitivity of Coefficient of Variation of Soil Moisture to D	81
Figure 3.2.5a Sensitivity of Mean of Soil Moisture to K_0	82
Figure 3.2.5b Sensitivity of Coefficient of Variation of Soil Moisture to K_0	82
Figure 3.2.6a Sensitivity of Mean of Soil Moisture to R	84
Figure 3.2.6b Sensitivity of Coefficient of Variation of Soil Moisture to R	84
Figure 3.2.7a Sensitivity of Mean of Soil Moisture to θ_0	85
Figure 3.2.7b Sensitivity of Coefficient of Variation of Soil Moisture to θ_0	85
Figure 4.1.1: Elevation Contours of Harvard Forest	98
Figure 4.1.2: Localized Elevation Contours around Prospect Hill	99
Figure 4.1.3: Topographic Map around Prospect Hill Showing Soil Moisture Showing Soil Moisture Access Tubes	100
Figure 4.2.1: Laboratory Calibration Curve of Neutron Probe Using Sandy Loam	103
Figure 4.2.2: Laboratory Estimation of Saturated Hydraulic Conductivity along Prospect Hill	105
Figure 4.2.3: Field Measurements of Porosity along Prospect Hill	108
Figure 4.2.4: Throughfall at Harvard Forest for Fall, 1995	112
Figure 4.2.5: Evaporation at Harvard Forest for Fall, 1995	113
Figure 4.2.6: Spatial Average of Soil Moisture for Fall, 1995	114
Figure 4.3.1a: Observations of θ plotted against Elevation	117
Figure 4.3.1b: Observations of θ plotted against Saturated Hydraulic Conductivity	117
Figure 4.3.1c: Observations of θ plotted against Porosity	117
Figure 4.3.2a: Observations of θ plotted against Elevation	118

Figure 4.3.2b: Observations of s plotted against Saturated Hydraulic Conductivity	118
Figure 4.3.2c: Observations of s plotted against Porosity	118
Figure 4.3.3a: Observations of K plotted against Elevation	119
Figure 4.3.3b: Observations of K plotted against Saturated Hydraulic Conductivity	119
Figure 4.3.3c: Observations of K plotted against Porosity	119
Figure 4.3.4: Comparison of Soil Moisture for Prospect Hill and a Flat Surface with the Same Porosity Distribution	123
Figure 4.4.1a: Predictions versus Observations of θ	128
Figure 4.4.1b: Predictions versus Observations of K	129
Figure 4.4.1b: Predictions versus Observations of s	130
Figure 4.4.2a: Unsteady Predictions for 10/3/95	133
Figure 4.4.2b: Unsteady Predictions for 10/9/95	133
Figure 4.4.2c: Unsteady Predictions for 10/20/95	134
Figure 4.4.2d: Unsteady Predictions for 10/27/95	134
Figure 4.4.2e: Unsteady Predictions for 11/3/95	135
Figure 4.4.2f: Unsteady Predictions for 11/11/95	135
Figure 4.4.2g: Unsteady Predictions for 11/17/95	136
Figure 4.4.2h: Unsteady Predictions for 11/25/95	136

LIST OF TABLES

Table 2.4.1: Normalized Kendall Ranking Statistic (τ) of the Mean (\bar{z}) and Variance (σ_z) of Elevation	41
Table 2.4.2: Parameters of the One-Dimensional Autocovariance Functions of Observed Elevation and Simulated Soil Moisture	42
Table 2.4.3: Values of Soil and Climate Parameters used in Monte Carlo Simulations	47
Table 2.6.1: Parameters of Covariance Functions of Observed Elevation and Simulated Soil Moisture	58
Table 3.1.1: Nominal Values of Soil, Climate, and Elevation parameters used in the Sensitivity Analysis	71
Table 3.1.2: Statistics of Unsaturated Hydraulic Conductivity and Soil Moisture For the Nominal Case Considered	73
Table 3.4.1: Stochastic Soil Properties from Mantoglou and Gelhar (1987b)	91
Table 3.4.2: Variability in Soil Moisture Resulting from Variability in Soil Properties	92
Table 4.2.1: Elevation along Prospect Hill	101
Table 4.2.2: Experimental Results for Saturated Hydraulic Conductivity along Prospect Hill	107
Table 4.2.3: Experimental Results for Porosity along Prospect Hill	109
Table 4.3.1: r^2 of regressions of z , θ_o , and K_o to θ , s , and K	120
Table 4.3.2: t-statistics of Linear Regressions	122
Table 4.4.1: Observed value of neglected term of $\frac{1}{\alpha K_o} \frac{\Delta K_o}{\Delta x}$ in Equation 2.1.9	127

Table 4.4.2: RMSE, r^2 between Steady-State Predictions and Average Soil Moisture	131
Table 4.4.3: r^2 of Unsteady Predictions versus Observations of Soil Moisture	137
Table 4.4.4: Spatial and Temporal Biases of Unsteady Predictions	138

LIST OF NOTATIONS

α	pore size distribution parameter
β	vertical divergence parameter
c	pore tension parameter
D	depth of the root zone
K	unsaturated hydraulic conductivity
K_0	saturated hydraulic conductivity
θ	volumetric water content of soil
θ_0	porosity
s	soil saturation, fraction
R	effective precipitation

CHAPTER 1

Introduction

1.0 Background

Soil moisture, the water occupying space in the unsaturated zone of soil, is a vital yet difficult to characterize component of the hydrologic cycle. Proper characterization of soil moisture has important implications ranging from pollution remediation to climatology. The main factors controlling soil moisture are soil properties, topography, and climate. Climate affects soil moisture through sources (e.g. precipitation) and sinks (e.g., evapotranspiration) of water. Soil properties control soil moisture by influencing the equilibrium of water flow. Topography is also expected to be a significant factor in soil moisture characterization. However, up to this point there has been no rigorous theory to explain the influence of topography on soil moisture.

1.1 Importance of Soil Moisture as a Hydrologic Variable

Soil moisture is a significant component of the hydrologic cycle; however, the expense and difficulty associated with taking soil moisture measurements makes it one of the least measured and hardest to quantify components of the hydrologic cycle. Most of the available information on soil moisture falls into two categories of spatial and temporal resolution: measurements at discrete locations at discrete points in time, as taken with soil tensiometers and neutron probes, and measurements which average soil moisture over large spatial scales and long time scales, as inferred from satellite measurements. These two categories represent the extremes of spatial and temporal averaging of soil moisture; little information is available regarding soil moisture behavior at an intermediate space-time scale. This discrepancy in the

measurement of soil moisture has traditionally lead to many simplified assumptions and parameterizations about soil moisture in studies in a wide range of scientific fields. Consequently, improving in the characterization of soil moisture fields in space and time could enrich a wide range of hydrologic studies.

Nearly all of the available information on soil moisture is actually the result of indirect measurements. Point observations of soil moisture measure hydraulic tension (with a tensiometer) or thermalized radiation (with a neutron probe); satellite information is derived from microwave emission. Thus it is common practice to use other forms of information to characterize soil moisture. Given the limitations of the resolution and the accuracy of current soil moisture information, it is worthy to attempt using new methods to add to the picture of soil moisture behavior. Topography is one factor which may have an important causal influence on soil moisture variability. The wealth of information on topography is enormous: elevation data is currently available for nearly all of the United States at a 30 m by 30 m scale. Furthermore, elevation is known to play a significant role in the flow of both groundwater aquifers and in surface runoff. It can therefore be expected that elevation will also play an important role in the flow of water in the vadose or unsaturated zone. The wide availability of elevation data and functional significance of topography suggest that it may be useful for obtaining information about soil moisture. The goal of this study is to derive an explicit relationship between soil moisture and topography, test the validity of this relationship with a field experiment, and utilize this relationship to infer information about the large-scale distribution of soil moisture.

1.2 Literature Review

The classical description of the flow of water in the unsaturated zone is Klute's (1952) reworking of Richard's Equation (1931):

$$\frac{\partial \theta}{\partial t} = \nabla \cdot (K \nabla \Phi) \quad (1.2.1)$$

(Philip, 1957). This equation describes the change in soil moisture content (referred to as soil moisture for simplicity), θ , as the divergence of the product of unsaturated hydraulic conductivity, K , and the hydraulic gradient, $\nabla \Phi$. In his paper, Philip (1957) uses Equation 1.2.1 to derive a fundamental theory of infiltration.

Later papers advance theories to quantify unsaturated hydraulic conductivity in terms of soil moisture content. One of the earliest and most widely used formulations was obtained by Gardner (1957), who began with Equation 1.2.1 above and derived an analytical form relating unsaturated hydraulic conductivity to capillary tension or suction head:

$$K = K_0 e^{\alpha \psi} \quad (1.2.2).$$

where ψ is the capillary tension in the soil. Soil moisture can then be expressed in terms of capillary tension through the relation

$$\theta = \theta_0 + c\psi \quad (1.2.3)$$

(Gelhar and Mantoglou, 1987a). This equation denotes a linear relationship between soil moisture and capillary tension, which can be a very good approximation for certain soils (Gelhar and Mantoglou, 1987b). Combining 1.2.2 and 1.2.3 together provides a simple but powerful formulation relating soil moisture to unsaturated hydraulic conductivity which has wide use in current theory and applications.

Another formulation, which is widely used in field applications, expresses unsaturated hydraulic conductivity in terms of soil water parameters

$$K(s) = K(1)s^{\frac{1}{m}} \quad (1.2.4)$$

$$\psi(s) = \psi(1)s^{-n}$$

(Brooks and Corey 1966), where s is the soil saturation (soil moisture content divided by porosity), $K(1)$ and $\psi(1)$ are the values of conductivity and capillary tension at 100% saturation, and m and n are constants used to fit the equations to a moisture retention curve. The advantages of this formulation is that it often agrees well with observed data and that the unsaturated parameters m , n , and $\psi(1)$ can all be obtained from one set of moisture retention measurements (Brooks and Corey, 1966). The disadvantage of this formulation is the highly non-linear relationship between unsaturated hydraulic conductivity and soil moisture, which makes the equations in 1.2.4 very difficult to deal with analytically.

In experimental work, it will be of interest to determine the properties of soils under study. Stephens (1996) provides an excellent description of many techniques used to characterize both saturated and unsaturated soil properties. Smith and Mullins (1991) also provide a great deal of information on standard techniques for characterization of soil properties; Revut and Rode (1981) present a wealth of techniques used by Russian scientists over a period of many years. Determination of properties in undisturbed field conditions is often preferable to using disturbed samples. Wooding (1968) and Shani *et al.* (1987) present field techniques for characterizing the parameter α in Gardner's formulation. Daniel (1990) reviews several field techniques for measurement of saturated hydraulic conductivity. For Brooks-Corey formulations, McCuen *et al.* (1981) and Gregson *et al.* (1987) present techniques for estimating the unsaturated parameters using information on soil type and employing efficient measurement techniques, respectively.

Many of the basic theories and studies of unsaturated flow began out of an interest in the infiltration in the vertical direction. However, it is expected that there will

be significant lateral flow in the unsaturated zone as well. Employing an experimental approach, Hewlett and Hibbert (1963) studied the flow of water in a sloping soil mass. After reviewing the works of Giorgini *et al.* (1984), Zaslavsky and Sinai (1981), and McCord and Stephens (1987) and carrying out qualitative unsaturated flow experiments, Eltahir (1989) concluded that significant lateral flow occurs within layers of soil with different moisture content. Genereux and Hemond (1990) state that up to 70% of the streamflow in a small stream in Central Massachusetts originates from the unsaturated zone. It is then expected that the flow of water unsaturated zone of the soil will be a significant component of the hydrologic cycle. Classical hydrologic theory is often incomplete in its description of unsaturated flow processes. Zaslavsky and Sinai (1981a,b,c,d,e) present a detailed investigation into unsaturated subsurface flow. Based on observations, theoretical considerations, and field experiments, they conclude that topographic slope and anisotropy of soils will be both be important factors influencing unsaturated flow. This important conclusion provides the motivation for this study.

Beven and Kirkby (1979) proposed the TOP model, a simple and widely approach model to relate the spatial distribution of soil moisture to topography. This model is based on the assumption that the water table intersects the ground surface in locations where the flux of water exceeds the capacity of saturated soil to transport water. Topography enters the model through the assumption that the hydraulic gradient of saturated flow is equivalent to the elevation gradient at the ground surface. However, this model neglects the lateral flow of water in the unsaturated zone: this in where the considerations of Zaslavsky and Sinai (1987a) can improve hydrologic characterizations of water flow.

Because of the many factor which affect unsaturated flow and the rule of heterogeneity of properties in many soils, a stochastic approach to characterizing unsaturated flow is often employed. Gelhar (1990) presents a thorough treatment on

stochastic subsurface hydrology, which demonstrates the mathematical techniques used in the formulation of subsurface problems. Bakr *et al.* (1978) consider a stochastic approach to the effect of anisotropy of saturated hydraulic conductivity on hydraulic head and conclude that dimensional consideration and the correlation scale of hydraulic conductivity are both very important. Gelhar and Mantoglou (1987b) present a stochastic unsaturated flow system and suggest that soil variability may be a cause of observed hysteresis observed in the field; in a companion paper (1987c), the same authors present an example of the differences in predicted of unsaturated flow made using both a classical and a stochastic approach. These results demonstrate that a stochastic formulation of an unsaturated flow system is valid and should better deal with natural variability than a deterministic approach.

1.3 Outline

This thesis is organized into five chapters. Chapter 2 formulates the basic unsaturated flow problem and employs a stochastic approach to derive an explicit relationship between soil moisture and topography. In Chapter 3, the effect of soil properties on the proposed relationship of soil moisture to topography and the variability in soil moisture arising from variability in soil properties is studied. Chapter 4 presents the results and explanations of a field experiment designed to test the relationship of soil moisture to topography. Finally, Chapter 5 presents a brief summary and the conclusions of this study.

CHAPTER 2

A Theory for the Relationship Between Soil Moisture and Topography

2.0 Introduction

In this Chapter, the basic principles relating soil moisture to topography are presented. Section 2.1 reviews the basic principles of unsaturated flow and develops a governing flux equation for the unsaturated zone. Special cases of this equation have analytical solutions; these are derived in Section 2.2. Spectral methods can be used to relate the statistical properties of soil moisture to the statistical properties of elevation; this procedure is presented for the one-dimensional case in Section 2.3, and the two-dimensional case in Section 2.5. Examples using real data from the New England region are shown for the one-dimensional case in Section 2.4 and the two-dimensional case in Section 2.6. The differences arising between the one- and the two-dimensional cases are discussed in Section 2.7, and conclusions are summarized in Section 2.8.

2.1 Formulation of the Problem

Darcy's equation describes the flow of water in porous media. Although this principle is most commonly used for saturated flow, an equation of form similar to Darcy's equation is valid for flow in the unsaturated zone. This unsaturated flow equation states that specific flow in the i -direction is equal to the product of isotropic unsaturated hydraulic conductivity and the hydraulic gradient in the i -direction:

$$q_i = -K(\psi) \frac{\partial h}{\partial x_i} \quad (2.1.1).$$

The quantity q_i is the specific flow in the i -direction. $K(\psi)$ is the unsaturated hydraulic conductivity, and $h (= \psi + z)$ is the hydraulic head, the sum of pressure head, ψ , and

elevation, z . In the unsaturated case, the pressure head, ψ , is capillary tension and will be negative in sign, decreasing (becoming more negative) with less water in the soil. The notation $K(\psi)$ suggests that the unsaturated hydraulic conductivity will be solely a function of the pressure head; in reality, it will depend on instantaneous hydraulic head, temperature, and the time history of wetting and drying of the soil (Bras, 1990). However, at long time scales the short-term influence of variable temperature, wetting, and drying can be expected to average to a negligible value. Since this study is concerned with long-term distributions of soil moisture, the effects of temperature and wetting and drying on unsaturated hydraulic conductivity will be considered negligible when compared to the effect of pressure head.

In general, the hydraulic tension, ψ , depends on the amount of water present in the soil. One measure of soil water is the available water content per unit total volume, represented by θ . Physically, θ is the volume of water occupying space in a given unit volume of soil. This quantity is easily (although indirectly) measured in the field using the neutron probe. On the other hand, ψ can be extremely difficult to measure *in situ* and will be used only as an intermediate quantity. Gardner (1958) and Mantoglou and Gelhar (1987) relate θ to unsaturated hydraulic conductivity with ψ as an intermediate variable using the two equations

$$K = K_o e^{\alpha\psi} \quad (2.1.2)$$

$$\theta = \theta_o + c\psi \quad (2.1.3).$$

Here, K_o is the saturated hydraulic conductivity, α is the dispersion coefficient, θ_o is the saturated water content (equivalent to the porosity of the soil), and c is the specific soil moisture capacity. By combining Equations 2.1.2 and 2.1.3 to eliminate ψ , unsaturated hydraulic conductivity and soil moisture are related directly. Taking the natural log of Equation 2.1.2 and solving for ψ ,

$$\psi = \frac{1}{\alpha} \ln\left(\frac{K}{K_o}\right) \quad (2.1.4).$$

This relates ψ to the ratio of unsaturated to fully saturated hydraulic conductivity of a soil. Substituting Equation 2.1.4 into the second equation in 2.1.3 to eliminate ψ , the relationship between the soil moisture and the unsaturated hydraulic conductivity of a soil becomes

$$\theta = \theta_o + \frac{c}{\alpha} \ln\left(\frac{K}{K_o}\right) \quad (2.1.5).$$

With this relationship, there is no longer dependence on the intermediate variable ψ , and it will be much easier to study soil moisture from unsaturated hydraulic conductivity.

Equation 2.1.1 can be expanded and substituted into Equation 2.1.2. Taking the derivatives of ψ and z in space,

$$q_i = -\frac{\partial}{\partial x_i} \left(\frac{1}{\alpha} \ln\left(\frac{K(\theta)}{K_o}\right) \right) - K(\theta, x) \frac{\partial z}{\partial x_i} = -\frac{1}{\alpha} \frac{\partial K(\theta)}{\partial x_i} + K(\theta) \left[\frac{1}{\alpha K_o} \frac{\partial K_o}{\partial x_i} - \frac{\partial z}{\partial x_i} \right] \quad (2.1.6)$$

which is a non-linear equation of K due to gradients in saturated hydraulic conductivity (assuming that the pore size distribution parameter, α , is constant in space).

However, the non-linear term $\frac{1}{\alpha K_o} \frac{\partial K_o}{\partial x_i}$ which multiplies $K(\theta, x)$ is generally expected to be of small order compared to elevation gradients, $\frac{\partial z}{\partial x_i}$. It is important to note that

Equation 2.1.6 treats elevation as an explicit variable in the horizontal direction. This treatment of elevation as a variable in space rather than as a spatial dimension will allow us to relate directly topography and unsaturated hydraulic conductivity.

Equation 2.1.6 describes flow in the unsaturated zone as the sum of flow due to unsaturated hydraulic conductivity gradients in the horizontal direction, which result in diffusion-like flow, and of flow due to elevation gradients, which force a Darcian gravity flow.

Since the region of interest in this study is the unsaturated zone, this region will be used as the control volume for conservation of mass. To determine changes in the water content of the unsaturated zone in time, conservation of mass can be applied to the control volume

$$D \frac{\partial \theta}{\partial t} = -D \frac{\partial q_i}{\partial x_i} - s + R \quad (2.1.7)$$

where D is the depth of the root zone, s is the vertical divergence of water, and R is infiltration rate into the soil. Equation 2.1.7 states that the overall change in water content in the root zone, $D \frac{\partial \theta}{\partial t}$ is equal to the loss of water due to horizontal fluxes, $D \frac{\partial q_i}{\partial x_i}$, minus the loss of water due to other sinks, s , plus the input of water due to precipitation, R . R , or effective precipitation, is the amount of rainfall infiltrating the soil and is equivalent to precipitation minus runoff for bare soils. When considerable vegetation is present, effective precipitation may be considerably reduced from actual precipitation through evaporative interception loss. For the purposes this analysis, R will be assumed a constant fraction of precipitation and constant in space. The sink of water due to vertical divergence, s , includes loss to evaporation and percolation. These flows may be combined and parameterized as proportional to hydraulic conductivity as $s = \beta K$. Conceptually, this parameterization is justifiable because divergence due to gravity (groundwater recharge) and to suction (from roots taking up water for evaporation) should result in a slow, Darcian flow that will be proportional to the hydraulic conductivity of a soil. With this parameterization, β can then be thought

of as the hydraulic gradient of sinks of water in the root zone. Substituting for q_i from Equation 2.1.6 into Equation 2.1.7 results in

$$D \frac{\partial \theta}{\partial t} = D \frac{\partial}{\partial x_i} \left(-\frac{1}{\alpha} \frac{\partial K(\theta)}{\partial x_i} + K(\theta, x) \left[\frac{1}{\alpha K_0} \frac{\partial K_0}{\partial x_i} - \frac{\partial z}{\partial x_i} \right] \right) - \beta K(\theta) + R \quad (2.1.8).$$

This equation quantifies the water balance in the root zone in terms of hydraulic conductivity gradients, $\frac{\partial K}{\partial x_i}$; soil properties, α , K_0 , and D ; topographic slope, $\frac{\partial z}{\partial x_i}$; and climatological forcings, R and β . Equation 2.1.8 can be used to establish the dependence of soil moisture conditions, K and θ , on elevation, z .

Often, it is of interest to consider the long-term behavior of soil moisture. In such cases, soil moisture should be near an equilibrium. Using the notation $E_t[]$ to denote the expected value, or average in *time*, Equation 2.1.8 can be averaged in time to obtain

$$D \frac{\partial E_t[\theta]}{\partial t} = D \frac{\partial}{\partial x_i} \left(-\frac{1}{\alpha} \frac{\partial E_t[K(\theta, x)]}{\partial x_i} - E_t[K(\theta, x)] \frac{\partial z(x)}{\partial x_i} \right) - \beta E_t[K(\theta, x)] + E_t[R] \quad (2.1.9)$$

where the effect of variability in saturated hydraulic conductivity is assumed to be negligible. Because soil moisture considered at seasonal or yearly time scales will be very near to equilibrium, the left-hand side of Equation 2.1.9 will be negligible, since the change in the time-average of soil moisture will be zero. This results in the equation

$$D \frac{\partial}{\partial x_i} \left(-\frac{1}{\alpha} \frac{\partial E_t[K(\theta, x)]}{\partial x_i} - E_t[K(\theta, x)] \frac{\partial z(x)}{\partial x_i} \right) - \beta E_t[K(\theta, x)] + E_t[R] = 0 \quad (2.1.10)$$

which is a special case of Equation 2.1.8 for which variability in saturated hydraulic conductivity is negligible and the long-term behavior of unsaturated hydraulic conductivity (which is used here as a surrogate for soil moisture) is considered. This equation is linear on $E_t[K]$, which makes it desirable for theoretical and analytical purposes.

2.2 Analytical Solutions to the Deterministic One-Dimensional Flow Equation

The equation describing flux of water in the unsaturated zone, Equation 2.1.8, can be studied for either the steady state or the transient case. In the steady-state case, soil moisture is considered as a long time scale (i.e., seasonal or yearly) process. As mentioned above, when the long-term expectation of this process is taken in time, the time-dependent term, $\frac{\partial \theta}{\partial t}$, can be considered nearly zero. The resulting equation is only dependent on distance, x , and becomes a second-order partial differential equation. In the case where hydraulic conductivity is constant, the derivatives of K_0 are also zero. These two conditions will transform equation 2.1.8 into a second-order ordinary differential equation. With knowledge of conditions at two boundaries, unsaturated hydraulic conductivity (and hence soil moisture) can then be completely described within the boundaries. Dropping the $E_t[]$ notation for simplicity of presentation, the ordinary differential equation derived from Equation 2.1.8 is

$$D \frac{d}{dx} \left(-\frac{1}{\alpha} \frac{dK(x)}{dx} - K(x) \frac{dz}{dx} \right) + \beta K(x) - R = 0 \quad (2.2.1)$$

where $K(x)$ and R are understood to mean $E_t[K(x)]$ and $E_t[R]$. All of the soil parameters K_0 , α , θ_0 , and c are characteristics of soil type; α and c are also somewhat dependent on soil moisture. However, all the soil parameters can be considered constant in space over the appropriate averaging scale, and α and c are

often constant for certain ranges of soil moisture. For constant soil parameters, topographic slope, $\frac{dz}{dx}$, and soil depth, this is a second-order, non-homogenous ordinary differential equation in K with constant coefficients. This type of equation has a solution given by

$$K(x) = C_1 e^{\lambda_1 x} + C_2 e^{\lambda_2 x} - \frac{\alpha R}{D} \quad (2.2.2)$$

where

$$\lambda_1 = \frac{\alpha}{2} \frac{dz}{dx} + \sqrt{\alpha^2 \left(\frac{dz}{dx} \right)^2 + 4 \frac{\alpha \beta}{D}} \quad (2.2.3)$$

$$\lambda_2 = \frac{\alpha}{2} \frac{dz}{dx} - \sqrt{\alpha^2 \left(\frac{dz}{dx} \right)^2 + 4 \frac{\alpha \beta}{D}} \quad (2.2.4)$$

are the roots of the characteristic equation of 2.2.1. The boundary conditions can be used to evaluate C_1 and C_2 ; Equation 2.2.1 can then be combined with Equation 2.1.8 to give predictions for soil moisture. This results in

$$\theta(x) = \theta_o + \frac{c}{\alpha} \ln \left[\frac{K(x)}{K_o} \right] \quad (2.2.5).$$

It is noteworthy that the soil properties θ_o and c do not appear in the solution of hydraulic conductivity in Equation 2.2.2. Since the solution $K(x)$ is independent of these two variables, they need not be constant over the domain of x . If these variables can be described as a function of distance, $\theta_o(x)$ and $c(x)$, then these descriptions can be substituted into 2.2.5 without any loss of generality. This more general solution for soil moisture is

$$\theta(x) = \theta_0(x) + \frac{c(x)}{\alpha} \ln \left[\frac{K(x)}{K_0} \right] \quad (2.2.6).$$

Further, if effective rainfall, R , is variable with distance and has a well-behaved functional form, the solution for K that includes this variability can be found in general by the method of variation of parameters. The resulting solution for $K(x)$ can then be incorporated into the solution of soil moisture, Equation 2.2.6. Thus, only the parameters α , β , $\frac{dz}{dx}$, K_0 , and D need be strictly constant in space in order to achieve an analytical solution to θ . Averaged over several months to a year to ensure equilibrium, this expression may be used to predict soil moisture conditions which can then be compared to observations of soil moisture data, thereby testing the proposed theory. This will be performed in Chapter 4.

At smaller time scales, it is not appropriate to take the temporal expectation of the $\frac{\partial \theta}{\partial t}$ term in Equation 2.1.8. For such cases, the solution of unsaturated hydraulic conductivity will be a function of both space and time. In order to find a solution to Equation 2.1.8, it will first be necessary to express θ in terms of K . Using Equation 2.1.5 to relate θ to K , the time derivative $\frac{\partial \theta}{\partial t}$ becomes

$$\frac{\partial \theta}{\partial t} = \frac{\partial \theta_0}{\partial t} + \frac{\partial}{\partial t} \left(\frac{c}{\alpha} \ln \left(\frac{K}{K_0} \right) \right) = \frac{c}{\alpha} \frac{\partial \ln(K)}{\partial t} = \frac{c}{\alpha} \frac{1}{K} \frac{\partial K}{\partial t} \quad (2.2.7).$$

soil properties θ_0 , c , α , and K_0 should remain constant in space in this case. For the case when saturated hydraulic conductivity is constant, $\frac{\partial \theta}{\partial t}$ can be substituted directly into 2.2.1, and K becomes the only unknown:

$$D \frac{c}{\alpha} \frac{1}{K} \frac{\partial K}{\partial t} = \frac{D}{\alpha} \frac{\partial^2 K}{\partial x^2} + D \frac{dz}{dx} \frac{\partial K}{\partial x} - \beta K + R \quad (2.2.8).$$

This equation can be solved numerically. However, the rainfall rate, R , will be non-zero only during precipitation events; for times with no rainfall, Equation 2.2.8 simplifies to a quasi-linear second-order form of the diffusion equation

$$D \frac{c}{\alpha} \frac{1}{K} \frac{\partial K}{\partial t} = \frac{D}{\alpha} \frac{\partial^2 K}{\partial x^2} + D \frac{dz}{dx} \frac{\partial K}{\partial x} - \beta K \quad (2.2.9).$$

By setting

$$\bar{K} = \frac{D}{\alpha\beta} K$$

$$\bar{x} = D \frac{dz}{dx} \beta x$$

$$\bar{t} = ct$$

(2.2.10a-d).

$$\omega = \frac{\beta}{\alpha D} \left(\frac{1}{\frac{dz}{dx}} \right)^2$$

Equation 2.2.9 simplifies to

$$\frac{1}{\bar{K}} \frac{\partial \bar{K}}{\partial \bar{t}} = \omega \frac{\partial^2 \bar{K}}{\partial \bar{x}^2} + \frac{\partial \bar{K}}{\partial \bar{x}} - \bar{K} \quad (2.2.11).$$

Using the concept of similarity solutions, which arise in similar problems of fluid mechanics, (Lister and Kerr 1989), the solution of Equation 2.2.11 should take the form

$$\bar{K} = \bar{t}^\epsilon H(\eta) \quad (2.2.12)$$

where

$$\eta = \frac{\bar{x}}{\bar{t}^v} \quad (2.2.13)$$

and ε and v are arbitrary constants. Taking the appropriate derivatives of this form of \bar{K} yields

$$\begin{aligned} \frac{\partial \bar{K}}{\partial \bar{t}} &= \varepsilon \bar{t}^{\varepsilon-1} H + \bar{t}^{-\varepsilon} \frac{\partial H}{\partial \bar{t}} = \varepsilon \bar{t}^{\varepsilon-1} H + \bar{t}^{-\varepsilon} \frac{\partial \eta}{\partial \bar{t}} \frac{dH}{d\eta} = \varepsilon \bar{t}^{\varepsilon-1} H + \bar{t}^{-\varepsilon} \left(-v \frac{\bar{x}}{\bar{t}^{v+1}} \right) \frac{dH}{d\eta} \\ \frac{\partial \bar{K}}{\partial \bar{x}} &= \bar{t}^{-\varepsilon} \frac{\partial H}{\partial \bar{x}} = \bar{t}^{-\varepsilon} \frac{\partial \eta}{\partial \bar{x}} \frac{dH}{d\eta} = \bar{t}^{-\varepsilon} \left(\frac{1}{\bar{t}^v} \right) \frac{dH}{d\eta} \\ \frac{\partial^2 \bar{K}}{\partial \bar{x}^2} &= \bar{t}^{-\varepsilon} \frac{\partial^2 H}{\partial \bar{x}^2} = \bar{t}^{-\varepsilon} \frac{\partial}{\partial \bar{x}} \left(\frac{\partial \eta}{\partial \bar{x}} \frac{dH}{d\eta} \right) = \frac{\bar{t}^{-\varepsilon}}{\bar{t}^v} \frac{\partial}{\partial \bar{x}} \left(\frac{dH}{d\eta} \right) = \frac{\bar{t}^{-\varepsilon}}{\bar{t}^v} \frac{\partial}{\partial \eta} \left(\frac{dH}{d\bar{x}} \right) = \frac{\bar{t}^{-\varepsilon}}{\bar{t}^{2v}} \frac{\partial^2 H}{\partial \eta^2} \end{aligned} \quad (2.2.14).$$

Substituting these expressions into Equation 2.2.11 results in

$$\frac{1}{\bar{t}^\varepsilon H} \left(\varepsilon \bar{t}^{\varepsilon-1} H + \bar{t}^{-\varepsilon} \left(-v \frac{\bar{x}}{\bar{t}^{v+1}} \right) \frac{dH}{d\eta} \right) = \omega \frac{\bar{t}^{-\varepsilon}}{\bar{t}^{2v}} \frac{\partial^2 H}{\partial \eta^2} + \frac{\bar{t}^{-\varepsilon}}{\bar{t}^v} \frac{dH}{d\eta} - \bar{t}^{-\varepsilon} H \quad (2.2.15).$$

Since ε and v are arbitrary, they can be selected to result in a manageable form of Equation 2.2.15. Choosing $\varepsilon = -1$ and $v = 0$ makes 2.2.15 linear and reduces the partial differential equation in x and t to an ordinary differential equation in η . This new equation is

$$-1 = \omega \frac{\partial^2 H}{\partial \eta^2} + \frac{dH}{d\eta} - H \quad (2.2.16)$$

which has the following solution

$$H = C_1 e^{\lambda_1 \bar{t}} + C_2 e^{\lambda_2 \bar{t}} - 1$$

$$\lambda_1 = -\frac{1}{2} + \frac{\sqrt{1+4\omega}}{2} \quad (2.2.17)$$

$$\lambda_2 = -\frac{1}{2} - \frac{\sqrt{1+4\omega}}{2}$$

which will be valid for times of no rainfall. To use this equation, rainfall events will need special consideration. H , \bar{K} , and θ , can be calculated from the following algorithm:

1) Given a set of initial conditions of K in space over the domain of x , the constants C_1 and C_2 can be determined. This will allow K to be calculated in both time and space as long as no rainfall occurs.

2) When precipitation does occur, previous procedure for calculating K must end. Typically, the rainfall events will be relatively short compared to the overall time; the changes in soil moisture due to unsaturated flow during the time-scale of the rainfall event should also be very small compared to the changes in soil moisture due to rainfall input. With this in mind, the total precipitation input to the soil can be added to the solution of θ (and thereby K) from the beginning of the rainfall event.

3) The new solution for K at the end of the rainfall event can be used as new initial conditions for the system. Starting again at step 1), the calculation of unsaturated hydraulic conductivity and soil moisture in time can continue through rainfall events.

2.3 One-dimensional Stochastic Analysis of the Steady-State Relationship Between Topography and Soil Moisture

Given the form of Equation (2.1.10), in which both unsaturated hydraulic conductivity and elevation are variable, it is possible to relate explicitly the characteristics of unsaturated hydraulic conductivity in space to the characteristics of elevation in space. Since soil moisture content can be directly related to unsaturated hydraulic conductivity by Equation 2.1.5, this is equivalent to relating soil moisture to elevation or topography. In the seasonal to yearly water balance studies used in many water resources and climatological applications, the long-term (near-equilibrium) behavior of soil moisture is needed. For these purposes, the equilibrium case in time will be considered in which the expectation of soil moisture in time can be used. Because the long-term expectation of soil moisture in time, $E_t[\theta]$, will be constant, the left-hand side of Equation 2.1.10, $\frac{\partial E_t[\theta]}{\partial t}$, will be zero. Taking the expectation in *time* (and dropping the $E_t[]$ notation for simplicity, as in the previous section), Equation 2.1.8 takes the form

$$D \frac{\partial}{\partial x} \left(-\frac{1}{\alpha} \frac{\partial K}{\partial x} - K \frac{\partial z}{\partial x} \right) + \beta K - R = 0 \quad (2.3.1)$$

where K and z are unsaturated hydraulic conductivity and elevation fields which vary in *space*. These two fields can be represented as stationary random fields composed of a spatial mean plus a random fluctuation in *space*. Using this concept, K and z may be described as

$$\begin{aligned} K &= \bar{K} + K' \\ z &= \bar{z} + z' \end{aligned} \quad (2.3.2a, b)$$

where \bar{K} and \bar{z} are the spatial means and K' and z' are the random spatial perturbations of K and z , respectively. The perturbation terms K' and z' are expected to be small compared to the spatial averages \bar{K} and \bar{z} and to average to zero in space. Taking the spatial expectation of K and z results in

$$E_x[K] = E_x[\bar{K} + K'] = E_x[\bar{K}] + E_x[K'] = \bar{K} \quad (2.3.3a)$$

and

$$E_x[z] = E_x[\bar{z} + z'] = E_x[\bar{z}] + E_x[z'] = \bar{z} \quad (2.3.3b).$$

where $E_x[\]$ is meant to emphasize that the expectation in *space* is being taken for K and z . Substituting for K and z from Equations 2.3.2a and 2.3.2b into Equation 2.3.1 yields

$$D \frac{\partial}{\partial x} \left(-\frac{1}{\alpha} \frac{\partial(\bar{K} + K')}{\partial x} - (\bar{K} + K') \frac{\partial(\bar{z} + z')}{\partial x} \right) + \beta(\bar{K} + K') - R = 0 \quad (2.3.4).$$

When this equation is averaged in *space*, all the perturbation terms become zero, resulting in an average equation

$$D \frac{\partial}{\partial x} \left(-\frac{1}{\alpha} \frac{\partial \bar{K}}{\partial x} - \bar{K} \frac{\partial \bar{z}}{\partial x} \right) + \beta \bar{K} - R = 0 \quad (2.3.5).$$

The expectation of the perturbation cross-products, $\overline{K' \frac{\partial z'}{\partial x}}$, has been assumed to be zero in this equation: this makes the equation linear and easier to work with analytically. For stationary field of K and $\frac{\partial z}{\partial x}$, the derivatives of \bar{K} and $\frac{\partial \bar{z}}{\partial x}$ in the horizontal directions are zero. These conditions will simplify Equation 2.3.5 to the form

$$\bar{K} = \frac{R}{\beta} \quad (2.3.5a)$$

which yields a simple expression for the spatial average hydraulic conductivity in terms of the average long-term rainfall and climatic conditions.

Unlike the spatial averages, the spatial perturbations K' and z' do vary in space and will have non-zero derivatives. Subtracting Equation 2.3.5 from 2.3.4, the resulting equation contains only perturbation terms:

$$D \frac{\partial}{\partial x} \left(-\frac{1}{\alpha} \frac{\partial K'}{\partial x} - \bar{K} \frac{\partial z'}{\partial x} - K' \frac{\partial \bar{z}}{\partial x} - K' \frac{\partial z'}{\partial x} \right) + \beta K' = 0 \quad (2.3.6).$$

Since the perturbation terms are expected to be of small order, products of perturbation terms will be even smaller; therefore, the cross-product involving multiplication of two perturbation terms, $K' \frac{\partial z'}{\partial x}$, is assumed to be small compared with the products containing only one perturbation term. This term will be ignored, simplifying Equation 2.3.6 to

$$D \frac{\partial}{\partial x} \left(-\frac{1}{\alpha} \frac{\partial K'}{\partial x} - \bar{K} \frac{\partial z'}{\partial x} - K' \frac{\partial \bar{z}}{\partial x} \right) + \beta K' = 0 \quad (2.3.7)$$

where \bar{K} and $\frac{\partial \bar{z}}{\partial x}$ are the spatial means discussed above. Using spectral representation of stationary random fields, K' and z' may be described as the integral sum of random complex amplitude dZ_K and dZ_z , each with an associated wave number, k . This representation of K' and z' is given by

$$z' = \int_{-\infty}^{\infty} e^{ikx} dZ_z(k) \quad \text{and} \quad K' = \int_{-\infty}^{\infty} e^{ikx} dZ_K(k) \quad (2.3.8a,b).$$

The random amplitudes have special properties useful in spectral analysis. In particular, they are related to the spectral density function, which gives the distribution of variance with frequency. The relationship of the spectral density function to the random amplitudes is given by

$$\begin{aligned} E\left[dZ_z(k)dZ_z^*(k)\right] &= S_z(k)dk \\ E\left[dZ_K(k)dZ_K^*(k)\right] &= S_K(k)dk \end{aligned} \quad (2.3.9a,b)$$

where $dZ_z^*(k)$ and $dZ_K^*(k)$ are the complex conjugates of $dZ_z(k)$ and $dZ_K(k)$, respectively, and $S_z(k)$ and $S_K(k)$ are the spectra of z and K , respectively. This result will be useful later in relating the variance of hydraulic conductivity to the variance of elevation.

Substituting the spectral representations of K' and z' in Equations 2.3.8a and 2.3.8b into Equation 2.3.7, results in the form

$$\begin{aligned} D \frac{\partial}{\partial x} \left(-\frac{1}{\alpha} \frac{\partial}{\partial x} \int_{-\infty}^{\infty} e^{ikx} dZ_K(k) - \bar{K} \frac{\partial}{\partial x} \int_{-\infty}^{\infty} e^{ikx} dZ_z(k) - \int_{-\infty}^{\infty} e^{ikx} dZ_K(k) \frac{\partial \bar{z}}{\partial x} \right) \\ + \beta \int_{-\infty}^{\infty} e^{ikx} dZ_K(k) = 0 \end{aligned} \quad (2.3.10).$$

Since the spectral amplitudes $dZ_z(k)$ and $dZ_K(k)$, and α and \bar{K} are independent of x , all differentiation can be taken inside of the integrals, resulting in

$$\int_{-\infty}^{\infty} \left[\left(-\frac{D}{\alpha} \frac{\partial^2 e^{ikx}}{\partial x^2} dZ_K(k) - D\bar{K} \frac{\partial^2 e^{ikx}}{\partial x^2} dZ_z(k) - \frac{\partial e^{ikx}}{\partial x} dZ_K(k) D \frac{\partial \bar{z}}{\partial x} \right) + \beta e^{ikx} dZ_K(k) \right] = 0 \quad (2.3.11).$$

After differentiating and grouping together terms with the same spectral amplitudes, 2.3.11 becomes

$$\int_{-\infty}^{\infty} e^{ikx} \left[\left(\frac{D}{\alpha} k^2 + \beta - iD \frac{\partial \bar{z}}{\partial x} k \right) dZ_K(k) + D\bar{K}k^2 dZ_z(k) \right] = 0 \quad (2.3.12).$$

In order for this equation to be satisfied in general, the entire expression inside the brackets must vanish at all values of k because of the uniqueness of the spectral amplitudes. This expression relates the spectral amplitudes of K to the spectral amplitudes of z by the following relation:

$$\left[\left(\frac{D}{\alpha} k^2 + \beta \right) - D \frac{\partial \bar{z}}{\partial x} ki \right] dZ_K(k) = D\bar{K}k^2 dZ_z(k) \quad (2.3.13a)$$

or

$$dZ_K(k) = \frac{D\bar{K}k^2}{\left[\left(\frac{D}{\alpha} k^2 + \beta \right) - D \frac{\partial \bar{z}}{\partial x} ki \right]} dZ_z(k) \quad (2.3.13b).$$

Now the complex conjugates of the spectral amplitudes will be related by

$$dZ_K^*(k) = \frac{D\bar{K}k^2}{\left[\left(\frac{D}{\alpha} k^2 + \beta \right) + D \frac{\partial \bar{z}}{\partial x} ki \right]} dZ_z^*(k) \quad (2.3.14)$$

which can be used with Equation 2.3.13b and the identities in Equations 2.3.9a and b to relate the spectrum of K to the spectrum of z :

$$\left[\left(\frac{D}{\alpha} k^2 + \beta \right)^2 + D^2 k^2 \left(\frac{\partial \bar{z}}{\partial x} \right)^2 \right] S_K(k) dk = \left(D\bar{K}k^2 \right)^2 S_z(k) dk \quad (2.3.15).$$

This relates the spectrum of K and z for every wave number k. If the spectrum of the elevation field can be determined, as from commonly available elevation maps, the spectral density function of unsaturated hydraulic conductivity can be estimated from 2.3.15. It is important to note that this relationship is dependent on the large-scale vertical elevation gradient, $\frac{\partial \bar{z}}{\partial x}$; this suggests that elevation slope will be an important factor in the relationship between topography and soil moisture.

A further property of the definition of spectrum is that the total integral of the spectrum is equal to the variance of the random field,

$$\int_{-\infty}^{\infty} S_z(k) dk = \sigma_z^2 \quad (2.3.16)$$

$$\int_{-\infty}^{\infty} S_K(k) dk = \sigma_K^2 \quad (2.3.17).$$

With the use of these identities, Equation 2.3.15 can be used to relate the variance of the elevation field to the variance of the hydraulic conductivity field. This relationship is given by

$$\sigma_K^2 = \omega_0^2 \alpha^2 \bar{K}^2 \sigma_z^2 \quad (2.3.18)$$

where

$$\omega_0^2 = \int_{-\infty}^{\infty} \left[\frac{k^4}{(k^2 + \frac{\alpha\beta}{D})^2 + \alpha^2 k^2 (\frac{\partial \bar{z}}{\partial x})^2} \right] \frac{S_z(k)}{\sigma_z^2} dk \quad (2.3.19).$$

ω_0^2 is a dimensionless coefficient which is a function of both the physical relationship between elevation and hydraulic conductivity (from the physics of Equation 2.3.1) and of the variability of elevation itself (from the spectral density function of elevation). The variance of unsaturated hydraulic conductivity is thus directly related to the variance of elevation through the mean unsaturated hydraulic conductivity, the pore size distribution parameter α , soil depth D , and the vertical divergence parameter β . Physically, the variance of soil moisture will be dependent on its relation to capillary tension (through the parameter α), the local climate (through mean unsaturated hydraulic conductivity and vertical divergence) and geologic properties (soil depth).

The variable of prime interest is soil moisture. To obtain this, it is necessary to relate the spectral properties of soil moisture to those of unsaturated hydraulic conductivity. Equation 2.1.5 expresses soil moisture in terms of unsaturated conductivity:

$$\theta = \theta_0 + \frac{c}{\alpha} \ln\left(\frac{K}{K_0}\right) \quad (2.3.20).$$

Soil moisture can be expressed as a stationary random field with mean and perturbation terms just as elevation and unsaturated conductivity, $\theta = \bar{\theta} + \theta'$. Substituting the perturbation notation for θ and for K as a random fields in *space* into Equation 2.3.20 yields

$$\bar{\theta} + \theta' = \theta_0 + \frac{c}{\alpha} \ln\left(\frac{\bar{K} + K'}{K_0}\right) = \theta_0 + \frac{c}{\alpha} \left[\ln\left(\left(\frac{\bar{K}}{K_0}\right)\left(1 + \frac{K'}{\bar{K}}\right)\right) \right] \quad (2.3.21).$$

This can be re-arranged using law of logarithms

$$\bar{\theta} + \theta' = \theta_o + \frac{c}{\alpha} \left[\ln\left(\frac{\bar{K}}{K_o}\right) + \ln\left(1 + \frac{K'}{\bar{K}}\right) \right] \quad (2.3.22).$$

Since K' should be small compared to \bar{K} , $\ln\left(1 + \frac{K'}{\bar{K}}\right)$ can be approximated by

$$\ln\left(1 + \frac{K'}{\bar{K}}\right) \cong \frac{K'}{\bar{K}} \quad (2.3.23).$$

Mean soil moisture can now be approximated by

$$\bar{\theta} + \theta' \cong \theta_o + \frac{c}{\alpha} \left[\ln\left(\frac{\bar{K}}{K_o}\right) + \frac{K'}{\bar{K}} \right] \quad (2.3.24).$$

Equation 2.3.24 can be used to evaluate both the expected mean and variance of θ . The mean of soil moisture can be derived by taking the mathematical expectation in space of each side of Equation 2.3.24. For the preliminary analysis in which the soil parameters θ_o , c , α , and K_o , and \bar{K} are constants, their expectation is simply the average values of these parameters. The expectation of the perturbation terms, θ' and K' , is zero. The expression for mean soil moisture becomes

$$E_x[\theta] \cong E_x \left[\theta_o + \frac{c}{\alpha} \left(\ln\left(\frac{\bar{K}}{K_o}\right) + \frac{K'}{\bar{K}} \right) \right] = \theta_o + \frac{c}{\alpha} \ln\left(\frac{\bar{K}}{K_o}\right) \quad (2.3.25).$$

Subtracting Equation 2.3.25 from 2.3.24 results in

$$\theta' = \frac{c}{\alpha} \frac{K'}{\bar{K}} \quad (2.3.26).$$

Using the spectral representations K' and θ' , Equation 2.3.26 may be written as

$$\int_{-\infty}^{\infty} e^{ikx} \left[dZ_{\theta}(k) - \left(\frac{c}{\alpha K} \right) dZ_K(k) \right] = 0 \quad (2.3.27).$$

This may be used to directly relate both the spectral density and the variance of soil moisture to elevation:

$$S_{\theta}(k) = \left(\frac{c}{\alpha K} \right)^2 S_K(k) \quad (2.3.28a)$$

$$\sigma_{\theta}^2 = \left(\frac{c}{\alpha K} \right)^2 \sigma_K^2 \quad (2.3.28b).$$

This relates the parameters of the distribution of soil moisture to the parameters of the distribution of unsaturated hydraulic conductivity. Since the statistics of hydraulic conductivity are already known from the statistics of elevation, elevation and soil moisture are now related through hydraulic conductivity. For the special case in which the large-scale topographic slope, $\frac{\partial z}{\partial x}$, is zero, combining 2.3.15 and 2.3.27 gives the spectral relationship between soil moisture and elevation:

$$S_{\theta}(k) dk = c^2 \frac{k^4}{\left(k^2 + \frac{\alpha \beta}{D} \right)^2} S_z(k) dk \quad (2.3.29a)$$

$$\sigma_{\theta}^2 = c^2 \omega_0^2 \sigma_z^2 \quad (2.3.29b).$$

Thus, if the spectrum of elevation is known, the spectrum of soil moisture can be inferred using 2.3.28. In the example in the next section, techniques for evaluating the distribution of soil moisture in one spatial dimension are presented.

2.4 One-Dimensional Example of the Distribution of Soil Moisture

Equation 2.3.29a expresses the spectrum of soil moisture in terms of the spectrum of elevation. This relationship can be exploited to infer the spectrum and the autocovariance function of soil moisture if either one of the corresponding functions of elevation is known. In order to characterize the distribution of soil moisture, the distribution of elevation must first be studied. The large-scale distribution of soil moisture can be described through its spectrum in the frequency domain, or by the autocovariance function in the spatial domain. With the large amount of available information on elevation, it is a straightforward procedure to estimate the autocovariance function of elevation for nearly any region of interest.

The observations of soil moisture that will to be described in Chapter 4 are from Central Massachusetts. For the purpose of illustration and to maintain consistency with the observations, an elevation field will be chosen from the same region. Elevation data was obtained from the USGS World Wide Web server (<http://edcwww.cr.usgs.gov/nsdi/gendem.htm>). The particular data set used covers the "Albany-East" region, a 1° by 1° region with equal arc-second ($2''$) resolution of elevation. This is equivalent to 92.5 m by 62.5 m resolution in distance. This large database provides freedom in selecting an area for analysis: in general, it is desirable to work with stationary elevation fields. Stationarity requires that the statistical properties (mean and variance) do not vary in space. The Kendall Ranking Test determines whether or not a particular set of data exhibits a trend: this can determine the stationarity of the data. To select a stationary elevation field, a code was written to implement the Kendall Ranking Test over multiple 30 km by 30 km subgrids of the elevation dataset. Trends were tested for in the mean and the variance in both the latitudinal (East-West) and longitudinal (North-South) directions. Based on the results of this test, the region with boundary enclosed from $42^\circ 19'$ to $42^\circ 51'$ W and $72^\circ 38'$ to $72^\circ 56'$ N was selected as the most stationarity region tested: the normalized Kendall-

Ranking Statistics (which will have a N(0,1) distribution) for the directional means and variances are presented in Table 2.4.1.

With a stationary elevation field, it is straightforward to estimate the sample autocovariance function for the region. The covariance function is a quantitative measure of the persistence of correlation of elevation over distance. For a stationary field, it can be calculated from the formula

$$\Gamma_z(i) = \sum_{i=0}^{nx} [z(x) - \bar{z}][z(x+i) - \bar{z}] \quad (2.4.1)$$

for a one-dimensional field in space (Jenkins and Watts, 1979). Once the covariance has been estimated numerically, curve-fitting techniques can be used to estimate the approximate analytical form for the covariance. The spectrum of elevation, $S_z(k)$, can be obtained from the covariance function, $R_z(x)$, chosen to describe the elevation field. From observations of a transect in Central New England, the covariance function of elevation can be estimated as

$$R_z(x) = \sigma^2 e^{-\lambda_1 |x|} \cos(A_x x) \quad (2.4.2)$$

where σ_z , λ , and A_x are estimated from elevation data using curve-fitting techniques. which has an exponentially-declining correlation with a sinusoidal modulation in space. The parameters λ_1 , σ^2 , and A_x are listed in Table 2.4.2. Elevation contours for the region are shown in Figure 2.4.1; the covariance function in the latitudinal direction is shown in Figure 2.4.2. The spectrum can then be evaluated from the Fourier Transform of the autocovariance function:

$$S_z(k) = \frac{1}{2\pi} \int_{-\infty}^{\infty} e^{-ikx} R_z(k) dx \quad (2.4.3).$$

Table 2.4.1: Normalized Kendall Ranking Statistic (τ) of the Mean (\bar{z}) and Variance (σ_z) of Elevation in the Latitudinal (x) and Longitudinal (y) Directions.

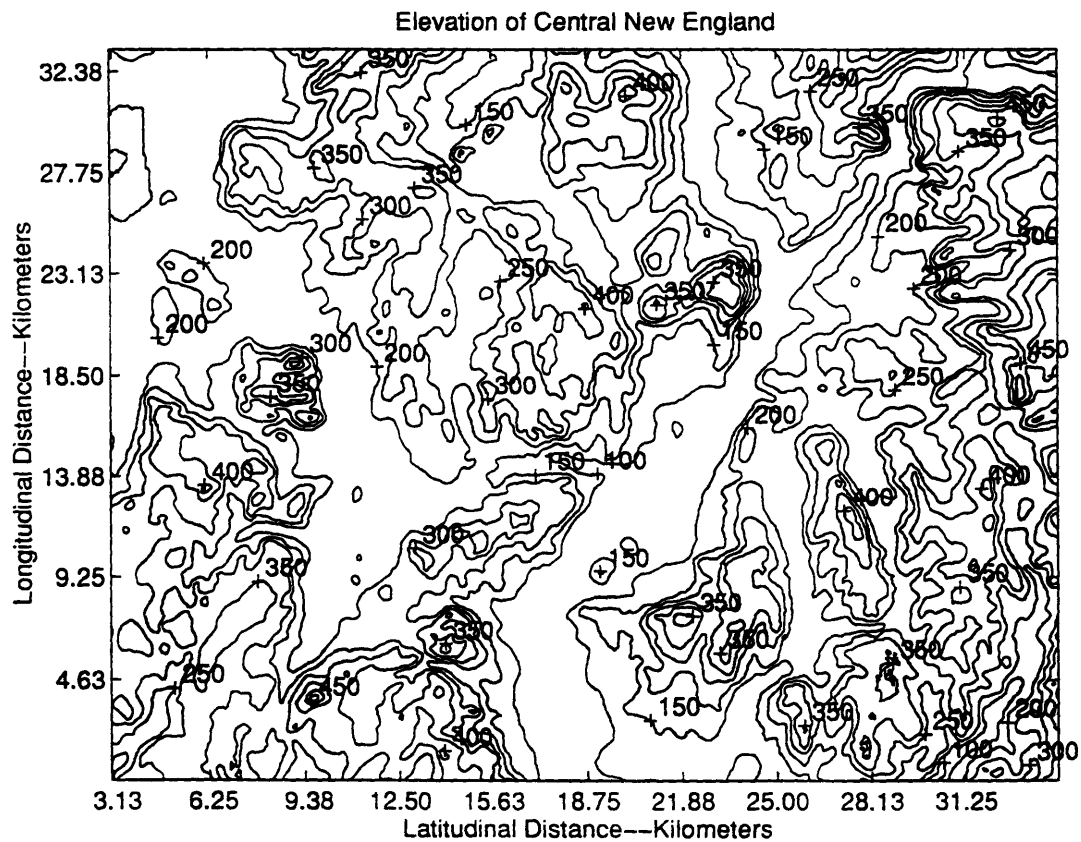
Statistic	Normalized τ †
\bar{z}_x	0.51
σ_{z_x}	-1.02
\bar{z}_y	1.03
σ_{z_y}	1.02

† The Normalized Kendall Ranking Statistics indicates the presence of a trend in the data at the 95% confidence level when it exceeds 1.996; all of these values of τ test negative for a trend in the data.

Table 2.4.2: Parameters of the One-Dimensional Autocovariance Functions of Observed Elevation and Simulated Soil Moisture.

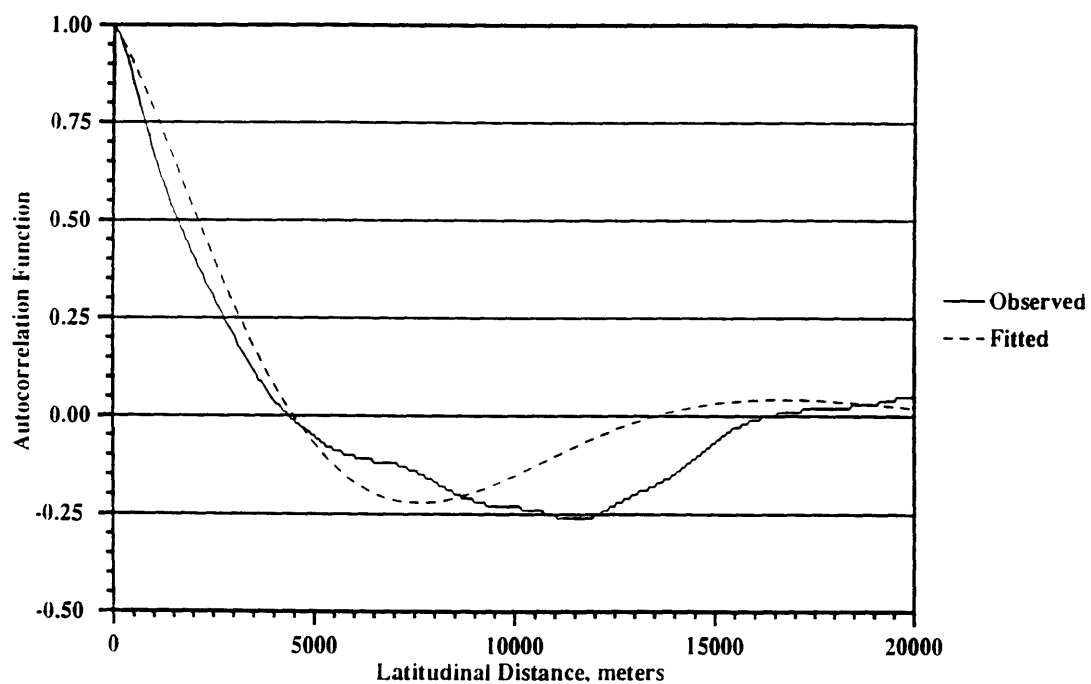
Parameter	Value	Units
σ_z^2	$(87)^2$	m^2
λ_x	$1/(5500)$	m^{-1}
A_x	$1/(5000)$	m^{-1}
σ_θ^2	$(0.0284)^2$	
λ_θ	$1/(60)$	m^{-1}

Figure 2.4.1: Elevation Contours in Central New England



Elevation is in meters; contour interval is 50 meters.

Figure 2.4.2: One-dimensional Observed Autocorrelation Function for New England Elevation



By substituting the identity

$$\cos(ax) = \frac{e^{iax} + e^{-iax}}{2} \quad (2.4.4)$$

into 2.4.3 and combining the exponentials, Equation 2.4.2 can be written

$$S_z(k) = \frac{1}{2\pi} \left\{ \int_{-\infty}^0 \sigma_z^2 \left[\frac{e^{[-i(k+a)+\lambda]x} + e^{[-i(k-a)+\lambda]x}}{2} \right] dx + \int_0^{\infty} e^{-ikx} \sigma_z^2 \left[\frac{e^{[-i(k+a)-\lambda]x} + e^{[-i(k-a)-\lambda]x}}{2} \right] dx \right\} \quad (2.4.5).$$

Equation 2.4.5 can be simplified analytically to

$$S_z(k, j) = \frac{\sigma_z^2}{2\pi} \left(\frac{\lambda}{\lambda^2 + (k-a)^2} + \frac{\lambda}{\lambda^2 + (k+a)^2} \right) \quad (2.4.6)$$

This form can be used in Equation 2.3.19 to evaluate ω_0^2 .

For this particular spectral density of elevation, there is no closed form expression for ω_0^2 , so Equation 2.3.19 can be integrated numerically using a simple iterative code. Using the nominal values of soil and climate conditions listed in Table 2.4.3, Equations 2.3.5a and 2.3.25 to evaluate the mean soil moisture, and Equations 2.3.19 and 2.3.29b to evaluate the variance of soil moisture, the value of σ_θ (standard deviation of soil moisture) is evaluated at 0.0284, or about 11% of the average value of soil moisture of 0.27.

Since the proposed spectrum of soil moisture for this region does not have an integratable form, the covariance function of soil moisture cannot be derived analytically. However, a Monte Carlo simulation of soil moisture as a random field can be carried out to approximate the covariance of soil moisture. In the simulation,

unsaturated hydraulic conductivity is simulated for 500 points in space using the spectrum given in Equation 2.3.15. This realization of unsaturated hydraulic conductivity can then be converted to soil moisture using Equation 2.1.5. Properly done, this procedure will result in a realization of soil moisture with the same spectral properties as the theoretical soil moisture field. It is important to make certain that the simulated spectrum of elevation has the same spectral properties as actual elevation; the observed and estimated covariance functions are shown in Figure 2.4.1. It is also crucial that the resulting soil moisture field have the same variance as the predictions from Equation 2.3.27 above. For the Monte Carlo simulation, the value of σ_θ is 0.0286, within 1% of the value from the numerical integration, for 500 samples. The covariance structure of soil moisture can be evaluated from the simulation as well. The functional form of the simulated covariance of soil moisture is approximated by:

$$R_\theta(x) = \sigma_\theta^2 e^{-\lambda_\theta |x|} \cos(A_\theta x) \quad (2.4.7).$$

The resulting correlation function of soil moisture is shown in Figure 2.4.3. The comparison of the spectral properties of soil moisture and elevation are shown in Table 2.4.2. Soil moisture in this case has a much shorter correlation scale than elevation: about 60 meters for soil moisture compared with 5 kilometers for elevation.

The distributions of elevation and of soil moisture from the simulation are shown in Figures 2.4.4 and 2.4.5. Whereas elevation has a flatter, more uniform distribution, soil moisture has a more centered, nearly Gaussian distribution. This result along with the results of the covariance analysis suggest that in a one-dimensional system, large-scale variability of a relatively unstructured distribution of topography will force small-scale variability in a more structured soil moisture distribution. Thus, topography is important as a soil moisture forcing because large-scale variability in topography is capable of introducing variability in soil moisture at much smaller scale.

Table 2.4.3: Values of Soil and Climate Parameters used in Monte Carlo Simulations

Symbol	Variable	Nominal Value
D:	Depth of Root Zone:	2 m
K_0 :	Saturated Conductivity:	12.2 cm/hr
α :	Dispersion Coefficient:	0.02 (cm) ⁻¹
c:	pore tension parameter:	0.001 (cm) ⁻¹
R:	Yearly Rainfall:	1 m/yr
β :	vertical divergence:	1
θ_0 :	porosity	0.4

Figure 2.4.3: Autocorrelation Function of Simulated Soil Moisture

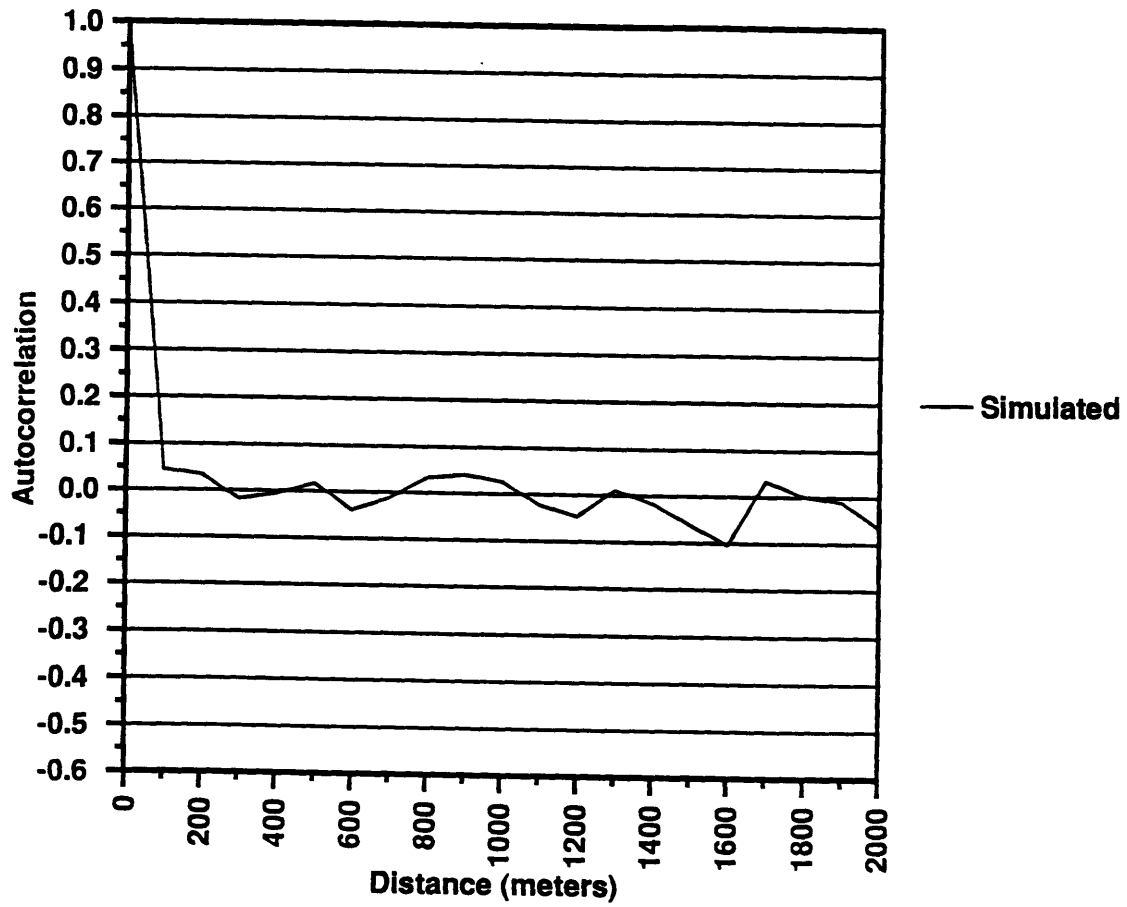


Figure 2.4.4: Distribution of Elevation in Central New England

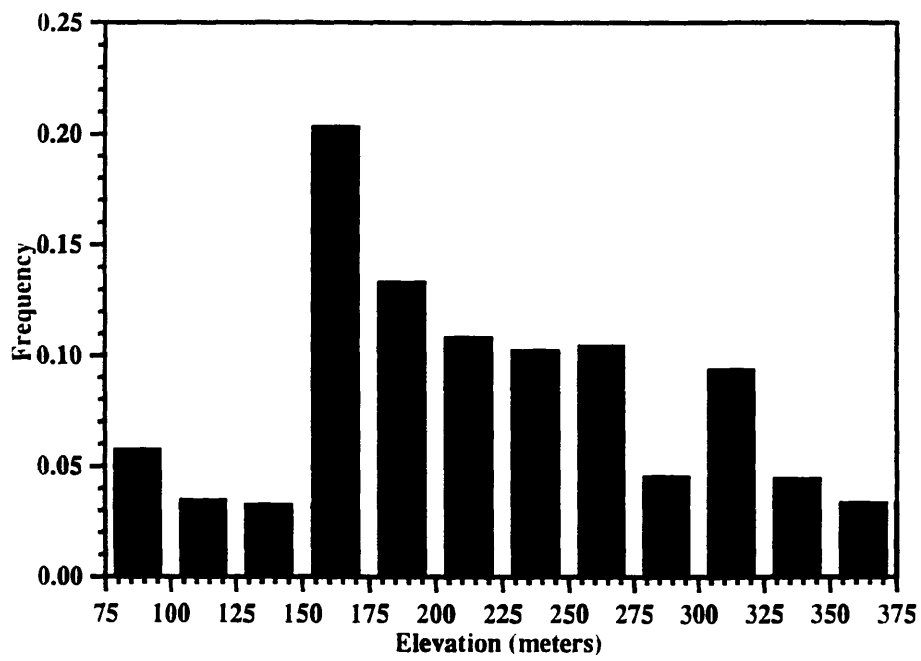
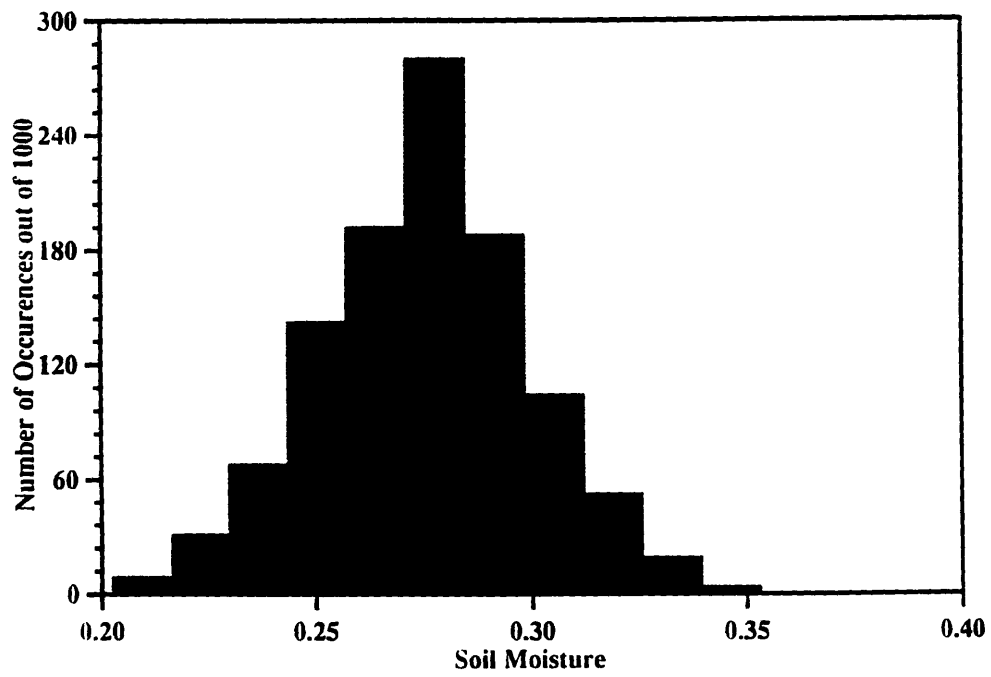


Figure 2.4.5: Distribution of Soil Moisture from One-Dimensional Simulation.



2.5 Two-Dimensional Stochastic Analysis of the Steady-State Relationship between Topography and Soil Moisture

In this section theory that describes the two-dimensional influence of topography on soil moisture distribution is developed. This begins with the combined flow and mass balance equation describing soil moisture. Again, long-term properties of soil moisture are of interest; since this deals with the long-term expectation of soil moisture in *time*, $E_t[\theta]$, the derivative $\frac{\partial E_t[\theta]}{\partial t}$ is again zero. This allows the simplification of dealing with only two spatial dimensions, x and y . Dropping the $E_t[\]$ notation and substituting the perturbation expressions for K and z , the two-dimensional flux equation is similar to the one-dimensional case, analogous to Equation 2.3.4

$$D \frac{\partial}{\partial x} \left(-\frac{1}{\alpha} \frac{\partial(\bar{K} + K')}{\partial x} - (\bar{K} + K') \frac{\partial(\bar{z} + z')}{\partial x} \right) + D \frac{\partial}{\partial y} \left(-\frac{1}{\alpha} \frac{\partial(\bar{K} + K')}{\partial y} - (\bar{K} + K') \frac{\partial(\bar{z} + z')}{\partial y} \right) + \beta(\bar{K} + K') - R = 0 \quad (2.5.1).$$

Taking the expectation of the entire equation in *space*,

$$D \frac{\partial}{\partial x} \left(-\frac{1}{\alpha} \frac{\partial \bar{K}}{\partial x} - \bar{K} \frac{\partial \bar{z}}{\partial x} \right) + D \frac{\partial}{\partial y} \left(-\frac{1}{\alpha} \frac{\partial \bar{K}}{\partial y} - \bar{K} \frac{\partial \bar{z}}{\partial y} \right) + \beta \bar{K} - R = 0 \quad (2.5.2).$$

This is the deterministic form of the two-dimensional problem. As with the one-dimensional case, if the spatial averages \bar{K} , $\frac{\partial \bar{z}}{\partial x}$, and $\frac{\partial \bar{z}}{\partial y}$ do not change in space, their derivatives in the horizontal direction are zero; this will again simplify the deterministic solution to the same result as the one-dimensional case

$$\bar{K} = \frac{R}{\beta} \quad (2.5.3)$$

which again specifies the average hydraulic conductivity as a function of precipitation. Subtracting Equation 2.5.2 from Equation 2.5.1, the differential equation describing the random fluctuation terms is

$$D \frac{\partial}{\partial x} \left(-\frac{1}{\alpha} \frac{\partial K'}{\partial x} - \bar{K} \frac{\partial z'}{\partial x} + K' \frac{\partial \bar{z}}{\partial x} \right) + D \frac{\partial}{\partial y} \left(-\frac{1}{\alpha} \frac{\partial K'}{\partial y} - \bar{K} \frac{\partial z'}{\partial y} + K' \frac{\partial \bar{z}}{\partial y} \right) + \beta K' = 0 \quad (2.5.4)$$

where cross products of perturbation terms have been assumed ignored. As in the one-dimensional case, this is justifiable when the cross-product terms are of small-order compared with the other terms. The spectral representations of K' and z' , which are now two-dimensional random fields, are

$$z' = \int_{-\infty}^{\infty} e^{i(jx+ky)} dZ_z(j,k) \quad \text{and} \quad K' = \int_{-\infty}^{\infty} e^{i(jx+ky)} dZ_K(j,k) \quad (2.5.5a, b).$$

These expressions may be substituted into Equation 2.5.4. Carrying out the differentiation with respect to x and y inside the integral of j and k , this becomes

$$\begin{aligned} & D \int_{-\infty}^{\infty} \left(-\frac{1}{\alpha} (-j^2) e^{i(jx+ky)} dZ_K(j,k) - \bar{K} (-j^2) e^{i(jx+ky)} dZ_z(j,k) + (ij) e^{i(jx+ky)} dZ_K(j,k) \frac{\partial \bar{z}}{\partial x} \right) + \\ & D \int_{-\infty}^{\infty} \left(-\frac{1}{\alpha} (-k^2) e^{i(jx+ky)} dZ_K(j,k) - \bar{K} (-k^2) e^{i(jx+ky)} dZ_z(j,k) + (ik) e^{i(jx+ky)} dZ_K(j,k) \frac{\partial \bar{z}}{\partial y} \right) + \\ & \beta \int_{-\infty}^{\infty} e^{i(jx+ky)} dZ_K(j,k) = 0 \end{aligned} \quad (2.5.6).$$

Grouping together similar spectral amplitudes, this becomes

$$D \int_{-\infty}^{\infty} \left(\frac{j^2 + k^2}{\alpha} + ik \frac{\partial \bar{z}}{\partial x} + ij \frac{\partial \bar{z}}{\partial y} + \frac{\beta}{D} \right) e^{i(jx+ky)} dZ_K(j,k) + \bar{K}(j^2 + k^2) e^{i(jx+ky)} dZ_z(j,k) = 0 \quad (2.5.7).$$

As in the one-dimensional case with Equation 2.3.12, Equation 2.5.7 relates the complex amplitudes of K to those of z. Because of the uniqueness of the spectral amplitudes, the terms inside the parentheses will vanish at all points leaving

$$D \left(\frac{j^2 + k^2}{\alpha} + \frac{\beta}{D} - ik \frac{\partial \bar{z}}{\partial x} - ij \frac{\partial \bar{z}}{\partial y} \right) e^{i(jx+ky)} dZ_K(j,k) = -D \bar{K}(j^2 + k^2) e^{i(jx+ky)} dZ_z(j,k) \quad (2.5.8a).$$

The complex conjugates of $dZ_K(j,k)$ and $dZ_z(j,k)$ are then related by

$$D \left(\frac{j^2 + k^2}{\alpha} + \frac{\beta}{D} + ik \frac{\partial \bar{z}}{\partial x} + ij \frac{\partial \bar{z}}{\partial y} \right) e^{i(jx+ky)} dZ_K(j,k) = -D \bar{K}(j^2 + k^2) e^{i(jx+ky)} dZ_z(j,k) \quad (2.5.8b).$$

The definition of the spectrum in two dimensions is analogous to that for one dimension:

$$E[dZ_z(j,k)dZ_z^*(j,k)] = S_z(j,k)djdk \quad (2.5.9a)$$

$$E[dZ_K(j,k)dZ_K^*(j,k)] = S_K(j,k)djdk \quad (2.5.9b).$$

Multiplying the right- and left-hand sides of Equations 2.5.8a and 2.5.8b, and using the identities in Equations 2.5.9a and 2.5.9b, this yields

$$S_K(j,k)djdk = \alpha^2 \bar{K}^2 \left(\frac{(j^2 + k^2)^2}{(j^2 + k^2 + \alpha \frac{\beta}{D})^2 + (j \frac{\partial \bar{z}}{\partial x} + k \frac{\partial \bar{z}}{\partial y})^2} \right) S_z(j,k)djdk \quad (2.5.10).$$

This expression relates the spectral density function of K to the spectral density function of z in two dimensions. As in the one-dimensional case, the variance of a two-dimensional random variable is the total integral of the spectral density function. Using this definition of variance in terms of the spectral density function, Equation 2.5.10 can be used to relate the variance of K to the variance of z

$$\sigma_K^2 = \int_{-\infty}^{\infty} \int_{-\infty}^{\infty} S_K(j,k) djdk = \int_{-\infty}^{\infty} \int_{-\infty}^{\infty} \alpha^2 \bar{K}^2 \left(\frac{(j^2 + k^2)}{(j^2 + k^2 + \alpha \frac{\beta}{D})} \right)^2 S_z(j,k) djdk \quad (2.5.11)$$

or as in equation 2.3.18

$$\sigma_K^2 = \gamma_0^2 \alpha^2 \bar{K}^2 \sigma_z^2 \quad (2.5.12)$$

where

$$\gamma_0^2 = \int_{-\infty}^{\infty} \int_{-\infty}^{\infty} \alpha^2 \bar{K}^2 \left(\frac{(j^2 + k^2)^2}{(j^2 + k^2 + \alpha \frac{\beta}{D})^2 + (j \frac{\partial z}{\partial x} + k \frac{\partial z}{\partial y})^2} \right) \frac{S_z(j,k)}{\sigma_z^2} djdk \quad (2.5.13)$$

which can be evaluated either analytically or numerically, depending on the form of the spectral density function. To get the variance of soil moisture, variance of unsaturated hydraulic conductivity must be used. The relation between the variance of soil moisture and the variance of unsaturated hydraulic conductivity derived in Section 3 made no general use of spatial dimension: thus, the same relation will be true for two dimensions as was true for one dimension. Variance of soil moisture in two

dimensions is thus related to variance of elevation in two dimensions by the same relation given in Equation 2.3.29b:

$$\sigma_{\theta}^2 = c^2 \omega_0^2 \sigma_z^2 \quad (2.5.14)$$

while the spectrum of soil moisture is related to the spectrum of elevation by

$$S_{\theta}(j,k)dj dk = c^2 \left(\frac{(j^2 + k^2)^2}{(j^2 + k^2 + \alpha \frac{\beta}{D})^2 + (j \frac{\partial \bar{z}}{\partial x} + k \frac{\partial \bar{z}}{\partial y})^2} \right) S_z(j,k)dj dk \quad (2.5.15).$$

For the special case in which the spatial average of topographic slope in both directions is zero, this reduces to:

$$S_{\theta}(j,k)dj dk = c^2 \left(\frac{(j^2 + k^2)^2}{(j^2 + k^2 + \alpha \frac{\beta}{D})^2} \right) S_z(j,k)dj dk \quad (2.5.16).$$

Now the statistics of soil moisture in two dimensions have been related to the statistics of elevation in two dimensions. In the next section, an example of the two-dimensional analysis of soil moisture distribution is presented.

2.6 Two-Dimensional Example of the Distribution of Soil Moisture

As in Section 2.4, prediction of the distribution of soil moisture begins with an analysis of elevation. The covariance function of elevation is of specific interest: a two-dimensional extension of the covariance function of z used in Section 4 results in

$$R_z(x,y) = \sigma_z^2 \exp(-\lambda_x|x| - \lambda_y|y|) \cos(ax) \cos(by) \quad (2.6.1)$$

This form merely allows the exponential and sinusoidal properties of the one-dimensional covariance function to extend into a second direction. For isotropic distributions, It is reasonable to expect that $\lambda_x = \lambda_y$ and $a = b$, although this condition is not necessary. The spectral density function of z can then be obtained by taking the inverse Fourier Transform:

$$S_z(j, k) = \frac{1}{4\pi} \int_{-\infty}^{\infty} \int_{-\infty}^{\infty} e^{-i(jx+ky)} R_z(x, y) dx dy \quad (2.6.2)$$

which can be evaluated in closed form in the same manner as for the one-dimensional case. This results in

$$S_{zz}(k, j) = \frac{\sigma^2}{4\pi^2} \left(\frac{\lambda_x}{\lambda_x^2 + (k-a)^2} + \frac{\lambda_x}{\lambda_x^2 + (k+a)^2} \right) \left(\frac{\lambda_y}{\lambda_y^2 + (j-b)^2} + \frac{\lambda_y}{\lambda_y^2 + (j+b)^2} \right) \quad (2.6.3).$$

This can be substituted into Equation 2.5.13 to evaluate ω_0^2 . It can also be combined with Equation 2.5.14 to evaluate the spectrum and the variance of soil moisture. The spectrum of soil moisture in two dimensions is then given by

$$S_{\theta\theta}(k, j) = \frac{c^2 \sigma_z^2}{4\pi^2} \frac{k^4 + j^4}{\left(k^2 + j^2 + \frac{\alpha\beta}{D} \right)^2} \left(\frac{\lambda_x}{\lambda_x^2 + (k-a)^2} + \frac{\lambda_x}{\lambda_x^2 + (k+a)^2} \right) \left(\frac{\lambda_y}{\lambda_y^2 + (j-b)^2} + \frac{\lambda_y}{\lambda_y^2 + (j+b)^2} \right) \quad (2.6.4).$$

For this example the same region in New England as in Section 2.4 is used. The values of λ_x , λ_y , a , and b given by the best-fit curves to observed elevation covariance are listed in Table 2.6.1. Integrating Equation 2.5.14 numerically using these values for elevation covariance and the same values of soil and climate as listed in Table 2.4.3,

the standard deviation of soil moisture is evaluated as 0.101, or about 37% of the value of the mean. This value of variance is approximately 3.5 times as large as in the one-dimensional case.

As with the one-dimensional case, there is no integratable form of the spectrum of unsaturated hydraulic conductivity with which evaluate the covariance function of unsaturated hydraulic conductivity. Again, we turn to Monte Carlo techniques to infer information about the covariance structure of unsaturated hydraulic conductivity and soil moisture. A Monte Carlo simulation of 90,000 points in space is carried out, creating a realization of unsaturated hydraulic conductivity in space. From this field of unsaturated hydraulic conductivity, the corresponding field of soil moisture can be determined at every point using Equation 2.1.5. The two-dimensional covariance function of soil moisture can then be estimated from the simulation. The simulated covariance of elevation is shown in Figure 2.6.2, which is comparable to the observed covariance of elevation shown in Figure 2.6.1. In the Monte Carlo simulation, the standard deviation is evaluated at 0.0982, very close to that evaluated numerically.

The two-dimensional covariance structure of soil moisture can be approximated by

$$R_{\theta}(x) = \sigma_{\theta}^2 e^{-\lambda_1|x| - \lambda_2|y|} \quad (2.6.5),$$

where the parameters λ_1 and λ_2 are given in Table 2.6.1. The simulated autocorrelation functions are shown in Figure 2.6.3 for the x-direction (latitude, $y=0$) and in Figure 2.6.4 for the y-direction (longitude, $x=0$); the two-dimensional autocorrelation function is shown in Figure 2.6.5.

The distribution of soil moisture resulting from the Monte Carlo simulation is shown in Figure 2.6.6. Compared with the same distribution of elevation as in Figure 2.4.4. Although much more centered than the elevation distribution, the two-

Table 2.6.1: Parameters of the Two-Dimensional Autocovariance Functions of Observed Elevation and Simulated Soil Moisture

Parameter	Value
σ_z^2	(87.3) m ²
λ_{x1}	(1/5500) m ⁻¹
λ_{x2}	(1/5500) m ⁻¹
a	(1/5000) m ⁻¹
b	(0)
σ_θ^2	(0.0248) ²
λ_{x1}	(1/1250) m ⁻¹
λ_{x1}	(1/2300)m ⁻¹
A_θ	(1/350) m ⁻¹
B_θ	(0)

Figure 2.6.1: Observed Two-Dimensional Autocorrelation Function for Selected Region in New England.

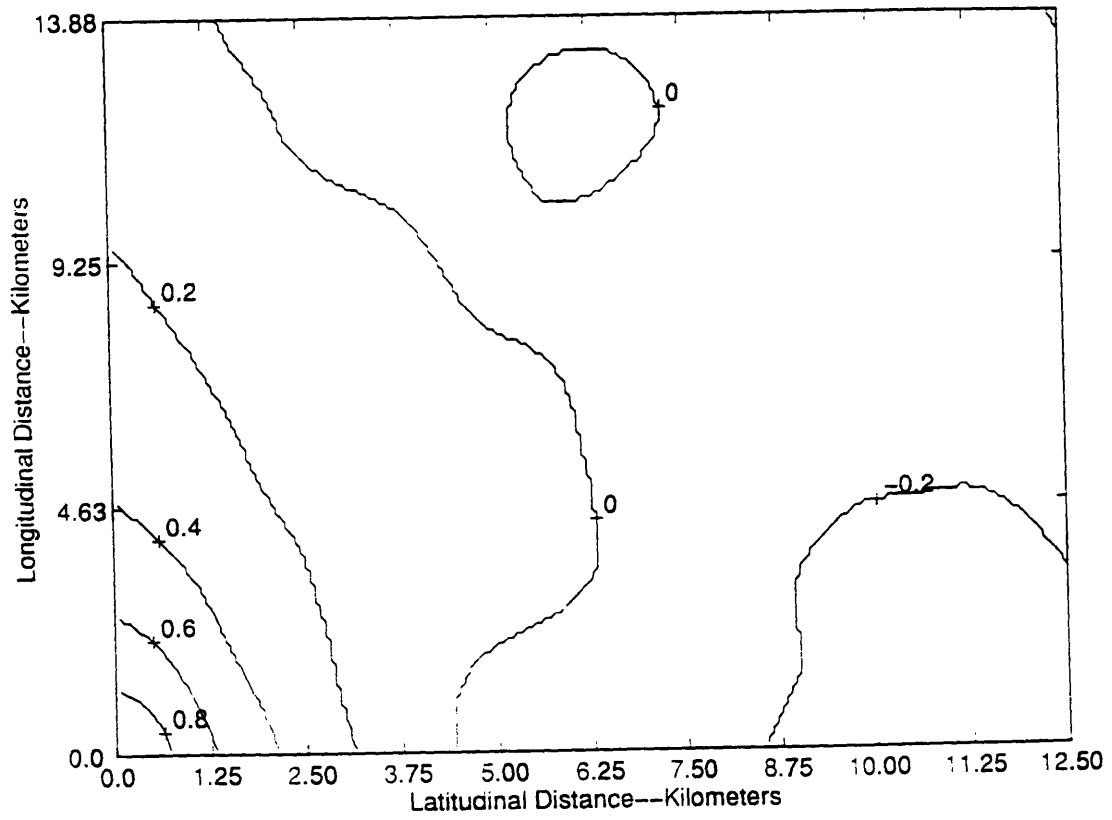


Figure 2.6.2: Simulated Two-Dimensional Autocorrelation Function for Selected Region in New England.

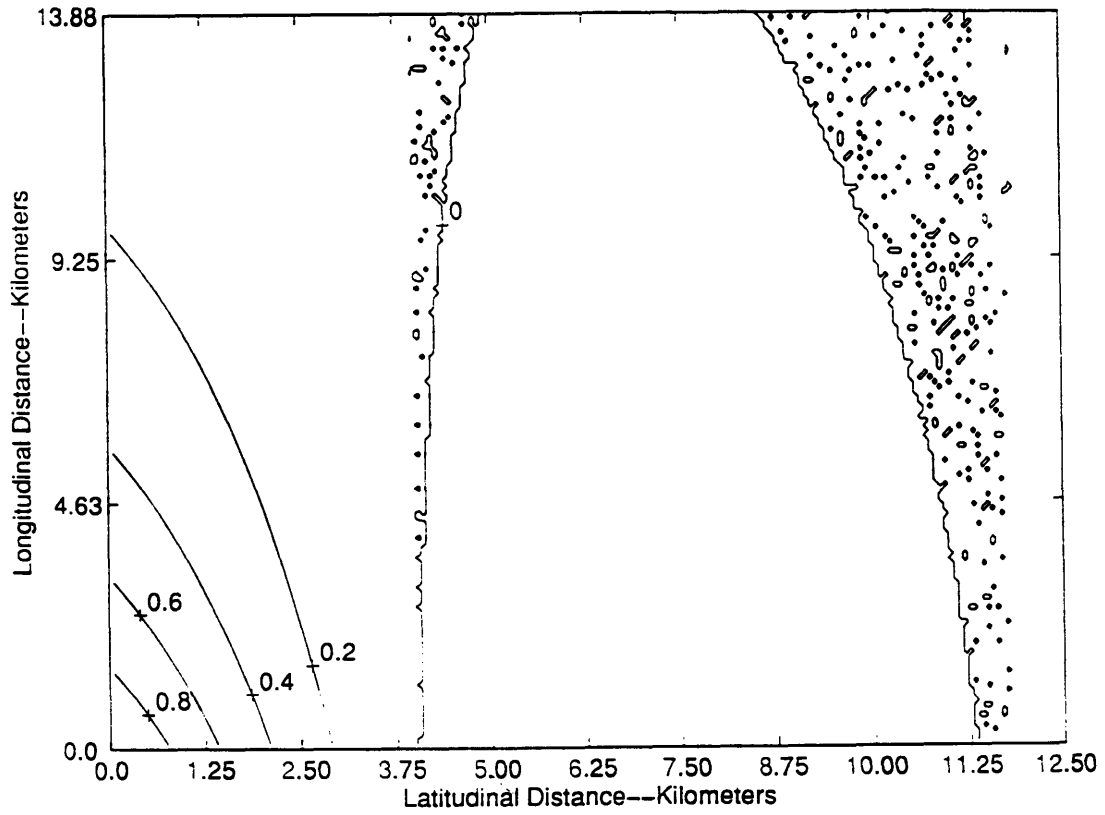


Figure 2.6.3: Latitudinal Autocorrelation of Two-Dimensional Simulation of Soil Moisture

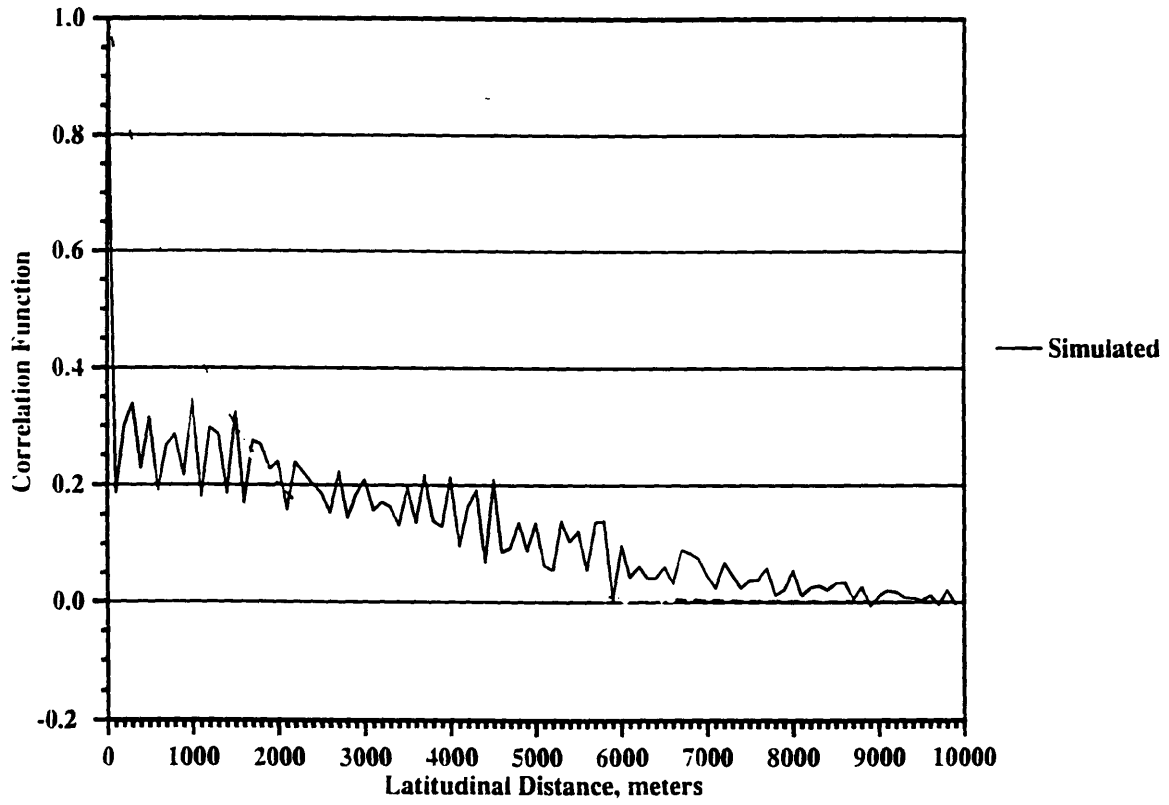


Figure 2.6.4: Longitudinal Autocorrelation of Two-Dimensional Simulation of Soil Moisture

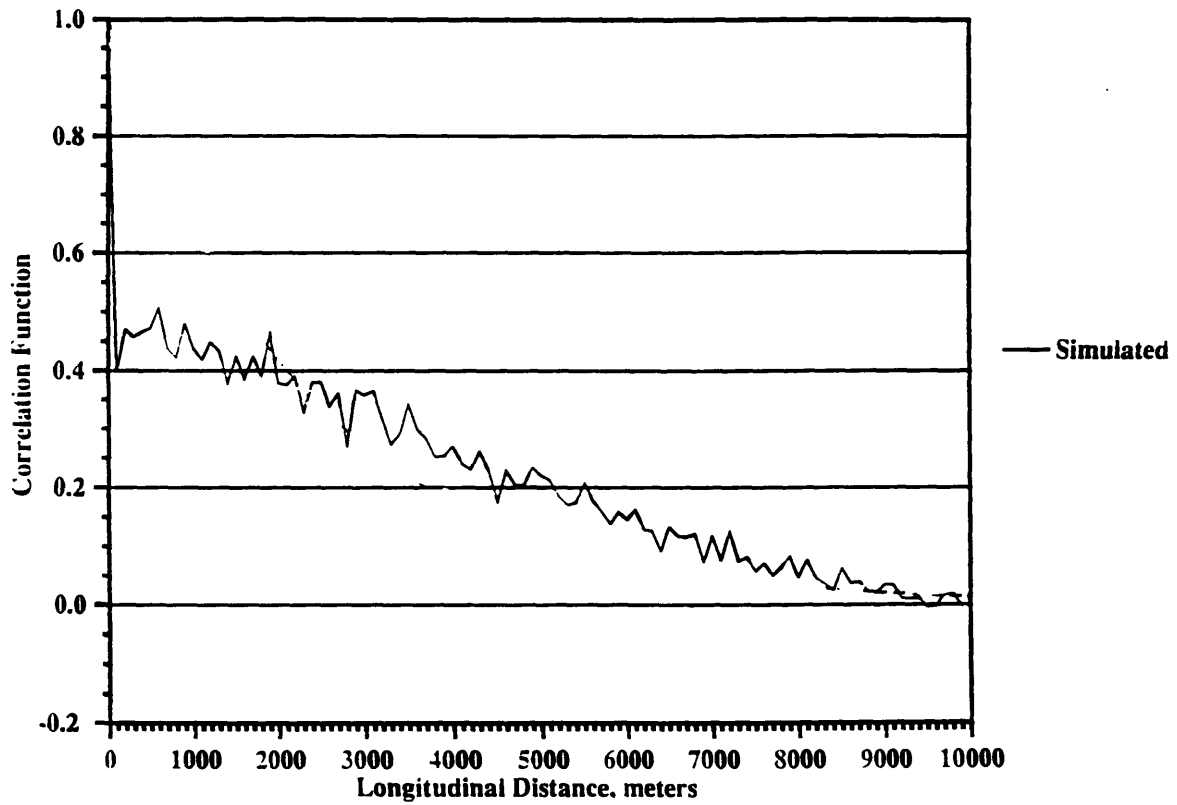


Figure 2.6.5: Autocorrelation Function of Two-Dimensional Simulated Soil Moisture Field in Two Dimensions.

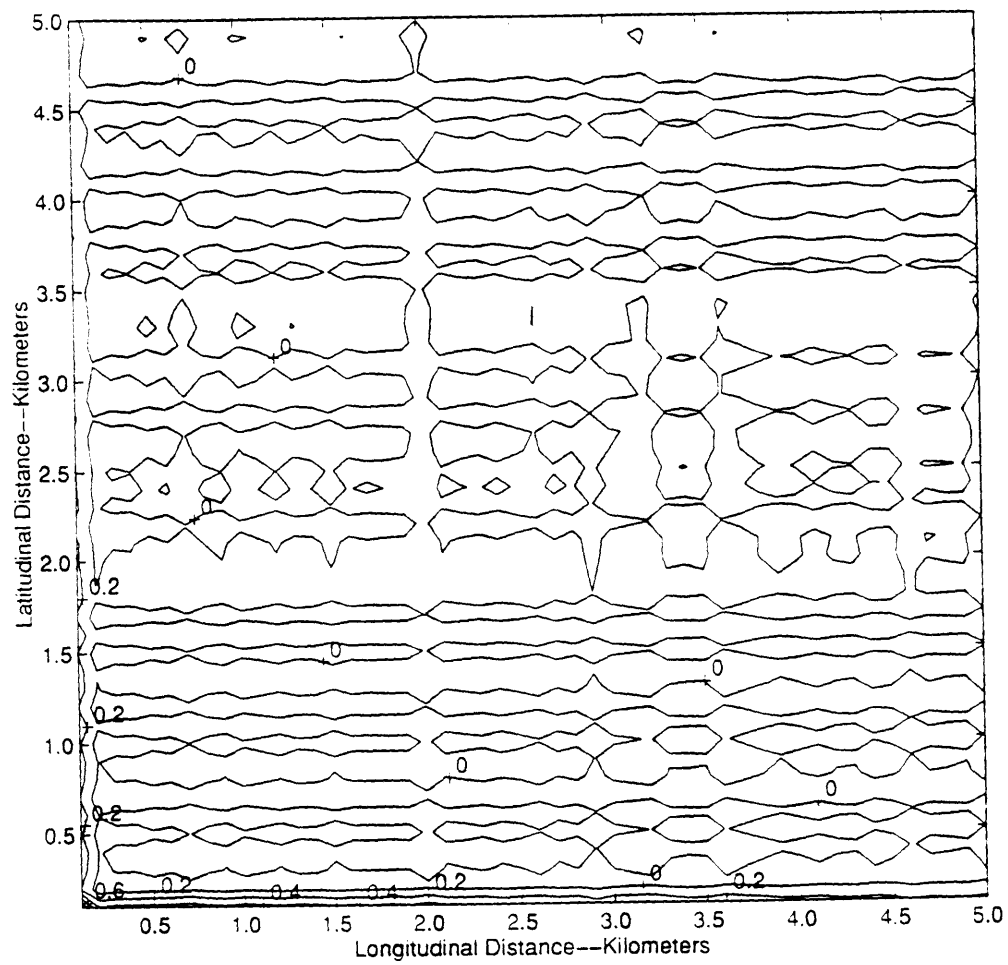
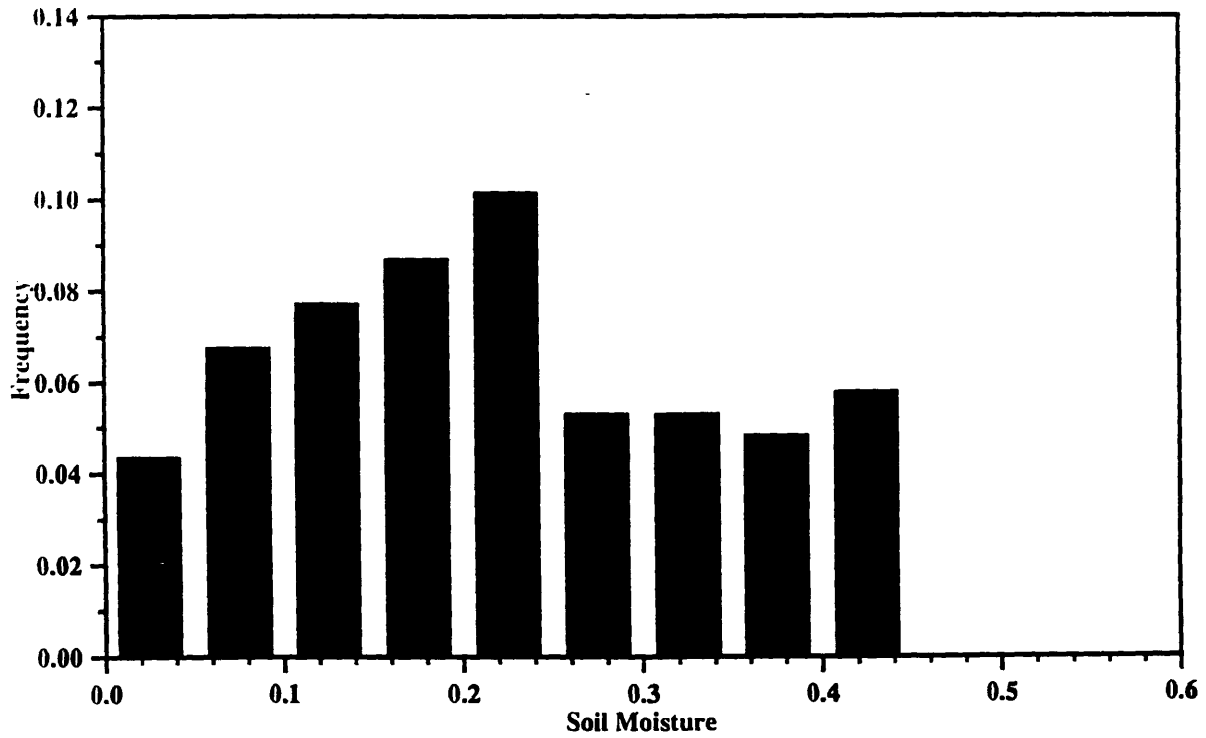


Figure 2.6.6: Distribution of Two-Dimensional Simulation of Soil Moisture.



dimensional distribution of soil moisture is more spread out than the one-dimensional case. Also, rather than a Normal distribution, it appears that the soil moisture distribution is more nearly Log-normal. Still, the effect of topography is clear: a nearly uniform distribution of elevation is capable of forcing a more structured distribution in soil moisture. In two dimensions, the theory predicts that topography will play an important role in shaping the distribution of soil moisture, in determining its variance, its correlation in space, and the shape of its distribution.

2.7 Comparison of One- and Two-dimensional results

It is important to study the differences that arise between the one- and the two-dimensional considerations of soil moisture flow. The statistics of mean and variance will be examined. The mean values for the two variables under consideration will determine if the overall behavior of the two systems are the same. The variance of the system will indicate whether the number of dimensions increases or decreases the variability of soil moisture to vary over the domain of the system. Information about the variance can in turn give insight to how the two-dimensional considerations allow for differences in the flow of soil moisture water.

The comparison of the statistics of soil moisture for the one- and the two-dimensional flow is straightforward. In the numerical evaluation of the one- and two-dimensions considerations, the means of K and θ are not affected by differences in the number of dimensions considered. Expressions for the mean hydraulic conductivity for the one-dimensional (Equation 2.3.5a) and the two-dimensional (Equation 2.5.3) problems reveal that the analytical expressions for the mean of unsaturated hydraulic conductivity are the same for the two cases. Since the expression relating the mean soil moisture to mean unsaturated hydraulic conductivity developed in Equation 2.3.39 has no dependence on dimension, it is expected that

mean soil moisture should also be the same for the one-and two-dimensional cases. Both of these results are reflected in the numerical experiments and suggest that the fundamental concepts used to formulate the two problems are similar.

Variance (and therefore the coefficient of variation), on the other hand, is substantially different for the two cases. The expression for the variance of K , Equation 2.3.20, shows that the variance of K (and therefore for θ) will be dependent on the functional form used to characterize the covariance function of elevation. This choice is somewhat arbitrary, but should be chosen by some objective criterion. For the purposes of illustration, a particular covariance function of elevation will be used to contrast the two cases. For the simple sinusoidally-modulated negative-exponential covariance function used to describe elevation (Equations 2.4.2 and 2.6.1), the numerical routines evaluate the variance in the two-dimensional case to be 3.5 times larger than the one-dimensional case.

The higher variance in the 2-D model has a physical basis. The flow of water due to elevation gradients can be expected to have a wider distribution in two spatial dimensions due to differing surface area for each elevation. The one-dimensional case will force soil moisture to be distributed in a thin slab with a single point describing each elevation and equal weighting for each value of θ used to determine σ_{θ} . In contrast, the two-dimensional case will allow soil moisture flow to be spread over a different range of points at each elevation, allowing for differential weighting of each value of θ used to calculate σ_{θ} . The one-dimensional case gives equal weighting to soil moisture values at each elevation in determining the variance. In contrast, the two-dimensional case has differential weighting at each elevation, according to the geometric structure of elevation. This differential weighting in the two-dimensional case will then result in a higher variance since the mean for each case is the same. The two-dimensional case will then have a broader distribution of soil moisture, resulting in greater variance than with the one-dimensional case. From the

perspective of variance, the two-dimensional consideration probably better describes the actual flux of water in the natural environment.

Also of consideration is the correlation structure of soil moisture in space. Whereas the one-dimensional case has a relatively weak correlation, the two-dimensional case has a strong correlation along the principal directions of topographic forcings. This suggests that in two dimensions, soil moisture is forced into a more regular pattern than in one dimension. Explanation of this behavior requires a further look at the spectrum of soil moisture. Going back to Equations 2.3.29 and 2.5.16, the one- and two-dimensional spectra of soil moisture are:

$$S_{\theta}(k) = c^2 \frac{\sigma_z^2}{2\pi} \left(\frac{k^4}{\left(k^2 + \frac{\alpha\beta}{D}\right)^2} \right) \left(\frac{\lambda}{\lambda^2 + (k-a)^2} + \frac{\lambda}{\lambda^2 + (k+a)^2} \right) \quad (2.7.1)$$

(One-Dimensional)

$$S_{\theta}(j,k) = \frac{c^2 \sigma_z^2}{4\pi^2} \left(\frac{k^4 + j^4}{\left(k^2 + j^2 + \frac{\alpha\beta}{D}\right)^2} \right) \times \left(\frac{\lambda_x}{\lambda_x^2 + (k-a)^2} + \frac{\lambda_x}{\lambda_x^2 + (k+a)^2} \right) \left(\frac{\lambda_y}{\lambda_y^2 + (j-b)^2} + \frac{\lambda_y}{\lambda_y^2 + (j+b)^2} \right) \quad (2.7.2)$$

(Two-Dimensional).

Each of these expressions is composed of two products: the spectrum of elevation, S_z , multiplied by the term describing spectral relationship of soil moisture to elevation, here referred to as Σ , where

$$\Sigma_1 = \frac{k^4}{\left(k^2 + \frac{\alpha\beta}{D}\right)^2} \quad (2.7.3)$$

$$\Sigma_2 = \frac{k^4 + j^4}{\left(k^2 + j^2 + \frac{\alpha\beta}{D}\right)^2} \quad (2.7.4)$$

In one dimension, Σ_1 is zero at $k=0$ and approaches the limit of 1 as k grows large; S_z , on the other hand, has a value close to 1 at $k=0$ and approaches a value of 0 as k grows large. These two opposing terms act to dampen the spectrum of soil moisture at all values of k , resulting in a flat spectrum and a soil moisture field with low correlation in space.

In two dimensions, the behavior of the spectrum of elevation is the same. S_z is large at small values of k and j and asymptotically approaches zero as either k or j grows large; when both k and j are large, the approach to zero is quickly increased. Σ_2 , on the other hand, will be significantly different from zero when either k or j is nonzero. Thus, when either k or j is zero, the product of $S_z \Sigma_2$ will be of significant value: the corresponding behavior of S_z and Σ_1 in one dimensional case does not occur along the k (or x) and j (or y) axes in the two-dimensional case. With a significant value of the spectrum in these directions, it is expected that there will be a significant correlation in space, which is the result reflected in Figure 2.6.5. The spectral relationship of soil moisture to elevation thus suggests that soil moisture will be correlated in space principally in the axes of anisotropy.

2.8 Conclusions

In this chapter, a general theory relating soil moisture to topography was developed. Both the one- and the two-dimensional case show that topography will create a significant component of variance in soil moisture fields, although topography

should not affect the mean value of soil moisture. Of the two cases, the two-dimensional case gives better consideration to true soil moisture behavior: the physical distribution of topography in two dimensions should account for larger variability in soil moisture. The two-dimensional case also predicts stronger correlation in space of soil moisture: this result is directly explainable in terms of the derived spectral relationship between soil moisture and topography.

The preceding theoretical study has shown that topography can be expected to have a strong influence on the distribution of soil moisture. Also, proper quantification of soil properties is necessary to obtain an idea of how significant soil moisture variability can be. In the next Chapter, soil and climate properties will be studied to ascertain their effect on soil moisture, both from the perspective of their influence on the relationship of soil moisture to topography and from the basis that they can introduce soil moisture variability on their own.

CHAPTER 3

Effect of Soil Properties and Climate on Soil Moisture Variability

3.0 Introduction

This chapter deals with the effect of soil properties and of climatic forcings on soil moisture. Each of these types of forcings can affect soil moisture variability in two ways. First, the magnitude of soil and climate forcings can strongly dampen or sharpen the significance of topography as a major forcing of soil moisture variability. The importance of soil and climate from this perspective is presented as a sensitivity analysis in Sections 3.1 and 3.2. Second, variability in soil properties may itself introduce significant variability into soil moisture. A general stochastic theory relating soil moisture and soil and climate properties is developed in Section 3.3 and discussed in Section 3.4. The overall summary and conclusions are made in Section 3.5.

3.1 Influence of Soil Properties on the Relationship of Soil Moisture to Topography

As seen in Equations 2.2.6 and 2.2.19, the influence of each soil property and parameter must be accounted for in order to use properly the theory developed in this study. Hence, the proposed relationship between soil moisture and topography will depend strongly on the properties of the soil. Depending on the value of certain soil properties, the effect of topography on soil moisture may be either enhanced or dampened. It is therefore necessary to determine quantitatively the sensitivity of the soil moisture-topography relationship to variations in soil properties. To accomplish this, a basic soil-climate-topography system is chosen for study. The parameters and properties that describe this system are listed in Table 3.1.1. With this nominal set of parameters, the mean and the variance of soil moisture can be evaluated numerically

Table 3.1.1: Nominal Values of Soil, Climate, and Elevation parameters used in the Sensitivity Analysis.

Symbol	Variable	Nominal Value
D:	Depth of Root Zone:	1.5 m
K ₀ :	Saturated Conductivity:	12.2 cm/hr†
α:	Dispersion Coefficient:	0.02 (cm) ⁻¹ *
c:	pore tension parameter:	0.001 (cm) ⁻¹ *
R:	Yearly Rainfall:	1 m/yr
β:	vertical divergence:	1
θ ₀ :	porosity	0.4†
σ _z ² :	variance of elevation	121.0 m ²
λ _x :	x-correlation scale of covariance	1.0/(1200) m ⁻¹
λ _y :	y-correlation scale of covariance	1.0/(1200) m ⁻¹
A _x :	x-modulation scale of covariance	1.0/(240) m ⁻¹
A _y :	y-modulation scale of covariance	1.0/(240) m ⁻¹

Autocovariance Function: $R_{zz}(x,y) = \sigma_z^2 \exp(-\lambda_x|x| - \lambda_y|y|) \cos(A_x x) \cos(A_y y)$

* from Mantoglou and Gelhar (1987b)

† from Bras(1990)

using Equations 2.5.3 and 2.5.14, respectively. The two-dimensional case of topography forcing soil moisture is considered, since it gives a more realistic consideration to actual conditions. Because these statistics are based on the formulation developed in Chapter 2, topography will be the main forcing of soil moisture.

For the nominal case listed in Table 3.1.1, the mean, variance, and coefficient of variation of soil moisture are presented in Table 3.1.2. The system under consideration is typical of a temperate climate with an isotropic elevation field of gently rolling hills. For this system, the topography-induced soil moisture variability, measured by its standard deviation, is about 7% of the mean, a small but significant value. It will be of interest to determine at what values of soil properties the variability induced by soil moisture will become more or less significant. For this purpose, a computer program was developed to evaluate the mean, variance, and coefficient of variation of soil moisture using the parameters listed in Table 3.1.1, varying the value of one parameter at a time from the nominal case. The on the statistics of soil moisture were carefully recorded for all the perturbed values of each soil parameter. This information can be used to evaluate the sensitivity of θ to each parameter and can act as an aid in future studies about soil moisture variability. More practically, this information will provide a guide to the limits of certainty required in each parameter to use the new soil moisture theory with accuracy.

By studying variability in the mean, variance, and coefficient of variation, it can be determined in which statistics each soil parameter will be important: in this topography-driven system, this information will show how each soil or climate parameter affects the relationship between soil moisture and topography. The effect on the mean will provide insights as to how strongly the parameters influence the overall behavior of the elevation-soil moisture system. Influences on the variance of θ , σ_θ , will be useful in determining how strongly topography forces variations in soil

Table 3.1.2: Statistics of Unsaturated Hydraulic Conductivity and Soil Moisture
For the Nominal Case Considered

Statistic	K (m/hr)	θ
μ	0.011	0.28
σ	0.0048	0.02
σ/μ (%)	42	7.4

moisture for given values of soil parameters. Finally, values of the coefficient of variation can be used to determine at what values of each parameter the significance of soil moisture variability due to topographic forcing will be damped or exaggerated. Study of these three statistics will therefore be useful in assessing the theoretical importance of topographic forcing of soil moisture in a given region and in determining which parameters need to be most strongly quantified. Some parameters affect only the mean or variance; others change both statistics. In all cases the coefficient of variation ($\sigma_{\theta} / \mu_{\theta}$) is affected by changing the parameters from the nominal values of the experiments. It is useful to elaborate the physical reasons for these changes. In the following section, the role and significance of each parameter is discussed.

3.2 Sensitivity of the soil-topography relationship to soil and climate properties

- **pore size distribution parameter**

The soil parameter α relates the unsaturated hydraulic conductivity, K , to ψ and the saturated conductivity, K_0 , through the relationship in Equation 2.1.2. Since there is an exponential relationship between K and ψ , the magnitude of α will strongly affect K ; soil moisture, on the other hand, is affected only through the calculations of mean soil moisture and of γ_0^2 . As can be seen in Equation 2.3.5, mean soil moisture is linearly related to $\frac{1}{\alpha} \ln\left(\frac{\bar{K}}{K_0}\right)$, where $\ln\left(\frac{\bar{K}}{K_0}\right)$ will be *negative*. For large values of α , sensitivity of mean soil moisture to mean unsaturated hydraulic conductivity will be dampened, resulting in larger (more positive) $\bar{\theta}$; for small values of α , this effect will be reversed and a smaller $\bar{\theta}$ is expected. The value of γ_0^2 is inversely proportional to the value of α , and σ_{θ}^2 is directly proportional to γ_0^2 . Small values of α should then result in higher variance of soil moisture and large values of α in smaller values of soil

moisture variance. This agrees with the result in Figures 3.2.1a and b, which demonstrate that mean soil moisture increases with α and that the variance of soil moisture decreases with α . Furthermore, as α increases, the coefficient of variation tends to decrease in magnitude, suggesting that larger values of α dampen the significance of soil moisture variability, as shown in Figure 3.2.1c. Thus, α is an important factor in determining how strongly topography will act as a forcing of soil moisture variability.

- **vertical divergence parameter**

β is proportional to the amount of water lost from the unsaturated zone due to vertical divergence, which includes evaporation and percolation. Since βK describes the vertical flux of water in the unsaturated zone Equation 2.1.10, β acts as the hydraulic gradient imposed by evaporation and percolation. For large values of β , water is taken from the unsaturated zone relatively rapidly and in large amounts; for small β , less water is lost and at a slower rate. At small values, β is then likely to result in a large volume of water retained in the unsaturated zone, with a resulting increased unsaturated conductivity and soil moisture. The larger hydraulic conductivity will increase the natural flow of water, resulting in a higher variance of θ . A large value of β indicates that very little water is retained in the unsaturated zone, resulting in a lower average θ as well as reduced natural unsaturated flow and variability of θ . These results are reflected in Figures 3.2.2 a and b, which shows that the mean and variance of θ grow small as β grows large. The coefficient of variation of θ also decreases as β grows large, suggesting that the significance of soil moisture variability will become smaller as shown in Figure 3.2.2c. It is then to be expected that in areas of high evaporation, percolation recharge, or other form of vertical divergence, the effect of variability of elevation on variability of soil moisture will be reduced, whereas in areas

Figure 3.2.1a: Sensitivity of Mean of Soil Moisture to α

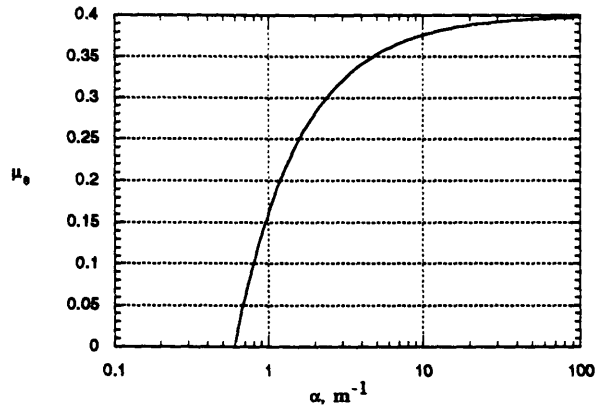


Figure 3.2.1b: Sensitivity of Standard Deviation of Soil Moisture to α

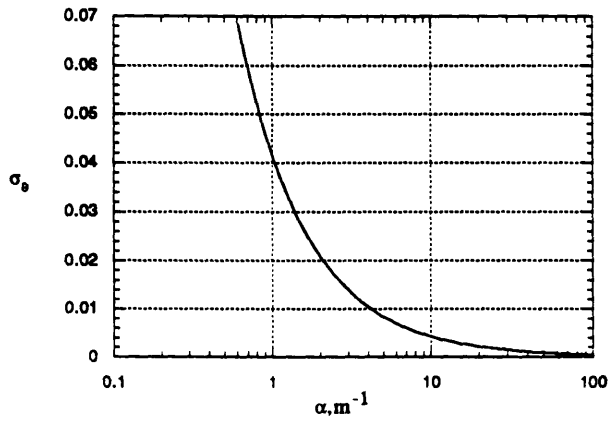


Figure 3.2.1c: Sensitivity of coefficient of variation of soil moisture to α

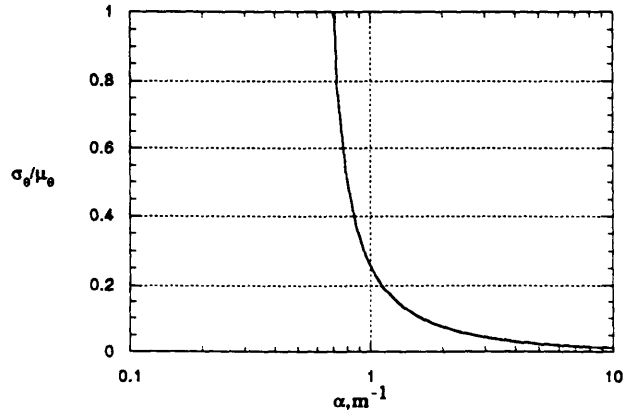


Figure 3.2.2a: Sensitivity of the Mean of Soil Moisture to β

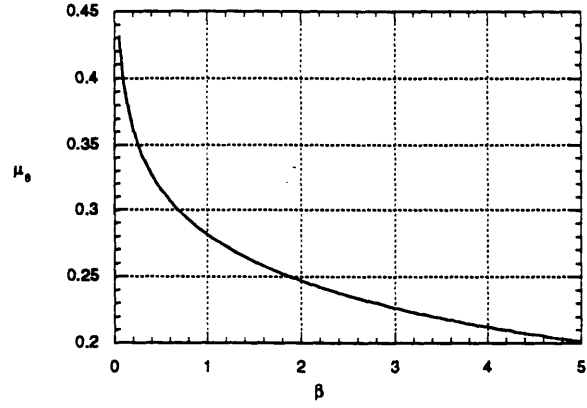


Figure 3.2.2b: Sensitivity of Standard Deviation of Soil Moisture to β

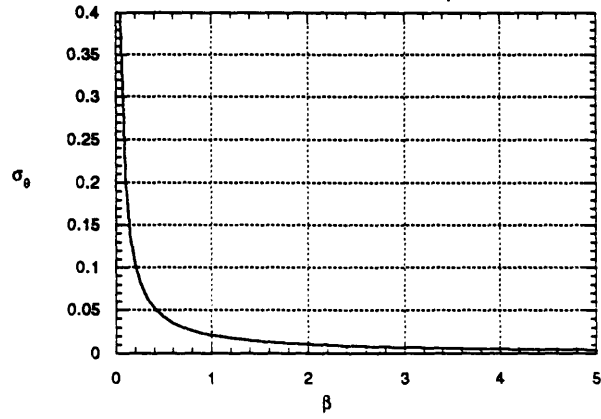
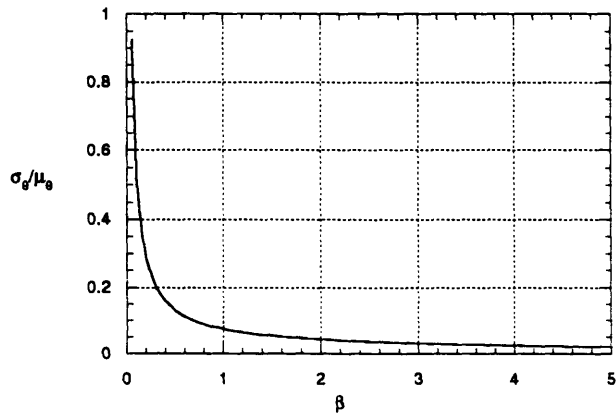


Figure 3.2.2c: Sensitivity of Coefficient of Variation of Soil Moisture to β



with lower vertical divergence, the influence of topography on soil moisture variability will be increased.

- **pore tension parameter**

The soil parameter c determines the sensitivity of θ to capillary tension; in effect, it is the derivative of soil moisture with respect to capillary tension, $\frac{\partial \theta}{\partial \psi}$. The pore tension parameter is therefore a direct sensitivity of θ to ψ : soils with large values of c will be more sensitive to changes in ψ than soils with smaller values of c . The parameter c could also be thought of as a measure of the amount of water drawn out of a soil subjected to a given capillary tension ψ . Soils with small values of c can be expected to have a higher average soil moisture, due to more water retained, and a reduced variability of topography-driven soil moisture, due to the relationship of σ_θ to σ_z in Equation 2.5.14. On the other hand, soil with large values of c can be expected to have lower average θ due to increased drainage for a given value of ψ and higher variance of θ due to increased sensitivity to variability of z . Higher values of c also result in a higher coefficient of variation due to the coupled effect of reduced mean and increased variance. These properties of c are reflected in the numerical experiments. The mean soil moisture decreases linearly with c , as shown in Figure 3.2.3a, while the variance of soil moisture increases linearly with c , as shown in Figure 3.2.3b. The coefficient of variation increases in a sharply nonlinear fashion with c , as shown in Figure 3.2.3c. Under certain conditions, the pore tension parameter is a very important soil property which can greatly amplify or dampen the significance of topographic soil moisture variability.

- **Soil Depth**

D is the depth of the unsaturated zone under consideration. Soil depth has no effect on mean soil moisture, which can be seen in Equation 2.3.5a. However, both

Figure 3.2.3a: Sensitivity of the Mean of Soil Moisture to c

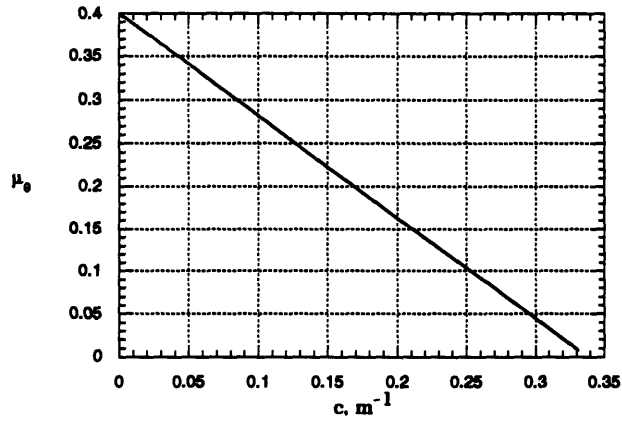


Figure 3.4.3b: Sensitivity of the Standard Deviation of Soil Moisture to c

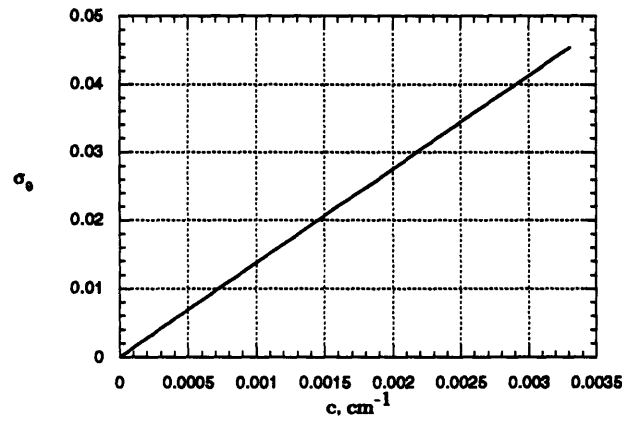
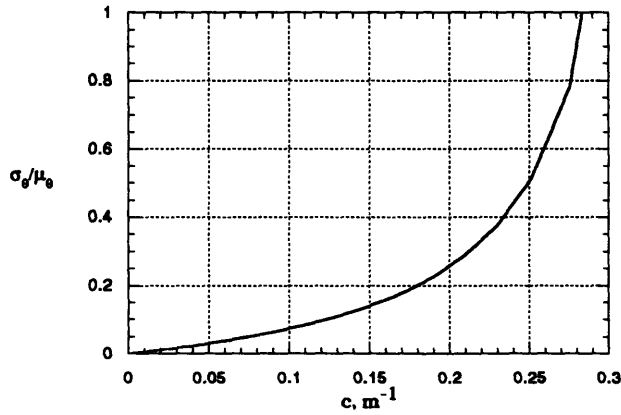


Figure 3.4.3b: Sensitivity of the Coefficient of Variation of Soil Moisture to c



the variance and the coefficient of variation of soil moisture increase linearly with depth of the root zone. Mathematically, γ_0^2 is directly proportional to depth, so that increasing depth increases the strength of the relationship between the variance soil moisture and topography. Physically, D is a factor in the divergence and the perturbation Equations, 2.3.7 and 2.5.4. The effect of increasing soil moisture variability with increasing depth can then be explained because large depth increases divergence of flow, resulting in more variability in the distribution of soil water. Depth also increases the coefficient of variation of soil moisture, so increased depth will act to increase the role of topography in bringing about variation in soil moisture. The effects of soil depth on the variance and coefficient of variation of soil moisture are shown in Figures 3.2.4a and b.

- **Saturated Hydraulic Conductivity**

The saturated hydraulic conductivity, K_0 , affects only the mean of soil moisture. Since K_0 does not affect either the mean Equation 2.3.5a or the variance Equation 2.3.7 of unsaturated conductivity, it has no effect on the divergence and therefore no effect on the variance of soil moisture in the unsaturated zone. K_0 affects only the mean of soil moisture, θ , through the saturation factor $\ln\left(\frac{\bar{K}}{K_0}\right)$ in Equation 2.3.36. Here, the ratio of unsaturated to saturated hydraulic conductivity is a measure of the saturation of a soil, which in turn determines soil moisture. Soil with a high saturated hydraulic conductivity will have smaller (more negative) values of $\ln\left(\frac{\bar{K}}{K_0}\right)$ and of θ for a given value of \bar{K} . However, this physical relationship has no bearing on the variance of soil moisture, as seen in Equation 2.3.27 and shown from the numerical experiments in Figure 3.2.5a. Average soil moisture show an inverse linear proportionality to K_0 . On the other hand, as K_0 increases, the coefficient of variation of soil moisture will also increase since average soil moisture will be smaller while the variance of soil moisture

Figure 3.2.4a: Sensitivity of the Standard Deviation of Soil Moisture to D

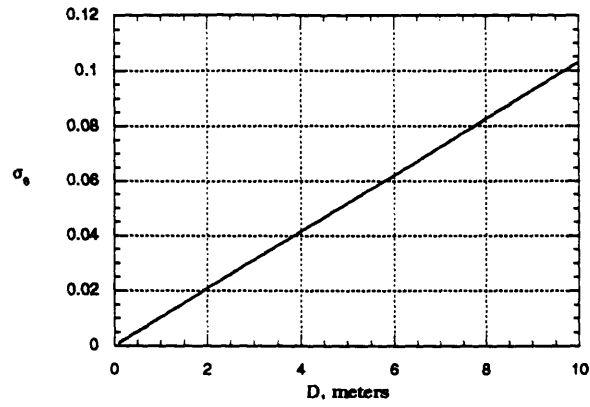


Figure 3.2.4b: Sensitivity of the Coefficient of Variation of Soil Moisture to D

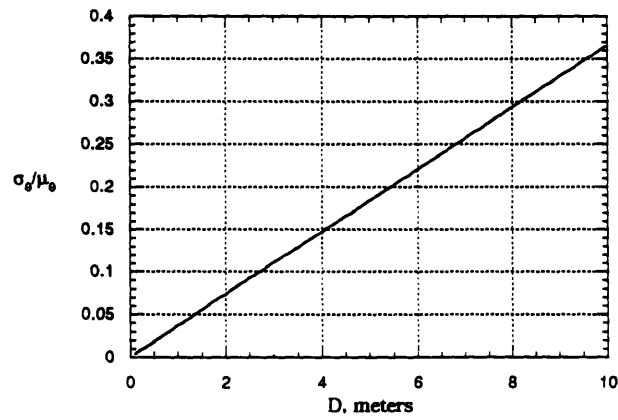


Figure 3.2.5a: Sensitivity of the Mean of Soil Moisture to K_0

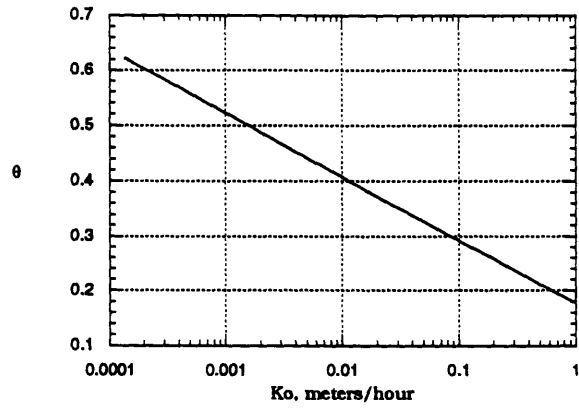
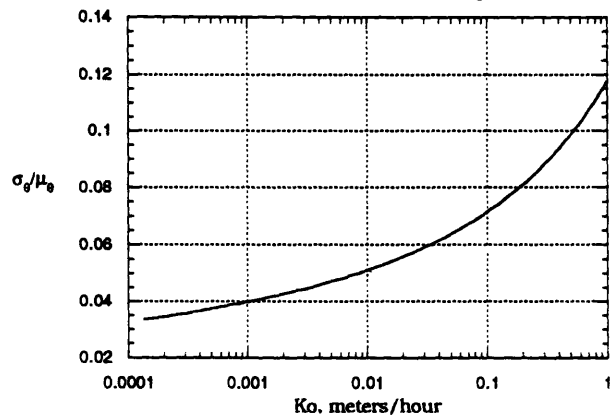


Figure 3.2.5b: Sensitivity of the Coefficient of Variation of Soil Moisture to K_0



remains constant. This effect is nonlinear as shown in Figure 3.2.5b. In general, soils with higher K_o will have a slightly more significant topography-driven soil moisture variability.

- **Rainfall Rate**

The amount of rainfall infiltrating the soil directly influences the average soil moisture, as well as the average unsaturated hydraulic conductivity. With more available water, the average soil moisture will be higher; with less available water, soil moisture will be lower. This effect is nonlinear, as depicted in Figure 3.2.6a. Rainfall rate does not affect the variability of soil moisture, since it has no effect on the horizontal flow of water. This is reflected in equation (2.3.29b), in which the variance of soil moisture has no dependence on rainfall rate or on average unsaturated hydraulic conductivity. Since more rainfall increases only the mean soil moisture, it will decrease the coefficient of variation and the overall significance of soil moisture variability, which is reflected in Figure 3.2.6b.

- **Porosity**

The porosity of a soil affects only the average soil moisture, which increases with increasing porosity. This can be expected since soils with higher porosity will be capable of storing greater amounts of soil water than soils with lower porosity; this is a one-to-one linear effect as depicted in Figure 3.2.7a. Increased porosity steadily decreases the coefficient of variation of soil moisture because as average soil moisture decreases, the same value of variance of soil moisture will become less significant. Porosity thus decreases the coefficient of soil moisture in a non-linear manner as shown in Figure 3.2.7b, and will be an important factor in the degree to which topography influences soil moisture variability.

Figure 3.2.6a: Sensitivity of the Mean of Soil Moisture to R

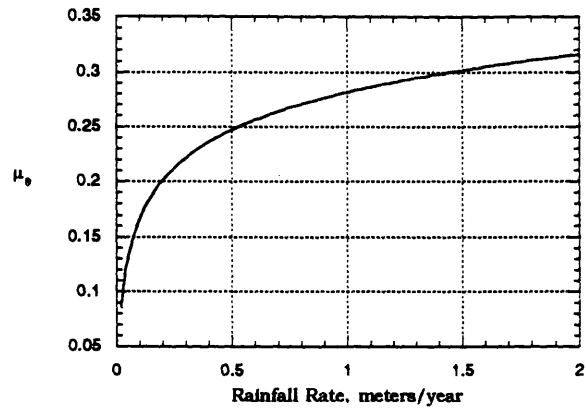


Figure 3.2.6b: Sensitivity of the Coefficient of Variation of Soil Moisture to R

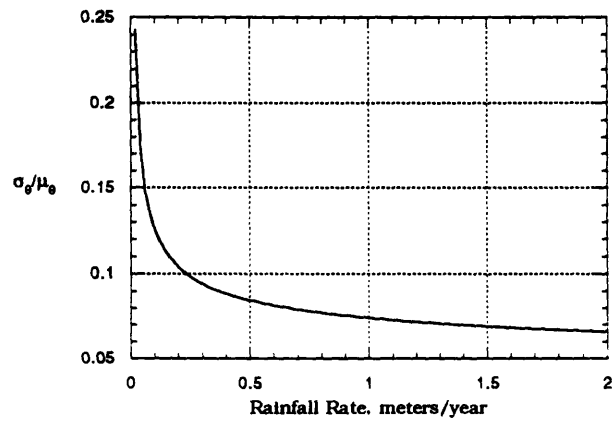


Figure 3.2.7a: Sensitivity of the Mean of Soil Moisture to Porosity

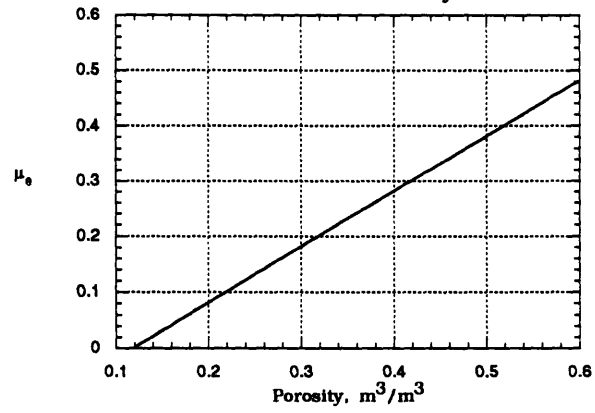
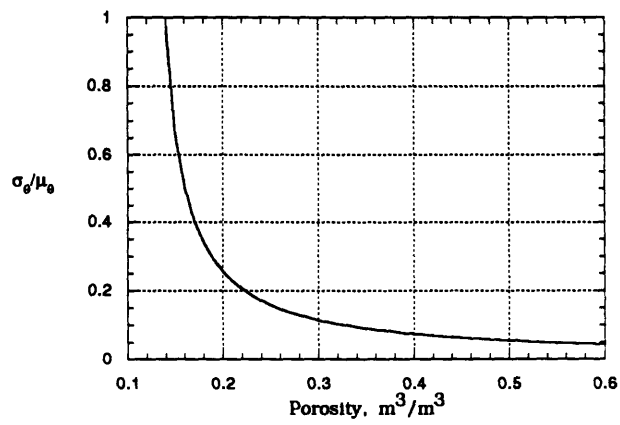


Figure 3.2.7b: Sensitivity of the Coefficient of Variation of Soil Moisture to Porosity



3.3 Stochastic Analysis of the Relationship Between Soil Moisture and Soil and Climate

The methods needed to relate the spectra of two variables have been demonstrated in the Section 2.3 using hydraulic conductivity (soil moisture) and elevation as examples. In reality, many factors will affect the nature of soil moisture variability: non-uniformity in all of the soil properties and parameters used to relate soil moisture to elevation will potentially influence variance in soil moisture. Consequently, it will be useful to know how the variability in these parameters will affect the variability of soil moisture. The same procedure used to relate the spectrum of soil moisture to elevation can be used to relate the spectrum of soil moisture to the spectrum of any soil property of interest. The spectrum of soil moisture is related to the spectrum of each individual parameter by the following equations:

$$S_{\theta}(k) = S_{\theta_0}(k) \quad (3.3.1)$$

$$S_{\theta}(k) = \frac{c^2}{\alpha^2} S_{\ln K_0}(k) \quad (3.3.2)$$

$$S_{\theta}(k) = \frac{1}{\alpha^2} \left[\ln \left(\frac{K}{K_0} \right) \right]^2 S_c(k) \quad (3.3.3)$$

$$S_{\theta}(k) = c^2 \left[\ln \left(\frac{K}{K_0} \right) \right]^2 S_{\frac{1}{\alpha}}(k) \quad (3.3.4)$$

$$S_{\theta}(k) = \left(\frac{c}{\alpha \bar{K}} \right)^2 S_K(k) \quad (3.3.5)$$

In addition, the spectral density of hydraulic conductivity, which can be directly related to soil moisture by Equation 3.3.5 above, is related to the spectral density of effective precipitation by

$$S_K(k) = \frac{\alpha^2}{D^2} \left(\frac{1}{k^2 + \frac{\alpha\beta}{D}} \right)^2 S_R(k) \quad (3.3.6)$$

or

$$S_\theta(k) = \left(\frac{c}{D\bar{K}} \right)^2 \left(\frac{1}{k^2 + \frac{\alpha\beta}{D}} \right)^2 S_R(k) \quad (3.3.7)$$

where $S_\theta(k)$ is the spectrum of precipitation in space only. Equations 3.3.6 and 3.3.7 are for the special case in which the overall elevation gradient, $\frac{\partial z}{\partial x}$, is zero. The variance of soil moisture will depend on the spectrum of each variable; however, for the equations in which the variable of integration k does not appear explicitly, the formal definition of the spectrum may be used to calculate the variance

$$\int_{-\infty}^{\infty} S_x(k) dk = \sigma_x^2 \quad (3.3.8)$$

for random variable x . Making use of this identity, Equations 3.3.1, 3.3.2, 3.3.3, 3.3.4, and 3.3.5 above can easily be simplified to

$$\sigma_\theta^2 = \sigma_{\theta_0}^2 \quad (3.3.9)$$

$$\sigma_\theta^2 = \frac{c^2}{\alpha^2} \sigma_{\ln K_0}^2 \quad (3.3.10)$$

$$\sigma_\theta^2 = \frac{1}{\alpha^2} \left[\ln \left(\frac{K}{K_0} \right) \right]^2 \sigma_c^2 \quad (3.3.11)$$

$$\sigma_\theta^2 = c^2 \left[\ln \left(\frac{K}{K_0} \right) \right]^2 \sigma_{\frac{1}{\alpha}}^2 \quad (3.3.12)$$

$$\sigma_\theta^2 = \left(\frac{c}{\alpha\bar{K}} \right)^2 \sigma_K^2 \quad (3.3.13)$$

where $\sigma_{\frac{1}{\alpha}}^2$ is the variance of $\frac{1}{\alpha}$ and $\sigma_{\ln K_0}^2$ is the variance of $\ln(K_0)$. It is further

important to note that these results have no dependence on the number of dimensions considered; they will be the same for the one- and the two-dimensional cases. For precipitation, the variance will have to be evaluated by integrating the factor

$\left(\frac{1}{k^2 + \frac{\alpha\beta}{D}} \right)^2$ times the spectrum with respect to k ; this will result in a form relating the

covariance of soil moisture and precipitation similar to that of the parameter γ_0^2 which described the correlation between the elevation and the hydraulic conductivity fields in one-dimension. Defining Ω_0^2 as

$$\Omega_0^2 = \int_{-\infty}^{\infty} \left(\frac{1}{k^2 + \frac{\alpha\beta}{D}} \right)^2 \frac{S_R(k)}{\sigma_R^2} dk \quad (3.3.14)$$

the variance of soil moisture may be related to the variance of precipitation by

$$\sigma_{\theta}^2 = \left(\frac{c}{DK} \right)^2 \Omega_0^2 \sigma_R^2 \quad (3.3.15)$$

A more realistic consideration will be to account for the effect of multiple variables. In particular, both elevation and rainfall are of considerable interest; extensive information should be available for both quantities. Using a stochastic analysis analogous to that in Section 2.3, the following relationship between unsaturated hydraulic conductivity, elevation, and rainfall can be derived

$$S_K(k) = \alpha^2 \bar{K}^2 \left(\frac{k^2}{k^2 + \frac{\alpha\beta}{D}} \right)^2 S_z(k) - \frac{\alpha^2 \bar{K}}{D} k^2 S_{Rz}(k) + \left(\frac{\alpha}{D} \right)^2 \left(\frac{1}{k^2 + \frac{\alpha\beta}{D}} \right)^2 S_R(k) \quad (3.3.16)$$

where $S_{Rz}(k)$ is the cross-spectrum of precipitation and elevation. $S_{Rz}(k)$ should be expected to be very nearly zero unless some known mechanism, such as orographic lifting, were present to link precipitation to topography. The spatial variability of precipitation described by $S_R(k)$ could be variability in precipitation infiltrating the ground surface over large areas where yearly precipitation is nearly uniform. $S_R(k)$ could then be a function of land cover and vegetation, which results in differential interception loss and therefore differential effective rainfall.

Ideally, soil properties would also be incorporated into this multi-variate spectral analysis. If enough reliable information on the large-scale saturated hydraulic conductivity and porosity fields of a region were available, both of these variables could be incorporated into the analysis. By using the relationship between the spectral amplitudes of K , z , and R , and substituting into the perturbation equation relating θ , $\ln(K_o)$, and θ_o , the following equation relating the effect of all four variables can be derived:

$$S_\theta(k) = C_1^2 S_{\ln(K_o)}(k) + C_2^2 S_{\theta_o}(k) + C_3^2 S_z(k) + C_4^2 S_R(k) + C_1 C_2 S_{\ln(K_o)\theta_o}(k) \quad (3.3.18)$$

$$+ C_1 C_3 S_{\ln(K_o)z}(k) + C_1 C_4 S_{\ln(K_o)R}(k) + C_2 C_3 S_{\theta_o z}(k) + C_2 C_4 S_{\theta_o R}(k) + C_3 C_4 S_{Rz}(k)$$

$$C_1 = \frac{1}{\alpha^2} \left[\ln \left(\frac{K}{K_0} \right) \right]^2$$

$$C_2 = 1$$

$$C_3 = c \frac{k^2}{\left(k^2 + \frac{\beta\alpha}{D} \right)}$$

$$C_4 = \frac{c}{D} \frac{1}{\left(k^2 + \frac{\beta\alpha}{D} \right)}$$

where $S_{xy}(k)$ is the cross-spectrum of variables x and y . Naturally, applications using Equation 3.3.18 will require a large amount of data on all four variables, z , R , K_0 , and θ_0 . In practice, all of this data may not be available, so Equation 3.3.18 may provide an upper bound on the characterization of soil moisture than cannot readily be put into practice. For the variables (such as K_0 and θ_0) which are not well characterized at a large scale, the terms involving those variables may be dropped in Equation 3.3.18, simplifying the final result. On the other hand, this theory can be extended to any number of variables desired, although the limit on data availability may create a practical limit of not more than three or four variables.

3.4 Examples of Soil as a Forcing of Soil Moisture Variability

Studying each parameter individually will give insight to how variability in that parameter alone will contribute to variability in soil moisture. Gelhar and Mantoglou (1987b) provide estimates of the variability of soil parameters for two soil types, as listed in Table 3.4.1. This information can be combined with the equations relating soil moisture variability to soil property variability described in Section 3.3 above. The values of soil moisture variability resulting from the relative effects of each soil parameter are listed for both soil types in Table 3.4.2. For example, using the values for the Panoche clay loam listed in Table 3.1.1, in Equation 3.3.10 above, $\frac{c^2}{\alpha^2}$ will be

Table 3.4.1: Stochastic Soil Properties from Mantoglou and Gelhar (1987b).

	Panoche Clay Loam	Maddock Sandy Loam
α (cm ⁻¹)	0.0294	0.147
c (cm ⁻¹)	0.0052	0.00245
\bar{K} (cm/s)	3.2e-6	3.2e-6
K_o (cm/s)*	6.8e-6	2.7e-4
n^*	0.4	0.35
$\sigma_{\frac{1}{\alpha}}^2$ (cm ²)*	100	36
σ_c^2 (cm ⁻²)	8.95e-8	N/A
$\sigma_{\ln K_o}^2$	2.48	7.45

* estimated

Table 3.4.2: Variability in Soil Moisture Resulting from Variability in Soil Properties.

	σ_{θ} resulting from variability in			
	z	α	c	K_o
Panoche	0.087	0.04	0.008	0.28
Maddock	0.012	0.066	N/A	0.045

evaluated at 0.032; variance in $\ln(K_0)$ is of order 2.5. It may be expected that variability in saturated hydraulic conductivity will make an important contribution ($\sigma_\theta=0.27$) to variance in soil moisture. For the nominal parameters in Table 3.1.1, the average soil moisture is evaluated at 0.27, so the variability introduced by saturated hydraulic conductivity will be nearly the same size as the average value of soil moisture. In contrast, in Equation 3.3.12, the quantity $c^2 \left[\ln \left(\frac{K}{K_0} \right) \right]^2$ will be about $1.5 \times 10^{-5} \text{ cm}^{-2}$; variability in $\frac{1}{\alpha}$ is estimated to be approximately 100 cm^2 , so that variability in the dispersion coefficient α will make a contribution to σ_θ of about 0.04. For the pore tension parameter, variance is estimated at about $9 \times 10^{-8} \text{ cm}^{-1}$; the coefficient $\frac{1}{\alpha^2} \left[\ln \left(\frac{K}{K_0} \right) \right]^2$ is approximately 700 cm^2 , creating a variance contribution to σ_θ of 0.008. For the elevation covariance parameters in Table 3.2.1, the topographic forcing alone would result in $\sigma_\theta=0.09$. This value is comparable in size to the variance created by α but less than the variance resulting from $\ln(K_0)$. Information on the variability of porosity is not available, but the natural variations in porosity will contribute directly to soil moisture variability, as shown in Equation 3.3.9. Also, the variability in infiltration described in the previous section would be difficult to quantify, so it is hard to characterize such effects in a real system. However, the available data shows that variability in soil properties will contribute very significantly to the variability in soil moisture at the large scale--this contribution will be larger than the contribution of topographic forcing for the clay loam.

The soil moisture variance resulting from soil properties of the Maddock sandy can also be calculated. In this case, average soil moisture is evaluated at 0.28. The contribution to σ_θ of saturated hydraulic conductivity will be greatly reduced from the previous case: for the Maddock loam, the variability introduced to σ_θ will be about 0.05. The contribution of the pore size distribution parameter will increase; the

addition to σ_θ by $\sigma \frac{1}{\alpha}$ will be about 0.07. The variability introduced by both of these soil properties will be larger than that brought about by topography. For the nominal case elevation field, the contribution to σ_θ given the Maddock loam soil parameters will be 0.02. Thus, for the case of the sandy loam, overall soil moisture variability will be smaller than for a clay loam, although the ratio of soil to topographic variance will be nearly twice as large for the Maddock loam as for the Panoche loam. From the results of these two examples, variability in soil properties is expected to be a significant source of variability along with the variability due to topography.

3.5 Conclusions

Soil and climate properties will be important in the large scale distribution of soil moisture in two ways. First, the value of soil and climate parameters will influence the significance of topographic forcing of soil moisture variability. In this situation, the soil and climate properties do add variability to soil moisture only in the sense that they influence the effect of topography. Among the parameters that are most important in this sense are α , β , c , and θ_o . Over certain ranges, all four of these parameters can greatly affect the importance of topographic forcing as evidenced through the value of the coefficient of variation of soil moisture. The properties D , K_o , R are less significant: over a wide range of values, these three soil and climate parameters tend to have a smaller effect on the significance of topography-induced soil moisture variability.

Second, variability in soil and climate variables can bring about significant variability in the distribution of soil moisture. Theoretically, variability in all of the soil and climate parameters will bring about soil moisture variability: verifying the significance of each parameters is more difficult. Using data available for two soil types, it was determined that typical variability in α and K_o will definitely bring about strong variability in soil moisture, whereas soil moisture variability arising from

variability in c was relatively insignificant for one soil type studied. Variability in the other soil and climate parameters was not quantified in this study. The importance of α both in affecting the influence on soil moisture due to topographic variability and in forcing soil moisture variability itself suggest that it is a very important parameter in the large-scale distribution of soil moisture. With increased study of the variability of soil properties, the relative importance of each soil parameter could be ascertained.

CHAPTER 4

Results of Field Experimentation

4.0 Introduction

This chapter examines the results of a field-scale soil moisture experiment designed to test the theory developed in Chapter 2: this will be the key to making practical use of the theory developed in Chapters 2 and 3. In Section 4.1, the experimental location is described. Section 4.2 covers the experimental procedures used to measure soil moisture and to determine the values of the relevant soil properties. The observed relationship of soil moisture to topography is presented and discussed in Section 4.3; the relationship between soil moisture and soil properties is discussed in Section 4.4. Predictions using the theoretical equations relating soil moisture to topography are made and then compared to observations in Section 4.5. Finally, the conclusions of this Chapter are presented in Section 4.6.

4.1 Background

In order to properly test the theoretical equations developed in Chapter 2, it is necessary to evaluate how well they describe soil moisture flow in a natural setting. To carry out this requirement, a field experiment to test the correlation of soil moisture on topography was carried out at the Harvard Forest research area. The forest contains a wide range of native species, almost completely undisturbed geologic formations, and topography characteristic of the New England area (Moore *et al.* 1996, Wofsy *et al.* 1994). Harvard Forest is unique in the wide range of meteorological measurements and other environmental studies taking place within its boundaries (Wofsy *et al.* 1994). This wide range of information available at the measurement location and the potential for cooperation with other research groups made Harvard Forest an excellent location to carry out the field experiment. The main experiment

was carried out along Prospect Hill, located approximately 1 km away from Harvard Forest's Environmental Monitoring System (EMS) tower, (Moore *et al.* 1996). The site at which the soil moisture measurements were taken was chosen for its uniformity of slope and soil type, and its proximity to other measurement locations. At the EMS Tower, sensible and latent heat flux measurements were made. Near the EMS Tower, precipitation was measured both above and below the forest canopy. These measurements will provide the necessary information about environmental forcings, such as evaporation and precipitation, that are required to properly evaluate the various forms of Equation 2.1.8 by using the experimental data. Localized maps of the Prospect Hill and of the EMS Tower showing local topography and measurement locations are shown in Figures 4.1.1 and 4.1.2, respectively. A topographic map showing the locations of the measurements along the hillslope is presented in Figure 4.1.3. As can be seen in that figure, the area covered by the measurement locations has uniform slope and covers a range of elevation of about 35 meters over a horizontal distance of about 150 meters, resulting in a slope $\frac{\partial z}{\partial x} = 0.24$. These conditions should provide a good testing grounds for unsaturated flow driven by topography, which will be proportional to the local slope as seen in Equation 2.1.8.

4.2 Experimental Procedure

The experiment is designed to sample soil moisture at different elevation levels to attempt to determine the relationship between soil moisture and topography. For this purpose, soil moisture was measured at the eight locations as previously shown in Figure 4.1.3; the elevation along the hillslope is listed in Table 4.2.1. Each location has three access tubes: a steel pipe driven into the ground to create an entry to the soil. The soil moisture measurements were taken with a neutron probe, which contains an Americium-241 radioactive source. To take measurements, the source is lowered down the access pipe where it emits neutrons into the surrounding soil. As

Figure 4.1.1: Elevation Contours of Harvard Forest

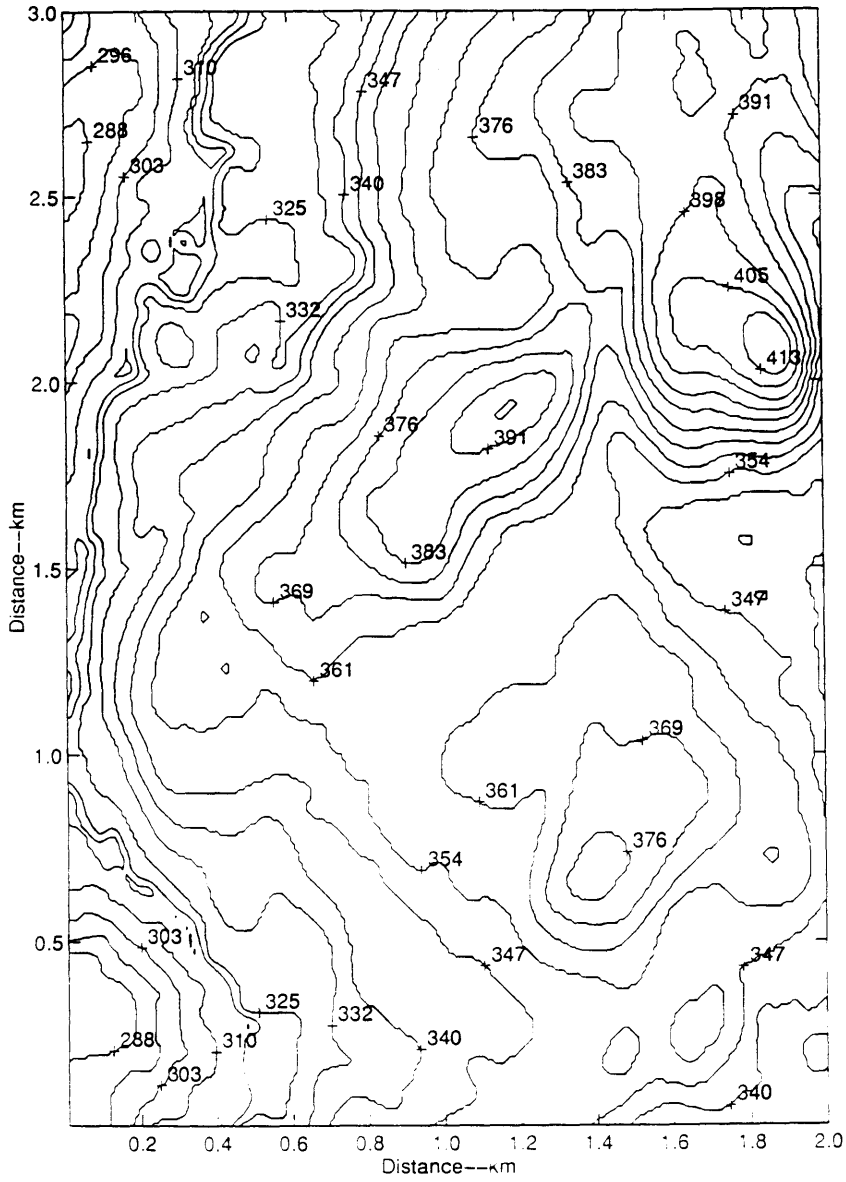


Figure 4.1.2: Localized Elevation Contours around Prospect Hill

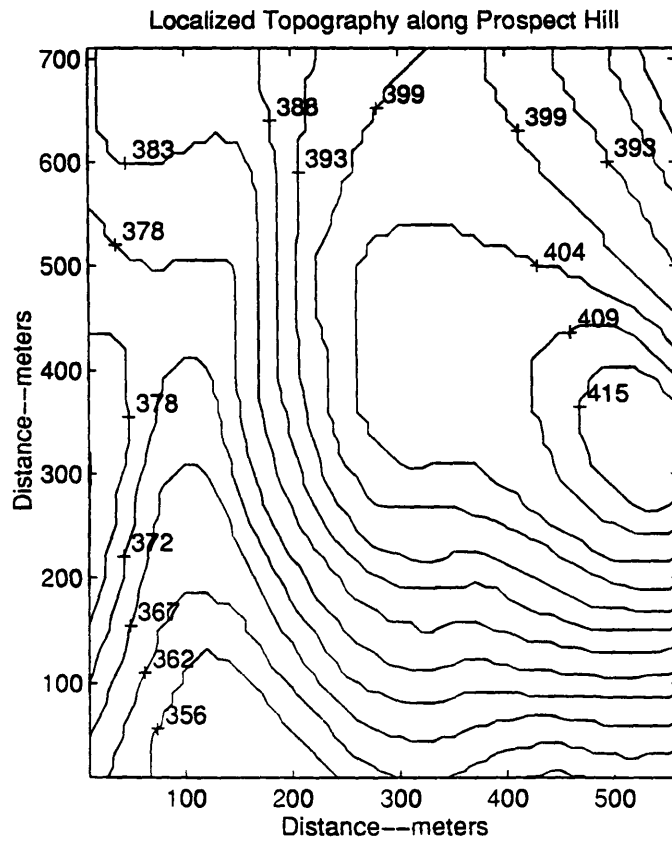


Figure 4.1.3: Topographic Map around Prospect Hill Showing the Locations of the Soil Moisture Access Tubes

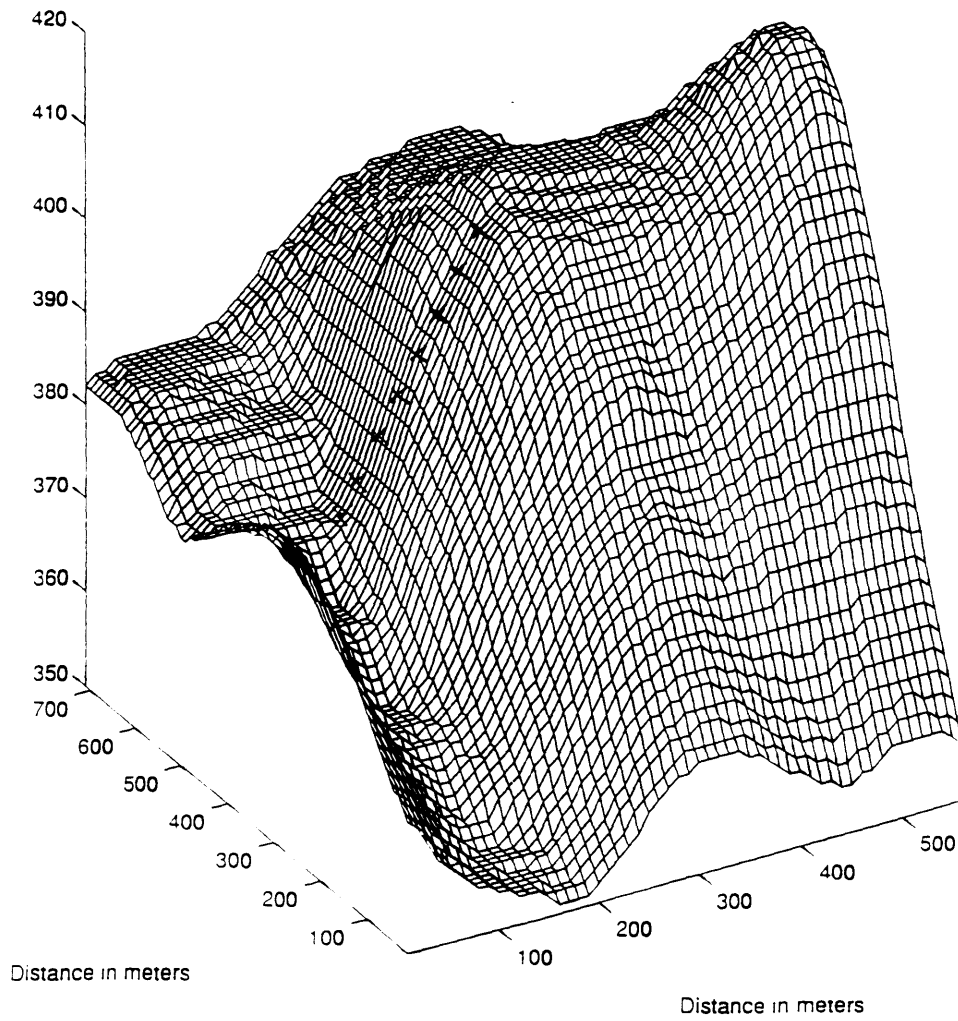


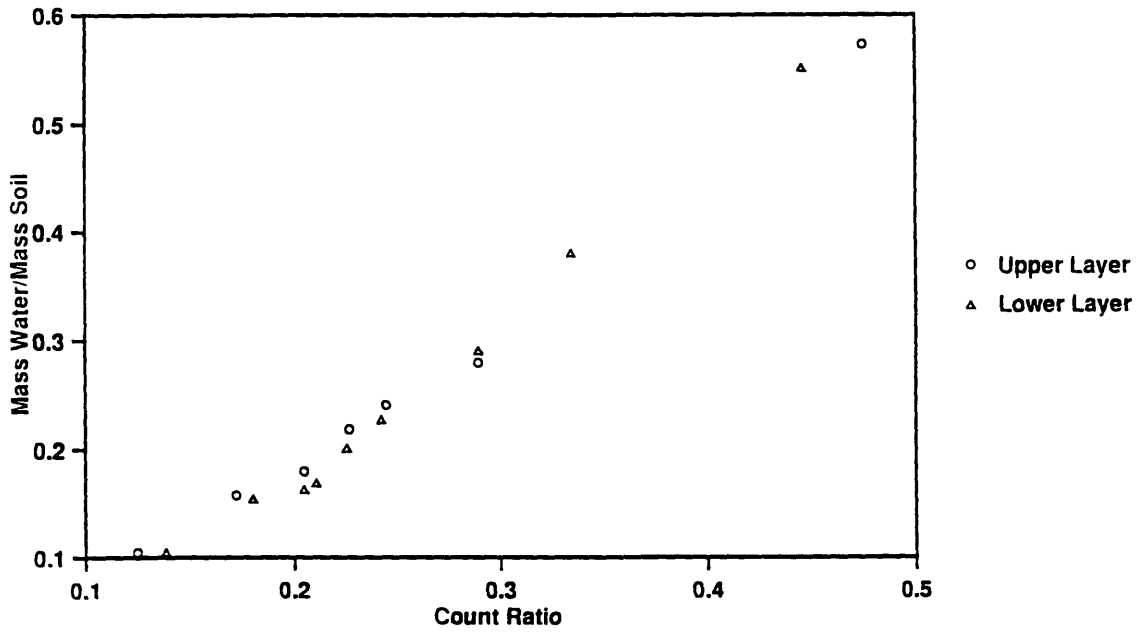
Table 4.2.1: Elevation along Prospect Hill

Distance Uphill (meters)	Elevation (meters)
0	365
22	370
44	375
66	381
89	386
111	392
133	397
155	401

the neutrons strike certain species of atoms, they lose energy and give off heat (undergo thermalization). The neutron probe measures the rate of thermalization (the *count measure*) during each measurement. Measurements can be taken using 30-second, 1-minute, or 4-minute sampling lengths: the neutron probe reading is the average rate of thermalization for the measurement interval, so the longer the measurement, the better the sampling of soil conditions. The count measure can then be compared with the current emission rate of the source (the *standard count*), which is measured every day on which soil moisture measurements are taken. The ratio of the count measure to the standard count (the *count ratio*) is then a measure of the thermalization potential of the soil. Because hydrogen atoms are exceptionally strong thermalization species, the count ratio is strongly proportional to the amount of water present in the soil. Thus, the number of thermalizations during a neutron probe reading can be taken as a measure of soil moisture. However, the neutron probe measurement cannot be used by itself to determine soil moisture. Since other thermalization species, such as iron atoms and organic molecules, occur naturally in the soil, the neutron probe needs to be calibrated in the laboratory to determine the exact relationship of the count ratio to soil moisture for a given soil type.

The laboratory calibration of the neutron probe was carried out with soil taken from the field site. This was done by placing the soil into a 2'x2'x2' crate and taking neutron probe measurements of the soil, using an access tube identical to those used in the field. The soil was then removed, samples were taken at several depths, and the moisture content of these samples was determined (ASTM Standard D-2216). The soil was allowed to dry to a new moisture content and then replaced to the same volume in the crate, after which the procedure was repeated. The neutron probe measurements were then plotted against soil moisture; the resulting curve can be used to give absolute soil moisture for future neutron probe measurements (Stephens, 1995). This curve is shown in Figure 4.2.1. The high degree of correlation ($r^2=0.95$)

Figure 4.2.1: Laboratory Calibration Curve of Neutron Probe Using Sandy Loam

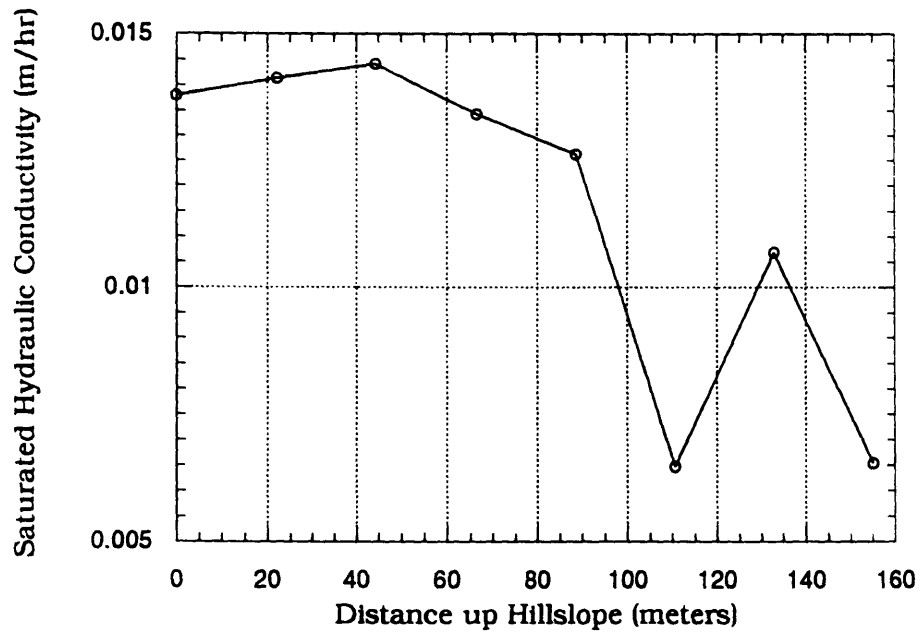


of the calibration curve shown in the diagram suggests that the laboratory results should be highly reproducible. Combined with the measurement uncertainty of the neutron probe, this curve can be used to quantify the uncertainty of the soil moisture measurements. The error inherent in the neutron probe measurements is proportional to the length of the sampling time and the amount of water in the soil (Troxler 1983). For the laboratory calibration curve, four-minute measurement intervals were used: this results in a 95% confidence that the measurement error is not more than 0.5% for natural soil moisture conditions. The field measurements were taken using a 30-second measurement, typically at eight different soil depths. This is equivalent to taking a four-minute measurement, so measurement error at each soil station is typically around 0.5% as well. Combined with the excellent fit of the calibration curve (uncertainty of about 2%), the error resulting from the translation of neutron probe readings to soil moisture should be minimal, on the order of 1-2%.

Saturated hydraulic conductivity, K_0 , was determined in the laboratory using the falling head permeameter test (Smith and Mullins, 1991). Disturbed soil samples were taken from near (80-100 cm) each of the eight soil moisture sampling locations. This was accomplished by driving a 3" pipe into the ground to a depth of approximately 30 cm, and then removing the pipe with the soil sample intact inside. Great care was taken to attain minimal disturbance of each sample. The volume that the sample occupied in the field was taken to equal the volume that the pipe intruded into the soil (Revut and Rode 1981); this record allows the sample to be returned to nearly the same volume in the laboratory as it held in the field. The falling head permeameter test was then executed for each soil sample. The results of these experiments are shown in Figure 4.2.2. K_0 shows a decreasing trend from the bottom to the top of the hillslope, with a sharp decrease near the top. This trend is a reflection of subtle changes in soil properties: near the bottom of the hill, the average particle size increases to include small pebbles, which result in higher saturated hydraulic

Figure 4.2.2

Laboratory Estimation of Saturated Hydraulic Conductivity along Prospect Hill



conductivity. Values of K_0 and coefficient of determination (which reflects the goodness of fit) of each falling head permeameter test are shown in Table 4.2.2.

Porosity was estimated in the field. This was done by fully saturating the soil around the soil access tubes at each elevation, measuring the residual capillary tension at depth, ψ , with a tensiometer, and taking neutron probe measurements and the calibration curve to determine soil moisture (Stephens, 1995). This procedure should give a very good measure of the water-holding capacity of soil in its undisturbed field condition. On the other hand, the standard test to determine porosity involves taking a large (0.1 ft³ minimum) field sample and to record carefully its volume by filling the hole either with sand or with a water-filled balloon (ATSM D-2167). Both the bulk density and the specific gravity of the soil (ASTM 854) are then determined in the laboratory, and porosity is estimated as

$$\theta_o = 1 - \frac{\text{bulk density}}{\text{specific gravity}} \quad (4.2.1).$$

With the proper equipment, this procedure can be expected to give reliable results (Revut and Rode 1981). However, given the constraints on availability of proper equipment to determine the volume of the soil in the field, the remote location of the experimental site, and the limitations on the determination of specific gravity of the soil, this test was deemed inappropriate. The much simpler neutron probe test is expected to give higher accuracy for less investment of time, minimal to no disturbance of soil structure, and without the use of heavy equipment which could severely damage the pristine state of the Harvard Forest. The results of the neutron probe tests are shown in Figure 4.2.3, and the values with error are presented in Table 4.2.3. The soil type at the experimental site is a fine sandy loam, which typically has a smaller porosity listed in the literature (on the order of 0.30 to 0.35) than was obtained from the field measurements. However, Bras (1990) notes that it is common for the actual field value

Table 4.2.2: Saturated Hydraulic Conductivity Results

Distance Uphill (m)	Hydraulic Conductivity (m/hr)	Coefficient of Determination
0	0.014	0.99
22	0.014	0.94
44	0.014	0.98
66	0.013	0.96
89	0.013	0.97
111	0.006	0.99
133	0.011	0.99
155	0.007	0.99

Figure 4.2.3

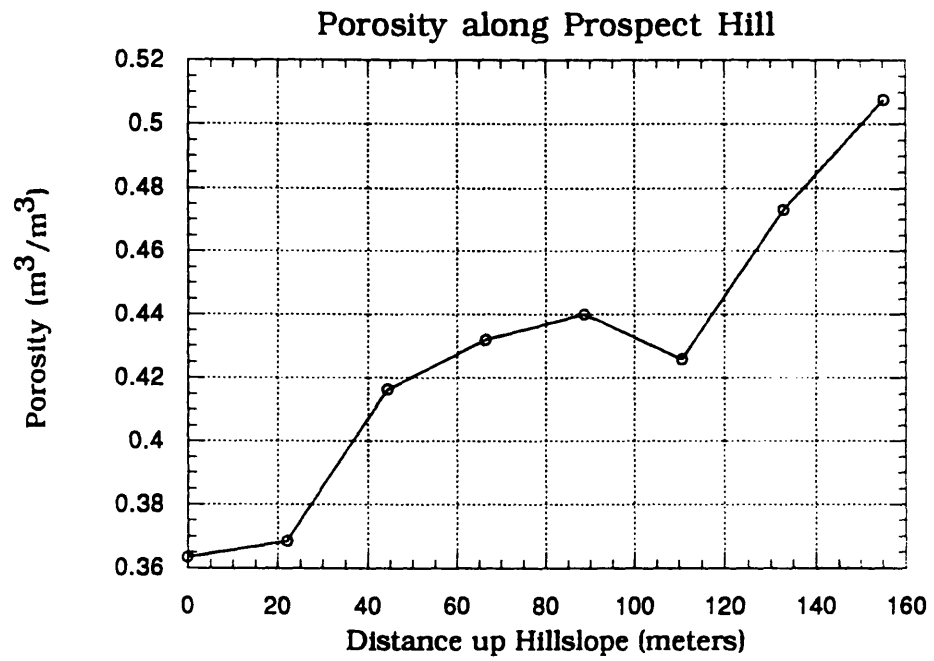


Table 4.2.3: Porosity Results

Distance	
Uphill (m)	Porosity
0	0.36
22	0.37
44	0.42
66	0.43
89	0.44
111	0.43
133	0.47
155	0.51

of porosity to be at least 0.1 larger than laboratory values: this may be a further indication of the acceptability and the usefulness of the neutron probe determination of porosity.

Values of the parameters relating soil moisture to unsaturated hydraulic conductivity, α and c , are also needed. Determination of these parameters in the field or in the laboratory requires specialized equipment that was unavailable for use. Since these parameters were not determined experimentally, values were determined from the instantaneous moisture profile and soil moisture retention experiments for a sandy loam (the same USDA soil classification as the soil along Prospect Hill) described by Smith and Mullins (1991, pp. 238-254). The values obtained from that study are $\alpha = 0.06 \text{ cm}^{-1}$ and $c = 0.0014 \text{ cm}^{-1}$; these values are acceptable in lieu of experimental values. However, it should be emphasized that these are estimates of α and c taken from laboratory experiments for a different soil and should be regarded strictly as parameters and not true soil properties. With further experimental resources, the values of α and c could be tested in the field and compared with the values used in this study.

It is also necessary to quantify the vertical fluxes of water in the unsaturated zone at the experimental site. Evaporation and precipitation are important sinks and sources of water for the experimental site. Fortunately, both of these components of the hydrologic cycle were measured at the Harvard Forest EMS Tower. Precipitation and throughfall (the amount of water reaching the forest floor) were measured with a network of twelve Texas Electronics tipping bucket raingauges; the measurements were recorded with an R.M. Young 26700 Programmable Translator. Because throughfall measurements were available and runoff was minimal, the amount of water infiltrating the ground surface is expected to be very nearly the same as the throughfall measurements. Evaporation was measured on the EMS Tower by the Wofsy research group at Harvard University. Eddy correlation measurements were

used to estimate evaporation, using a five-minute time interval of measurement (Wofsy 1993 *et al.*, Moore *et al.* 1996). The EMS tower is south-southwest (slightly downwind on the average) of the Prospect Hill Site. Using the formulation in Gash (1986) and the estimates for the roughness length of the forest surface from Choi (1996), the 95% effective fetch or contributing distance upwind of the EMS Tower is estimated at 7000 meters: this measurement along with the average wind direction suggest that the EMS measurements should provide a good estimate of the evaporation at the hillslope site. Throughfall and evaporation for September through November are shown in Figures 4.2.4 and 4.2.5. These two estimates together should provide excellent quantification of the vertical hydrologic sinks and sources of moisture at the measurement site.

It is noteworthy that precipitation for the period greatly exceeds evaporation. Because the Prospect Hill site is directly adjacent to the stream channel running through Harvard Forest, visual observations of runoff were made every time soil moisture measurements were taken: from September to November, no noticeable runoff was observed in the stream channel. Using a simple mass balance, this implies that there should be a net accumulation of water in the unsaturated zone for the measurement period. This is reflected in Figure 4.2.6, which shows the spatially averaged soil moisture for each soil moisture measurement date. A sharp increase in soil moisture occurs in early October, coinciding with the decline of the forest canopy and the resulting decrease in evapotranspiration. For the period of October 1 to November 25, soil moisture remains fairly constant, increasing at an average rate of $D \frac{\partial \theta}{\partial t} = 0.001 \text{ cm/hr}$. This estimate was determined by dividing the change in soil moisture for period, multiplying by the average soil depth, and dividing by total time. This is smaller than, though comparable to, the average rate of evaporation and rainfall measured at the EMS Tower (approximately 0.005 cm/hr and 0.025 cm/hr, respectively). This large differential in the precipitation and evaporation rates are consistent with the increase in unsaturated zone soil moisture seen in Figure 4.2.6.

Figure 4.2.4

Daily Throughfall at Harvard Forest

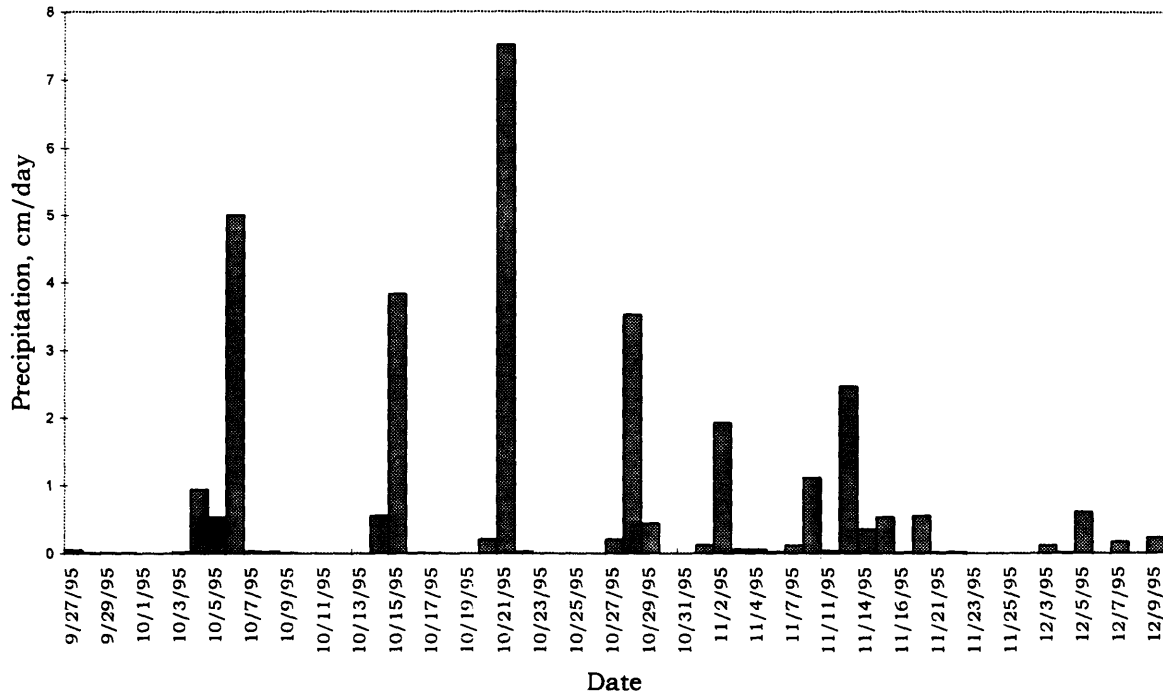


Figure 4.2.5

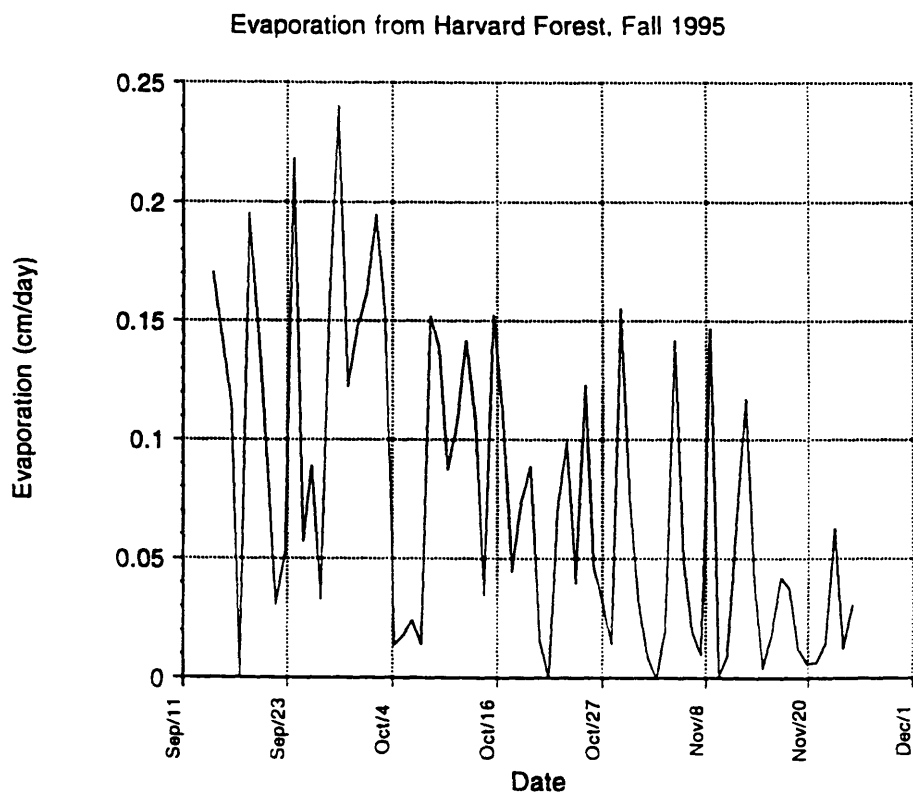
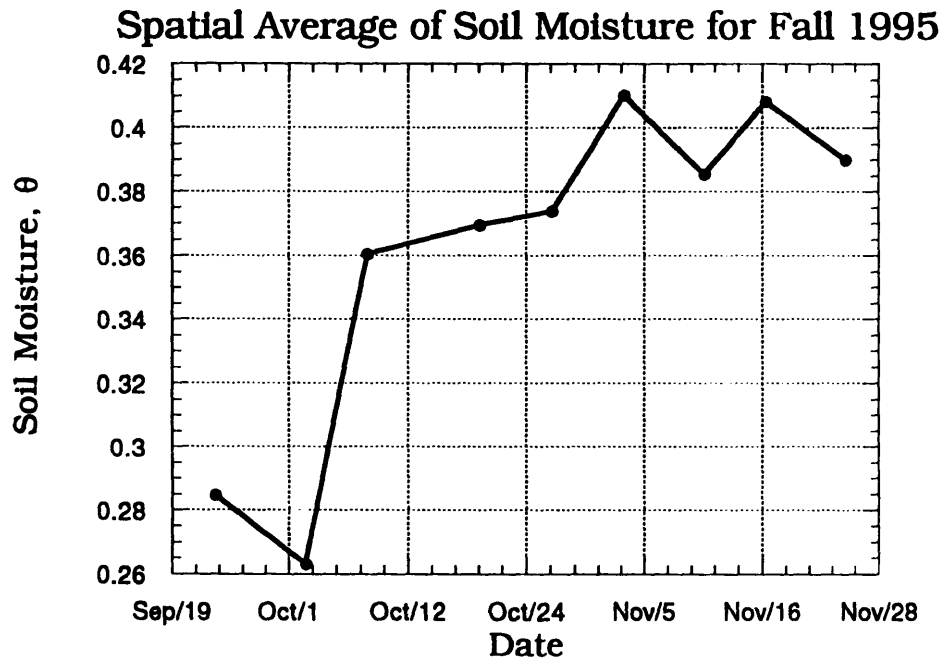


Figure 4.2.6



From October 27 to November 25, soil moisture decreases at an even smaller average rate (0.000023 cm/hr), so that the rate of change of the time average of soil moisture for that period is practically zero (0.1%) compared with the other fluxes of water. This condition is consistent with the assumptions involved in deriving Equation 2.2.1, in which the time-average rate of change of soil moisture is assumed zero: the resulting solution to Equation 2.2.1 should be valid for this period.

4.3 Relationship of Soil Water to Topography and Soil Properties

The ultimate goal of the field experiments is to test the notion that there is a noticeable and predictable correlation of soil water with elevation. Here, soil water refers to the general concept of water contained in the soil. Three specific measures of soil water can be directly compared using the experimental results. Soil moisture, θ , is measured almost directly using neutron probe measurements and the neutron probe calibration curve. Unsaturated hydraulic conductivity, K , can be estimated at each observation point using the observations of θ and the estimates of soil properties, α , c , θ_o , and K_o . Soil saturation, s , can also be estimated at each observation point by dividing the θ measurement by the porosity at each elevation. Of the three quantities, θ , is most directly a measured quantity, since the neutron probe readings measure attenuation of radiation, which is strongly proportional to soil moisture. Saturation, s , is dependent only on the measurements of θ and on the determination of θ_o . Unsaturated conductivity, K , is more an inferred quantity rather than a measured quantity: values of K are actually soil moisture observations translated into unsaturated hydraulic conductivity using the equation:

$$K = K_o e^{\frac{\alpha(\theta - \theta_o)}{c}} \quad (4.3.1)$$

and substituting for measurements of θ and the appropriate soil properties, α , c , θ_o , K_o . Since estimation of K involves the largest number of estimated parameters, it is most subject to experimental error of the three quantities. However, because of the high degree of accuracy of the soil moisture and soil property results (Tables 4.2.2 and 4.2.3), and the fact that the same values of α and c are used in each conversion, error of this sort should not be significant and K can also be considered an accurate measure of actual soil water conditions.

The observed data are presented in two fashions. First, observations of soil moisture(θ), soil saturation (s), and unsaturated hydraulic conductivity (K) are plotted against elevation (z), saturated hydraulic conductivity, (K_o) and porosity(θ_o) in Figures 4.3.1(a-c), 4.3.2(a-c), and 4.3.3(a-c). Examination of these figures shows that the observed relationship between the three measures of soil water and the three forcings (z , K_o , θ_o) can be approximated as linear. With this in mind, linear regressions between the three measure of soil water and the three forcings can be calculated. Two statistics from these regressions will be used to evaluate the dependence of soil moisture on the three forcings. First, r^2 , which is the percent of variability observed in the soil water explained by a linear relationship with the forcing will be used. This will measure the correlation between soil water and the forcings and how well each forcing explains the observations. r^2 can also be calculated for regressions of soil water to multiple forcings: the gain in r^2 from the simple regressions is a measure of the independent information contained in each forcing. This can be used to evaluate which of the three forcings are most informative in explaining soil water behavior. r^2 for the single and multiple regressions is shown in Table 4.3.1

The slope of the regression line is an important statistic. The slope of the regression line divided by its standard error is a t-statistic which can be used to give the level of confidence that the slope is significantly different from zero. When this is the case, then there is a significant associative statistical relationship between the

Figure 4.3.1a Observations of θ plotted against Elevation

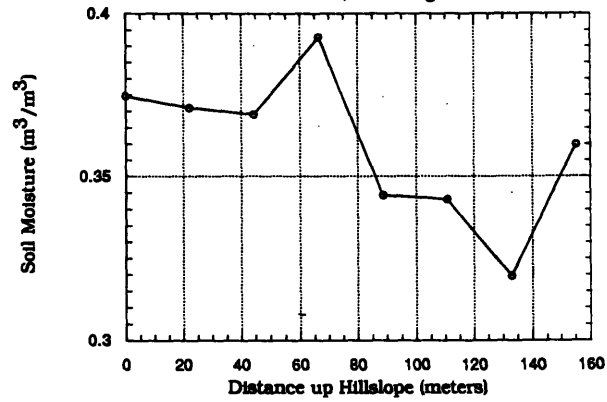


Figure 4.3.1b Observations of θ plotted against Saturated Hydraulic Conductivity

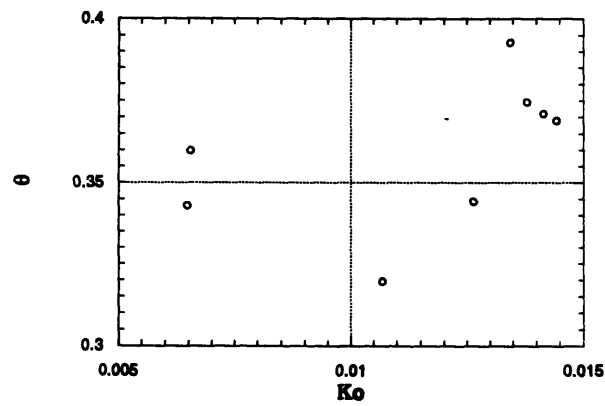


Figure 4.3.1c Observations of θ plotted against Porosity

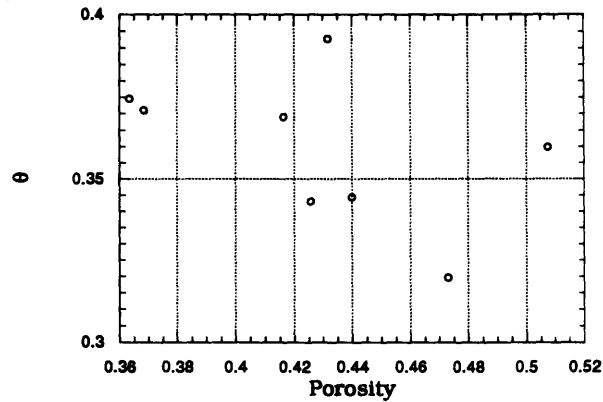


Figure 4.3.2a Observations of s plotted against Elevation

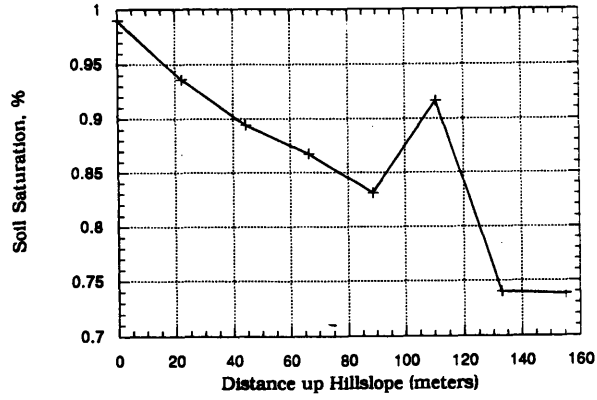


Figure 4.3.2b Observations of s plotted against Saturated Hydraulic Conductivity

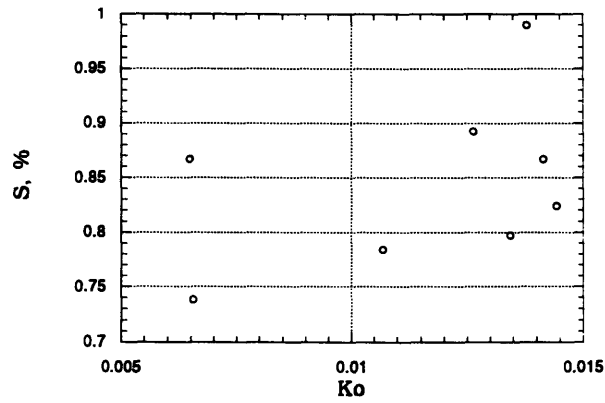


Figure 4.3.2c Observations of s plotted against Porosity

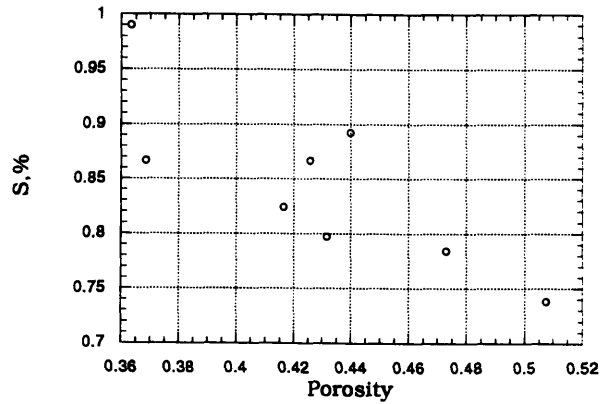


Figure 4.3.3a Observations of K plotted against Elevation

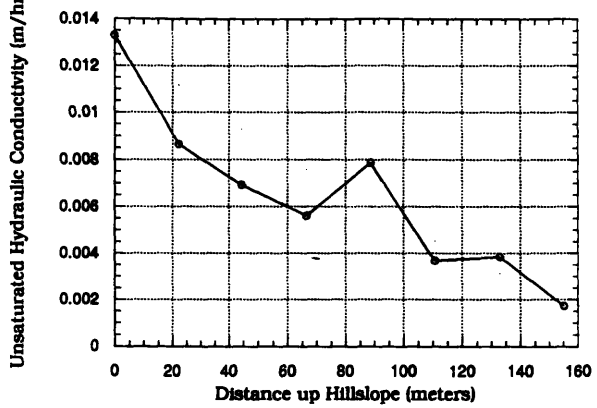


Figure 4.3.3b Observations of K plotted against Saturated Hydraulic Conductivity

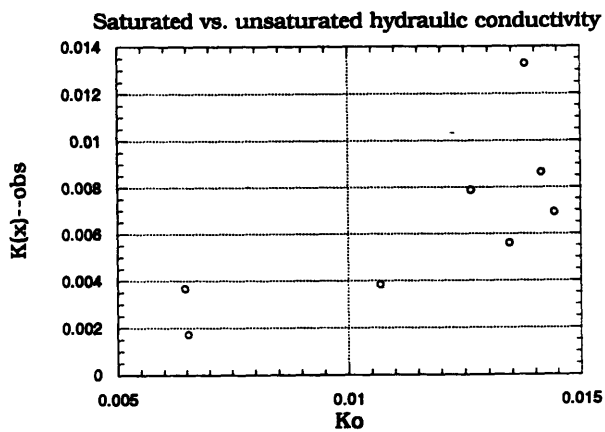


Figure 4.3.3c Observations of K plotted against Porosity

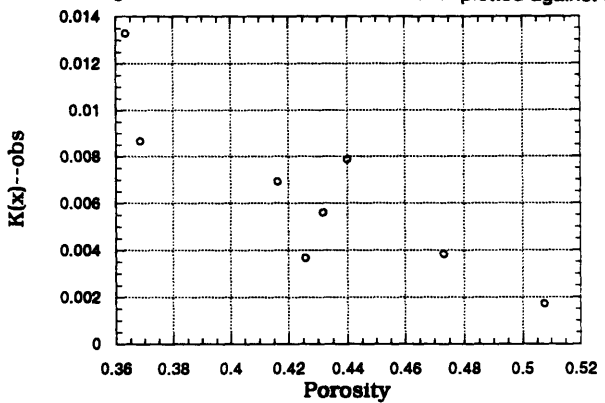


Table 4.3.1: r^2 of regressions of z , θ , and K_0 to θ , s , and K

Dependent Regression Variable	r^2 of Regression with Independent Variable(s)				
	z	K_0	n	z and z'	z and K_0
K	0.82	0.55	0.74	0.82	0.82
θ	0.39	0.28	0.35	0.39	0.39
s	0.54	0.18	0.66	0.67	0.64

measure of soil water and the forcing. The value of these statistics along with critical values of the t-distribution are shown in Table 4.3.2.

Soil moisture, θ , the preliminary variable of interest, shows a weak correlation to elevation ($r^2 = 0.38$, slope of regression significant at 90% confidence level). This result is somewhat discouraging at first. However, it is important to note that θ does not appear explicitly in the divergence equation of soil moisture (Equation 2.2.1). Soil moisture has a dependence on topography through its relation to unsaturated hydraulic conductivity, a relation which is dependent on four soil properties: θ_o , K_o , α , and c . Although the values of α and c along the hillslope are unknown and assumed to be constant, there is measured variability in saturated hydraulic conductivity and porosity, as shown in Figures 4.2.2 and 4.2.3. Thus, topography is not the only force at work on the distribution of soil moisture: soil properties will also affect the behavior of soil moisture at the experimental site.

It is enlightening to consider the effect that soil properties along Prospect Hill would have on soil moisture in the absence of an elevation gradient. A qualitative example of the soil properties along Prospect Hill and the equivalent flat slab of soil is shown in Figure 4.3.4. In the flat surface, the elevation is constant but porosity and hydraulic conductivity have gradients identical to those observed along Prospect Hill. Since the time-average soil moisture along Prospect Hill is nearly constant during Late October into November (see Section 4.2 above), the simple equilibrium case can be considered. Inside this flat surface, soil moisture at equilibrium would flow until the hydraulic head were constant at all points: since z is constant, capillary potential would also need to be constant. The condition of constant capillary potential in the soil is approximately equivalent to the condition of constant saturation throughout the soil. Since porosity increases uphill, soil moisture in the flat slab of soil must increase to maintain a constant level of saturation. If the elevation gradient along Prospect Hill had no effect on soil moisture, then the same pattern of soil moisture would be seen

Table 4.3.2 t-statistics of Linear Regressions

<u>Dependent</u> <u>Variable</u>	<u>Independent</u> <u>Variable</u>	<u>Slope/</u> <u>Standard Error</u>
θ	z	1.974†
θ	K_0	-1.508*
θ	θ_0	1.807*
s	z	-2.652‡
s	K_0	1.147°
s	θ_0	-3.417‡
K	z	-5.291‡
K	K_0	2.745‡
K	θ_0	-4.117‡

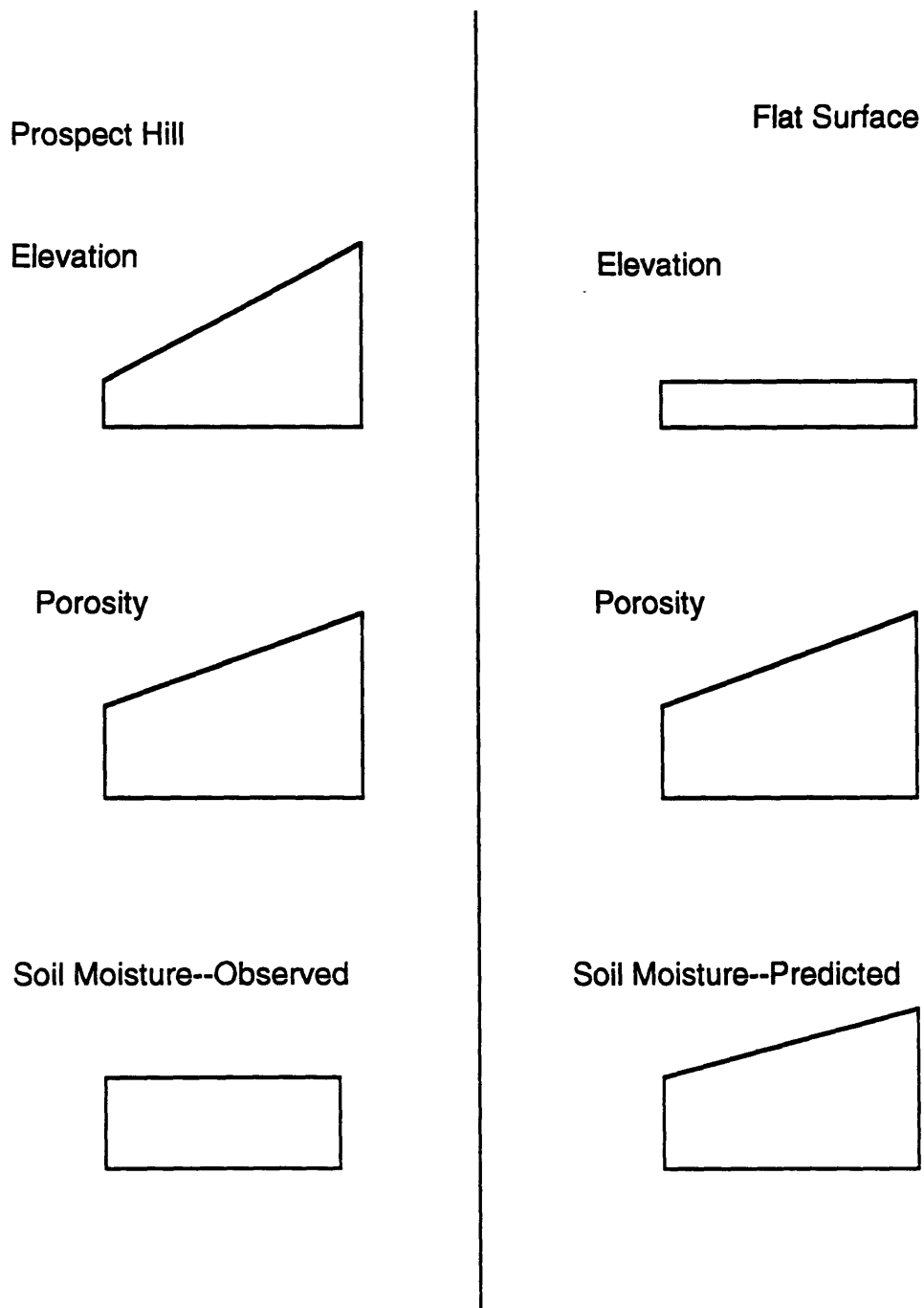
° insignificant

* exceeds critical value of 80% certainty of significant slope

† exceeds critical value of 90% certainty of significant slope

‡ exceeds critical value of 95% certainty of significant slope

Figure 4.3.4: Comparison of Soil Moisture for Prospect Hill and a Flat Surface with the Same Porosity Distribution



along the hillslope: soil moisture would increase uphill due to the effects of porosity alone. However, soil moisture along Prospect Hill remains nearly constant. In order to account for the observed behavior of soil moisture, another force must be at work. The most logical suggestion is that the elevation gradient along Prospect Hill is the factor that re-distributes the soil moisture away from the equilibrium condition predicted by soil properties alone.

Soil saturation observations, s , are also important to examine. The time average saturation is plotted against elevation in Figure 4.3.2a: the result is a striking correlation of soil saturation to elevation ($r^2 = 0.54$, slope significant at 95% confidence). As previously stated, soil saturation is directly proportional to the capillary tension head in the soil, ψ . Soils with high saturation are being forced to hold more of their potential of water; in the observational results, these are areas of lower elevation. The soil at the lower elevation therefore has lower ψ and is holding a greater percentage of its potential to draw in water. Again, if there were no effect from the elevation gradient, soil saturation would be constant along the hillslope. Since saturation displays a strong increase with elevation it can be reasonably concluded that elevation is at work driving the soil saturation higher downhill than would be observed if elevation had no role in soil moisture behavior.

Unsaturated hydraulic conductivity, K , also shows a strong correlation to elevation, with $r^2 = 0.82$ and regression slope significant at the 95% confidence level. The dependence of K on elevation is physically important: as water travels down the hill, the hydraulic conductivity increases. This indicates that soil at higher elevation has less capacity to transport water per unit area than soil at lower elevations. This is a valuable property because the "observed" unsaturated conductivity is dependent on soil properties and yet is still observably affected by elevation. That unsaturated hydraulic conductivity shows such a strong correlation to elevation is especially significant since the proposed equation relating soil water to elevation (Equation 2.1.8)

has an explicit dependence between the soil moisture surrogate, K , and z , elevation. Of the three measures of soil water, K much more strongly accounts for soil variability than θ or s , and has a more robust relationship with elevation. This suggests that there is a definite dependence of unsaturated hydraulic conductivity on topography and that unsaturated hydraulic conductivity is a significant variable in studies of topographic and geologic forcings on soil water.

4.4 Predictions of the Theory Relating Soil Moisture to Topography

The final step in testing the relation of soil moisture to topography is to evaluate how well predictions from the governing flow equation compare to actual observations. Both the steady state (Equation 2.2.1) and the transient (Equation 2.2.7) flux equations can be tested. The steady equation can be used to evaluate how well the theory predicts the long-term soil moisture behavior in space if the rate of change of soil moisture ($\frac{\partial\theta}{\partial t}$) is near to zero; this condition is close to being satisfied for the period of October 27 to November 25. The value of the neglected term $\frac{D}{\alpha K_0} \frac{\partial K_0}{\partial x}$ from Equation 2.1.6 is compared to topographic slope in Table 4.4.1: this confirms that the contribution of this term is indeed negligible and that the simplified version Equation 2.1.6 can be used.

The measurements of evaporation can be used to infer the vertical divergence parameter, β . Since the soil at the measurement site is shallow (1 meter in depth) and lies directly on bedrock, downwards percolation from the unsaturated zone is expected to be minimal. Evaporation should therefore be the main component vertical sink of water from the unsaturated zone. Since vertical sinks of water are parameterized as $s=\beta K$ in Equation 2.1.8, β can be estimated for the measurement site with the formulation

$$\beta = (\text{evaporation}) / (\text{average unsaturated hydraulic conductivity})$$

Using the data from Figures 4.2.5 and 4.3.3, β is estimated at a value of 0.004 for the experimental site.

Figures 4.4.1a-c show the predictions versus observations made with Equations 2.2.2 and 2.2.6 for the time average of θ , K , and s for Fall 1995 for the eight elevation levels. The average RMS error for these predictions (not including the boundaries, which are automatically satisfied) is 0.022 for θ , or about 6.3% of the average: RMSE, r^2 , and the significance of the regression between predictions and observations are presented in Table 4.4.2. This results indicate that the steady-state equation is reasonable for predicting the idealized soil saturation, s , and unsaturated hydraulic conductivity, K , behavior in a natural system: heterogeneity in the natural environment will be expected to produce some degree of model error. Soil moisture, θ , is not predicted as well as K and s . Predicted θ is translated from predictions of unsaturated hydraulic conductivity by Equation 2.1.5 which depends highly on soil properties; observed θ is relatively independent of soil properties. It is to be expected that the two values will not be in strong agreement.

Unsaturated hydraulic conductivity is the basic variable of the steady-state predictions: the predictions of K depend only on the boundary conditions of soil moisture and on the quantities D , β , α , and $\frac{\partial z}{\partial x}$ in Equations 2.2.3. The predictions agree very strongly with the observations, which are highly dependent on the soil properties α , c , θ_0 , and K_0 . These two sets of values for K are expected to vary relatively independent of each other: their only similarity is the value of α , which is used in two completely separate equations, and in the two boundary conditions. However, the agreement of the observations to predictions is excellent: the regression of observations to predictions yields an r^2 of 0.85 and significance of slope at over 95% confidence. The agreement of these two independent quantities is extremely significant and strongly indicates that the theory relating unsaturated hydraulic

Table 4.4.1: Observed value of neglected term of $\frac{1}{\alpha K_0} \frac{\Delta K_0}{\Delta x}$ in Equation 2.1.9.

Elevation level (m)	$\frac{1}{\alpha K_0} \frac{\Delta K_0}{\Delta x}$	$\frac{\partial z}{\partial x}$	ratio of $\frac{\partial z}{\partial x}$ to $\frac{1}{\alpha K_0} \frac{\Delta K_0}{\Delta x}$
133 to 155	0.0018	0.24	0.72%
111 to 133	-0.0011	0.24	-0.46%
89 to 111	0.0026	0.24	1.1%
66 to 89	0.00018	0.24	0.07%
44 to 66	0.0020	0.24	0.08%
22 to 44	-5.4e-5	0.24	-0.02%
0 to 22	-7e-5	0.24	-0.03%

Figure 4.4.1a

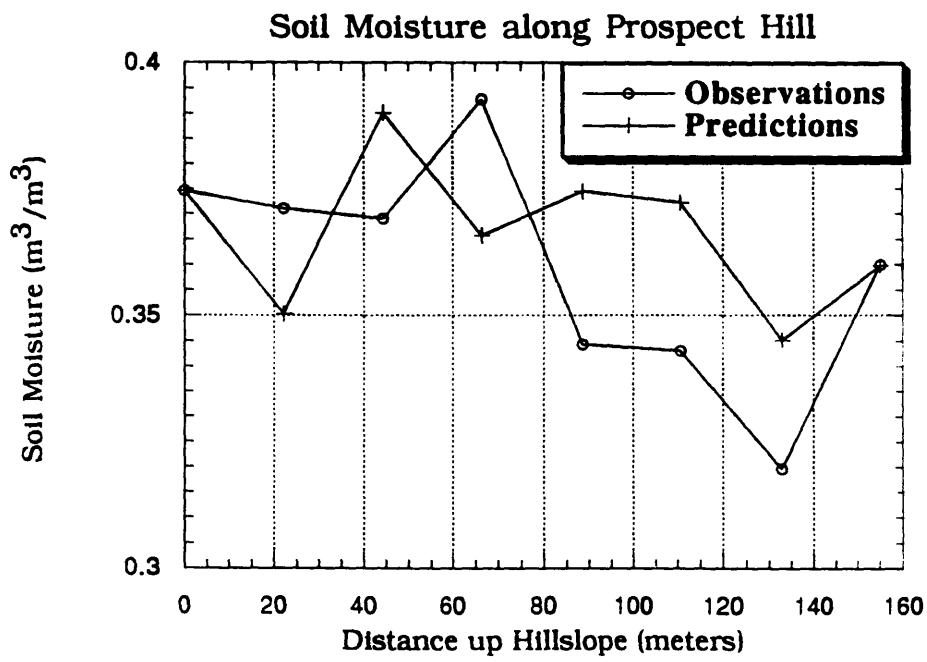


Figure 4.4.1b

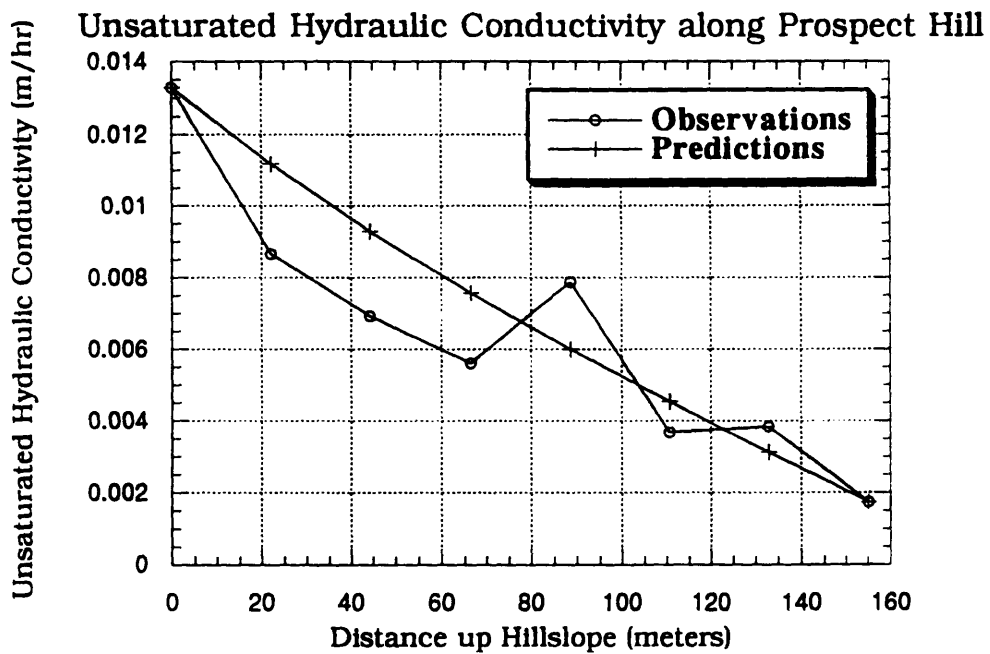


Figure 4.4.1c

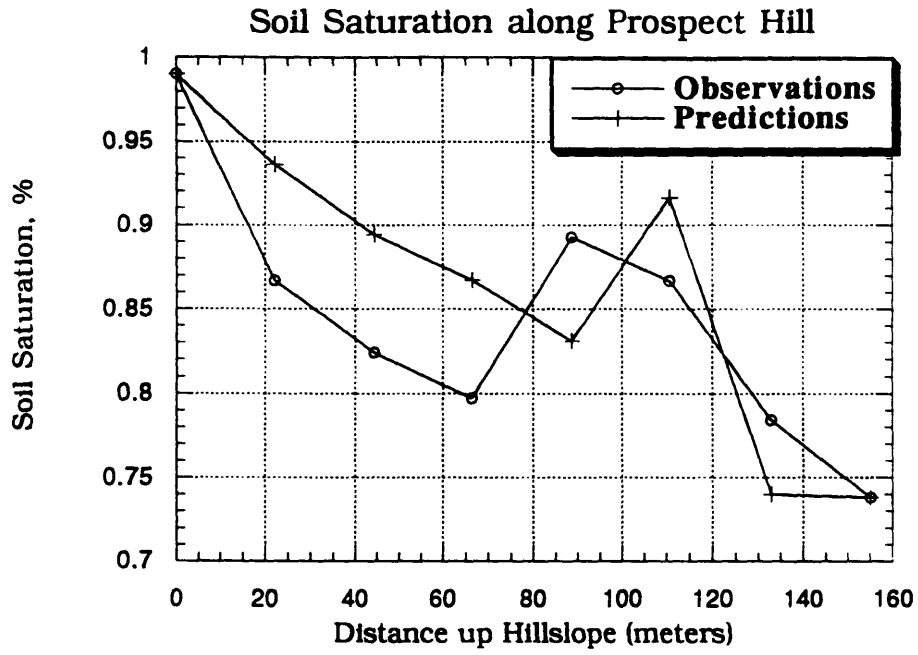


Table 4.4.2: RMSE, r^2 , between Steady-State Predictions and Average Soil Moisture

	Variable		
	K	θ	s
Average	0.0065	0.36	0.85
RMSE	0.0016	0.022	0.053
%RMSE	24.9%	6.3%	6.3%
r^2 of predictions			
vs. observations	0.85	0.11	0.65

conductivity in Equation 2.2.1 is capable of accurately describing the behavior of soil water in space for topography-driven flux.

The next step is to determine how well the unsteady equation predicts soil moisture: this will test the ability of the theory to make predictions in time as well as space. Using each measurement date as a set of initial conditions, along with the rainfall and the evaporation record, Equations 2.2.10, 2.2.12, and 2.2.17) can be used to make predictions for the next measurement date. This involves predicting the initial conditions in space and then predicting the future behavior of soil moisture in time, as described in the algorithm for unsteady predictions in Section 2.2. The predictions can then be compared with the observed results as shown in Figure 4.4.2a-h. The agreements between the two is not perfect. However, the coefficient of determination of a simple linear regression between observations and predictions of soil moisture θ in time is quite good at each location, as shown in Table 4.4.3; RMSE for the eight dates on which predictions were made is about 20% of the mean, or three times as large as when steady-state predictions made in space alone.

It is also important to note that the bias of the unsteady predictive error changes with time. At the beginning of the experimental period, the unsteady equation underpredicts soil moisture on the average: as autumn progresses, the bias goes to zero and then to overprediction towards the end of the fall. Since predictions of the initial conditions of soil moisture do not show this bias (and actually show a positive bias for the period) as shown in Table 4.4.4, this bias must arise from predictions in time. The bias of the predictions of initial conditions has no correlation with the bias of the predictions for the next time measurement date. As shown by Equation 2.2.11, the predictions in time are the initial conditions divided by time: the temporal rate of decay for unsteady predictions is $(ct)^{-1}$, from the formulation in Equation 2.2.10c. Since time is always known, it follows that c , the pore tension parameter, may possibly change in time. This would not be unexpected behavior, since c is in general dependent of the

**Figure 4.4.2a:
Unsteady Predictions for 10/3/95**

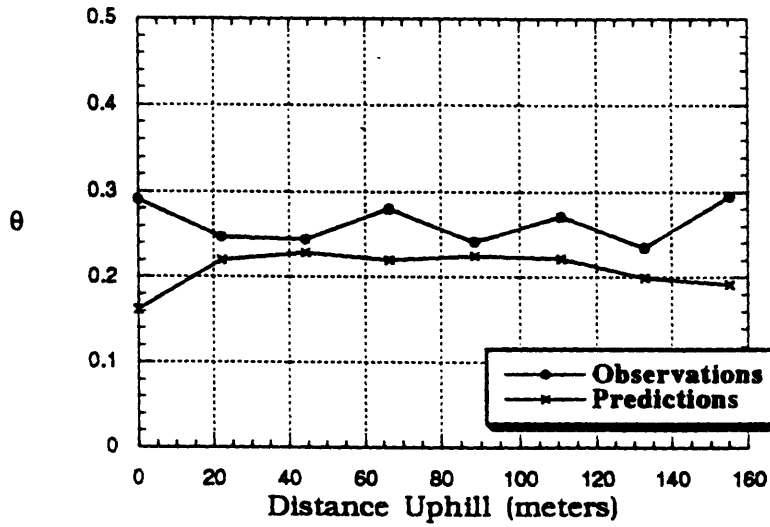


**Figure 4.4.2b:
Unsteady Predictions for 10/9/95**

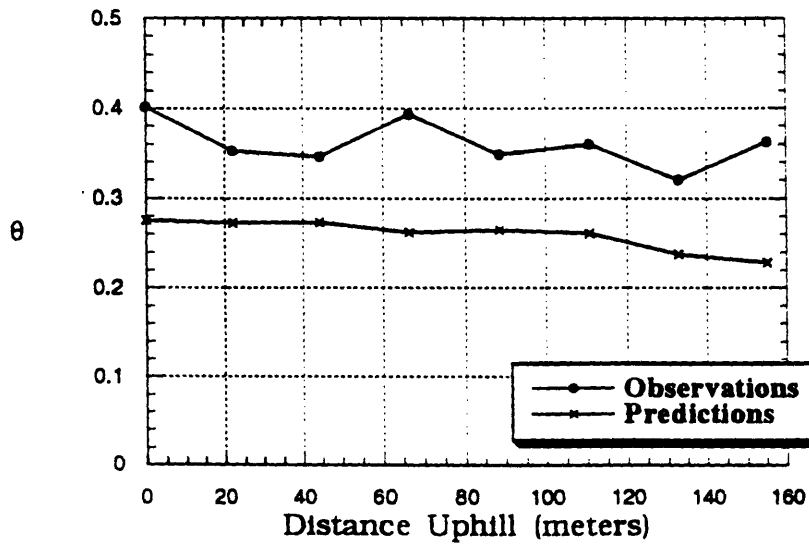


**Figure 4.4.2c:
Unsteady Predictions for 10/20/95**

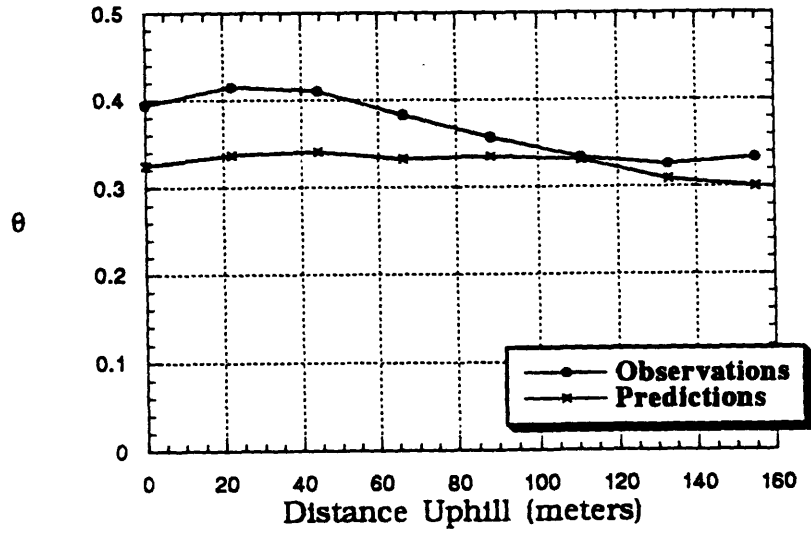


**Figure 4.4.2d:
Unsteady Predictions for 10/27/95**

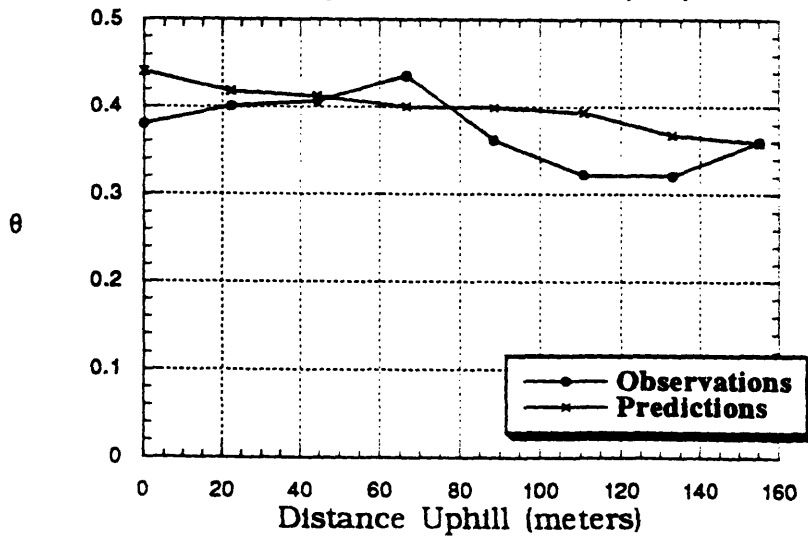


**Figure 4.4.2e:
Unsteady Predictions for 11/3/95**

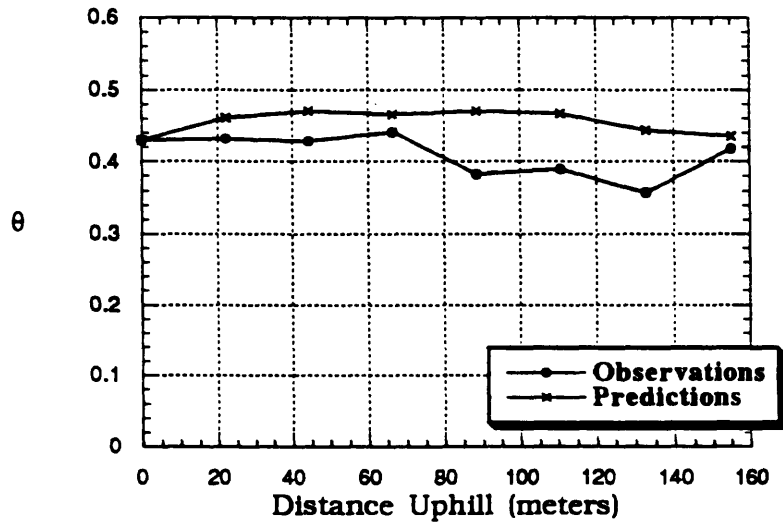


**Figure 4.4.2f:
Unsteady Predictions for 11/11/95**

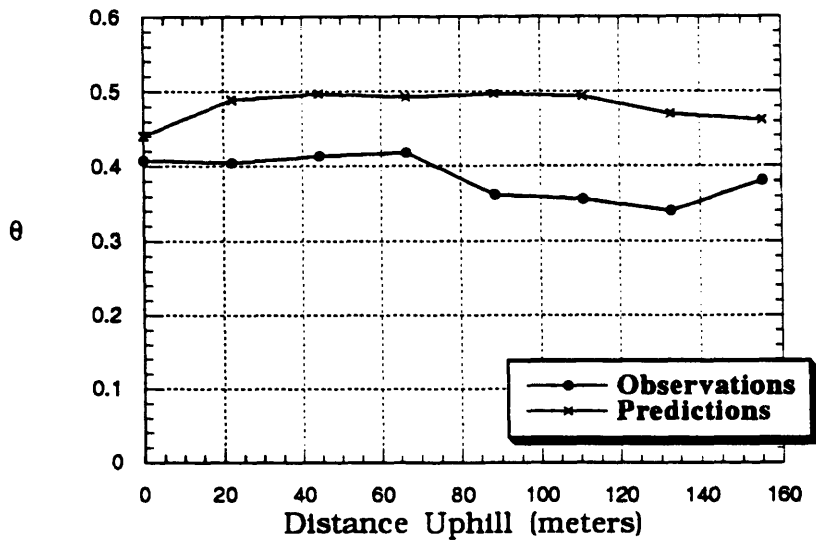


**Figure 4.4.2g:
Unsteady Predictions for 11/17/95**

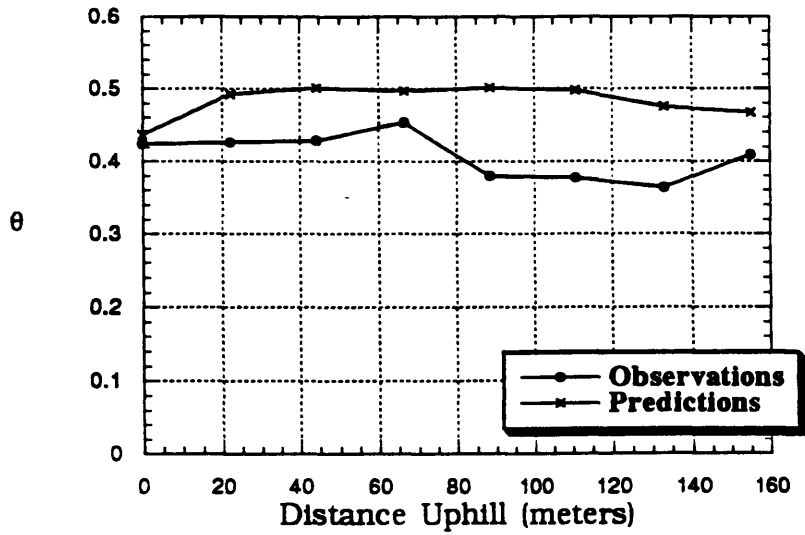


**Figure 4.4.2h:
Unsteady Predictions for 11/25/95**

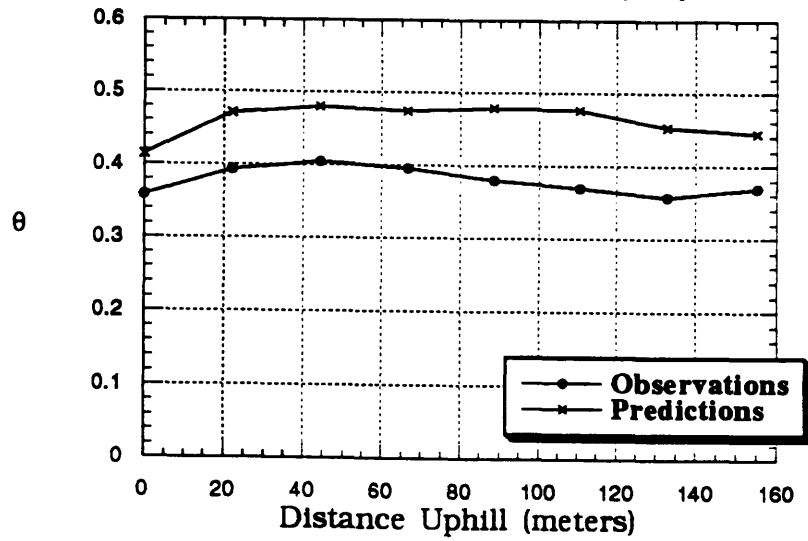


Table 4.4.3: r^2 of Unsteady Predictions versus Observations of Soil Moisture

<u>Distance Uphill (meters)</u>	<u>r^2</u>
0	0.67
22	0.71
44	0.54
66	0.61
89	0.63
111	0.72
133	0.66
155	0.51

Table 4.4.4: Bias of Unsteady Predictions of Soil Moisture

Date	Bias of Initial Conditions	Bias in Resulting Prediction
9/24/95	0.34	0.22
10/3/95	0.43	-0.48
10/9/95	0.25	-0.18
10/20/95	-0.01	-0.22
10/27/95	0.10	-0.34
11/3/95	0.26	0.22
11/11/95	0.19	-0.11
11/17/95	0.21	0.21
11/25/95	0.09	N/A
Average:	0.21	-0.09

r^2 of regression of temporal to spatial biases = 0.01

moisture content of the soil, the time history of wetting and drying, and temperature (which may significantly affect the viscosity of water as well). The assumption that c is constant may not be entirely accurate for the flux system under consideration. The dependence of c on soil moisture would need to be quantified in order to test if this is true. One immediate limit of the predictive use of the theory is the present capability to quantify soil parameters. Although the predictions are acceptable using a simplified approach to unsaturated behavior of soil, they will ultimately be limited by the complexity of unsaturated soil behavior.

4.5 Conclusions

The field experiment shows some very significant results. Observed soil moisture, θ , soil saturation, s , and unsaturated hydraulic conductivity, K , all show significant dependence on topography and on soil properties. These forcings of topography and soil properties act on soil moisture in significant but opposing manners. The effect of soil properties can be predicted by elementary physics: soil moisture should increase and saturation should remain constant uphill due to increasing porosity. In the observations, soil moisture remains constant and saturation decreases: the best explanation for this behavior is the proposed effect of topographic forcing.

Predictions in space made with the steady-state theory show K to have an important relationship with topography and soil properties. Observations of K are primarily dependent on soil properties such as α , c , θ_0 , and K_0 , while predictions of K are made using boundary conditions and the values of D , β , α , and $\frac{\partial z}{\partial x}$. These two sets of K are determined in a relatively independent manner: strong agreement with the experimental observations to the theoretical predictions prove the significance of the theory.

Unsteady predictions also agree well with observations. Using observations to make predictions for the next measurement date, predictions of soil moisture were made in space as well as time. The results are quite good, with high r^2 and RMSE about three times as large as for predictions in space alone.

In summary, the field experiment demonstrates 1) a significant role of topography in explaining the observations of soil moisture and 2) reasonable agreement of predictions to observations of unsaturated hydraulic conductivity made using the governing flow equation.

CHAPTER 5

Conclusions

5.0 Introduction

This chapter summarizes the theoretical and experimental results and the conclusions based on the findings of this study.

5.1 Soil Moisture Theory.

The main theory developed in this study is a formulation relating the distribution of soil moisture to topography. Using an explicit representation of elevation, the relationship between soil moisture and topography is derived from the basic principles of unsaturated flow. Both the one- and the two-dimensional cases are considered. Using spectral techniques, the spectrum of soil moisture can then be expressed in terms of the soil and climate properties and spectrum of topography. This effectively relates the distribution of soil moisture to the distribution of topography.

The theory predicts that the two-dimensional case will result in larger variance and stronger spatial correlation of soil moisture. Of the two cases, the two-dimensional consideration gives better regard to true soil moisture behavior: the flow of soil moisture in the real world will inherently be multidimensional. In two physical dimensions, the distribution of topography is expected to result in a larger variability of soil moisture. Mathematically, the spectral relationship between soil moisture and topography will also predict a higher variance and stronger spatial correlation in the two-dimensional case.

Soil and climate will also be important in the large scale distribution of soil moisture. To test the importance of soil and climate in the relationship of soil moisture distribution to topography, a sensitivity analysis was carried out for a ideal system with topography as the main forcing. The pore size distribution parameter (α), vertical

divergence parameter (β), pore size distribution parameter (c), and porosity (θ_0) most significantly affect the significance of soil moisture variability. This is demonstrated by the changes in the coefficient of variation of soil moisture resulting from changes in these properties. The properties of root zone depth (D), saturated hydraulic conductivity (K_0), and effective precipitation (R) have a less significant impact on topography-driven soil moisture variability.

Theoretically, variations in all soil properties can bring about significant soil moisture variability. The magnitude of this variability was examined using data for two soil types. It was determined that variability in α and K_0 bring about significant soil moisture variability of the same magnitude or larger than the variability resulting from topography. It can be concluded that both topography and soil properties will create important contributions to soil moisture variability.

5.2 Field Observations

For the theory in Chapters 2 and 3 to be validated, it is necessary to test the actual impact of topography on soil moisture. For this purpose, measurements of soil moisture and soil properties were taken along a hillslope at a research facility in Central Massachusetts. In the observations, soil moisture remains nearly constant with elevation while porosity increases with elevation. The effect of porosity alone would be to redistribute soil moisture to a constant saturation level along the hill, resulting in higher soil moisture uphill. The observations of a nearly constant soil moisture profile strongly suggests that the elevation gradient acts to redistribute soil moisture downhill. Therefore, forcings of topography and soil properties act on soil moisture in significant but opposing manners.

Predictions in space made with the steady and unsteady theory also show unsaturated hydraulic conductivity, K , to have an important relationship with topography and soil properties. Observations of K are primarily dependent on soil

properties such as α , c , θ_o , and K_o , while predictions of K are made using boundary conditions and the values of D , β , α , and $\frac{\partial z}{\partial x}$. These two sets of K are determined in a relatively independent manner: strong agreement of the experimental observations with the theoretical predictions prove the significance of the theory.

5.3 Future Research

Several aspects of the work in this study can be continued. First, the next step in advancing the theory relating soil moisture distribution to topography is to consider the unsteady case in which soil moisture will vary in time as well as space. This consideration will add a third dimension to the theory developed in Chapter 2. Second, the soil moisture experiments are currently in progress, so the opportunity exists to create a picture of the long-term behavior of soil moisture. This information will aid in further understanding the spatial and temporal processes which affect soil moisture. Third, with quantitative large-scale information on the variability of soils, the general theory developed in Section 3.3 can be used to make predictions about the large-scale distribution of soil moisture based on considerations of topography and soil properties. Finally, the theory developed in this study could be combined with other techniques for estimating the large-scale distribution of soil moisture. This could potentially improve operational predictions of the distribution of soil moisture. As these refinements are carried out, it is hopeful that the scope and impact of hydrologic studies will be improved and that the value of this research will be significant.

References

- ASTM**, Soil and rock, Vol 4.08, Philadelphia (1995):
"D-854: Standard test for specific gravity of soils", p.80-83.
"D-1556: Standard test for density and unit weight of soil in place by the sand- cone method", p.112-117.
"D-2167: Standard test method for density and unit weight of soil in place by the rubber balloon method", p.167-172.
"D-2216: Standard test for laboratory determination of water (moisture) content of soil and rock", p.178-181.
- Bakr**, A.A., L.W. Gelhar, A.L. Gutjahr, and J.R. MacMillan, "Stochastic analysis of spatial variability in subsurface flows, I : Comparison of one- and three-dimensional flows", *Water Resour. Res.*, 14, 2, 263-281, (1978).
- Beven**, K. J. and M. J. Kirkby. "A physically based, variable contributing area model of basin hydrology", *Hydrological Sciences Journal*, 24, 1, 43-69, (1979).
- Bras**, R.L., Hydrology. An Introduction to Hydrologic Science, Addison-Wesley (1990).
- Brooks**, R. H., and A. T. Corey, "Properties of porous media affecting fluid flow", *ASCE j. Irr. Drainage Div.*, IR2, 61-88 (1966).
- Choi**, J., "Evaporation from Harvard Forest", Bachelor's Thesis, MIT (1996).
- Daniel**, D. E., "In Situ hydraulic conductivity tests for compacted clay", *ASCE J. Geotech Eng.*, 115, 1205-1226 (1989).
- Eltahir**, E.A.B., "Lateral unsaturated flow", term paper, MIT, (1989).
- Gardner**, W.R., "Some steady state solutions of the unsaturated moisture flow equation with application to evaporation from a water table", *Soil Sci.* 85, 4, 228-232 (1958).
- Gash**, J.H., "A note on estimating the effect of a limited fetch on micrometeorological evaporation measurements", *Boundary-Layer Meteorology*, 35, 409-413 (1986).
- Gelhar**, L.W., Stochastic subsurface hydrology, Prentice-Hall (1993).
- Genereux**, D.P., and H.F. Hemond, "Naturally occurring radon 222 as a tracer for stream flow generation: steady state methodology and field example", *Water Resour. Res.*, 26, 12, 3065-3076 (1990).
- Giorgini**, A., M. Bergman, J. Pravia, and A. Hamidi, "Lateral moisture movements in unsaturated anisotropic media", Purdue University, Water Resources Research Center, TR #169, (1984).
- Gregson**, K., D. J. Hector, and M. McGowan, "A one-parameter model for the soil water characteristic", *J. Soil Sci.*, 38, 483-486 (1987).

Hewlett, J. D., and A. R. Hibbert, "Moisture and energy conditions within a sloping soil mass", *Journal of Geophysical Research*, 68, 1081-1087, (1963).

Jenkins, G.M., and D.G. Watts, Spectral analysis and its applications, Holden-Day (1968).

Lister, J. R., and P. Kerr, "The propagation of two-dimensional and axisymmetric viscous gravity currents at a fluid interface", *J. Fluid Mech.*, 203, 215-250, (1989).

Kendall, M, and J. D. Gibbons. Rank Correlation Methods, Oxford University Press, (1990).

Klute, A., "A numerical method for solving the flow equation for water in unsaturated materials", *Soil Sci*, 73, 105-116 (1952).

Mantoglou, A. and L.W. Gelhar, "Stochastic modeling of large-scale transient unsaturated flow systems", *Water Resources Research*, 23, 1, 37-46 (1987a).

Mantoglou, A., and L.W. Gelhar, "Capillary tension head variance, mean soil moisture content, and effective specific soil moisture capacity of transient unsaturated flow in stratified soils", *Water Resour. Res.* , 23, 1, 47-56 (1987b).

Mantoglou, A., and L.W. Gelhar, "Effective hydraulic conductivities of transient unsaturated flow in stratified soils", *Water Resour. Res.* , 23, 1, 47-68 (1987c).

McCord, J.T., and D. B. Stephens, "Lateral moisture flow beneath a sandy hillslope without an apparent impeding layer", *Hydrological Process*, 1, (1987).

McCuen, R. H., W. H. Rawls, and D. L. Brakensisk, "Statistical analysis of the Brooks-Corey and the Green-Ampt parameters across soil texture", *Water Resour. Res.*, 27, 1005-1013 (1981).

Moore, K.E., D.R. Fitzjarrald, R.K. Sakai, M.L. Goulden, J.W. Munger, and S.C. Wofsy, "Seasonal variation in radiative and turbulent exchange at a deciduous forest in central Massachusetts", *J. of Applied Meteorology*, 35, 122-134, (1996).

Philip, J. R., "The theory of infiltration: 1. The infiltration equation and its solution", *Soil. Sci*, 83, 345-347 (1957).

Revut, I.B., and A.A. Rode, Experimental methods of studying soil structure, Kolos Publishers, Leningrad, (1969), Published for U.S. Department of Agriculture and the National Science Foundation by Amerind Publishing Co., New Delhi (1981).

Richards, L. A., "Capillary conduction of liquids through porous mediums", *Physics* 1, 318-333 (1931).

Shani, U., R. J. Hanks, E. Bresler, and C. A. S. Oliveira, "Field method for estimating the hydraulic conductivity and matric potential-water content relations", *Soil Sci. Am. J.*, 51, 298-302 (1987).

Sloan, P.G., and I.D. Moore, "Modeling subsurface stormflow on steeply sloping forested watersheds", *Water Resour.Res.* , 20, 12, 1815-1822 (1984).

Smith, K.A., and C.E. Mullins, Soil Analysis - physical methods, Marcel Dekker, Inc. (1991).

Stephens, D.B., Vadose zone hydrology, Lewis Publishers (1996).

Troxler Electronic Laboratories, Inc., RTP, NC, 3300 Series instruction manual: depth moisture gauges, (1983).

Wofsy, S.C., M.L. Goulden, J.W. Munger, S.-M. Fan, P.S. Bawkin, B.C. Daube, S.L. Bassow, and F.A. Bazzaz, "Net exchange of CO₂ in a mid-latitude forest", *Science*, 260, 1314-1317 (1993).

Wooding, R. A., "Steady infiltration from a shallow circular pond", *Water Resour. Res.*, 4, 1259-1273 (1968).

Zaslavsky, D., and Sinai, G., "Surface hydrology: I-Explanation of the phenomena", ASCE, *J. Hydr.Div.* , 107, 1-16 (1981).

Zaslavsky, D., and G. Sinai, "Journal of the hydraulics division - Surface Hydrology: II-Distribution of raindrops", ASCE, *J. Hydr.Div.* , 107, 17-36 (1981).

Zaslavsky, D., and G. Sinai, "Journal of the hydraulics division - Surface Hydrology: III-Causes of lateral flow", ASCE, *J. Hydr.Div.* , 107, 37-52 (1981).

Zaslavsky, D., and G. Sinai, "Journal of the hydraulics division - Surface Hydrology: IV-Flow in sloping layered soil", ASCE, *J. Hydr.Div.* , 107, 53-64 (1981).

Zaslavsky, D., and G. Sinai, "Journal of the hydraulics division - Surface Hydrology: V-In-surface transient flow", ASCE, *J. Hydr.Div.* , 107, 65-93 (1981).